# Antimicrobial Surfaces

## (Silver-bearing Surfaces)

**Ph.D. Thesis**

**by**

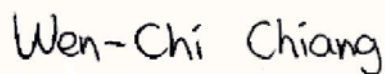**Wen-Chi Chiang**

**January 2009**

**Department of Mechanical Engineering**

**Technical University of Denmark**

# Preface

The present thesis is submitted in candidacy of a Ph.D. degree from The Technical University of Denmark (DTU). The project was carried out at the Department of Mechanical Engineering (MEK) and the Department of Systems Biology in the period of August 2005 to January 2009. The project was supervised by Professor Per Møller and co-supervised by Associate Professor Lisbeth Rischel Hilbert and Associate Professor Tim Tolker-Nielsen. This work combined with the knowledge of thermodynamics, electrochemistry, alloy design, and microbiology, validating the effective bacteria inhibiting effect, has resulted in new selections of antimicrobial surfaces which can be used to help reduce the occurrence of bacterial (re-)contamination giving primarily an inhibiting effect close to the surfaces.

The structure of the thesis is an introductory chapter to the field itself, giving also the background motivations. Then the following chapters 2 and 4 introduce the two major modes of antimicrobial effect studied in this work. The chapters 3 and 5 collect and discuss the obtained results and studies on silver-palladium surfaces and on silver-bearing stainless steels. Chapter 6 is an overview of the experimental techniques applied and chapter 7 summarizes the papers in this thesis. Chapter 8 closes the thesis with an overall discussion, conclusion and outlook.

Wen-Chi Chiang

Konges Lyngby, January 2009

**A paper award is included in the thesis:**

A new method to inhibit microbial and biofilm adhesion: *International Water Association Biofilm Technologies Conference*, Singapore, January 2008.

**The following papers are included in the thesis:**

1. Study of electroplated silver-palladium biofouling inhibiting coating: <u>W. C. Chiang</u>, L. R. Hilbert, C. Schroll, T. Tolker-Nielsen, and P. Møller. *Corrosion Engineering, Science and Technology*, Vol. 43, No. 2, pp. 142-148, 2008.

2. Bacterial inhibiting surfaces caused by the effects of silver release and/or electrical field: <u>W. C. Chiang</u>, L. R. Hilbert, C. Schroll, T. Tolker-Nielsen, and P. Møller. *Electrochimica Acta*, 2008, Vol. 54, No. 1, pp. 108-115, 2008.

3. Anti-biofilm properties of a silver-palladium surface: <u>W. C. Chiang</u>, C. Schroll, L. R. Hilbert, P. Møller, and T. Tolker-Nielsen. *Applied and Environmental Microbiology*, Vol. 75, No. 6, pp. 1674-1678, 2009.

4. Influence of silver additions to type 316 stainless steels on bacterial inhibition, mechanical properties, and corrosion resistance: <u>W. C. Chiang</u>, I. S. Tseng, P. Møller, L. R. Hilbert, T. Tolker-Nielsen, and J. K. Wu. *Materials Chemistry and Physics*, Vol. 119, No. 1, pp. 123-130, 2010.

5. Influence of bacteria on silver dissolution from silver-palladium surfaces: <u>W. C. Chiang</u>, L. R. Hilbert, C. Schroll, T. Tolker-Nielsen, and P. Møller. A conference paper presented at *European Corrosion Congress*, Nice, France, September 2009.

# Acknowledgements

# Abstract

Bacterial (re-)contamination is a major concern in many areas, and it is therefore of high priority to develop effective and low-toxic methods for combating bacteria. In this work, silver-palladium surfaces and silver-bearing stainless steels were designed and investigated focusing on electrochemical principles to form bacteria inhibiting effects. It is expected that these designs could be integrated in areas where hygiene is a major requirement.

The main results of this work are included in form of journal papers given in appendices. Papers I and II are focused on the investigation of microstructures, electrochemical properties and bacteria inhibiting effects of silver-palladium surfaces, and the preliminarily discussions of their bacteria inhibiting mechanisms. Paper II also covers the investigation of the bacteria inhibiting effects of Ag-bearing ferritic/austenitic (duplex) stainless steels as compared with silver-palladium surfaces. Paper III is focused on the evaluation of the biofilm inhibition efficacy and study of the biofilm inhibition mechanism of silver-palladium surfaces under conditions of low and high bacterial load, which were performed by using flow-chamber and batch setups respectively. Paper IV investigates the influence of silver additions to type 316 austenitic stainless steels on bacterial inhibition, mechanical properties, and corrosion resistance. The possible mechanisms of silver dissolution from silver-bearing surfaces are also discussed. Paper V is a study of the phenomenon of increased silver dissolution from silver-palladium surfaces under exposure to some specific environments.

For silver-palladium surfaces, the experiments conducted showed that the surfaces can

inhibit bacteria and biofilms due to generating micro-electric fields and electrochemical redox processes from the surfaces. For silver-bearing stainless steels, experiments showed that silver addition to stainless steels can generate a bacteria inhibiting property due to the release of toxic levels of silver from the surfaces, but can slightly degrade mechanical and corrosion properties as compared to traditional stainless steels. However, as bacterial microcolonies may occur if these bacteria inhibiting surfaces become covered with a conditioning layer of dead surface-associated bacteria or are used for a long time, highest efficiency of these surfaces may be achieved under conditions where appropriate cleaning practices can be applied.

It is not surprising that chemicals aggressive to silver and silver compounds can accelerate silver dissolution due to the formations of silver ions and silver complex ions, but in this work a phenomenon of increased silver dissolution was found associated directly with the presence of bacteria. Experiments showed that surface-associated bacteria greatly increased silver dissolution from the silver-bearing surfaces due to the interactions between cell components and the surfaces, and the amount of surface-associated bacteria enhanced this effect. Thus the presence of bacteria could be the switch that turns on the release of toxic silver ions, which leads to a killing effect in solutions otherwise not aggressive to silver.

# Resumé

Forurening med bakterier og bakterievækst skaber i mange sammenhænge væsentlig bekymring, og udvikling af effektive metoder til at bekæmpe bakterier uden anvendelse af giftige stoffer er derfor af høj prioritet. I dette forskningsarbejde er der fokuseret på anvendelse af elektrokemiske principper til at skabe en bakteriehæmmende effekt. Dette er realiseret i form af udvikling og undersøgelse af sølv-palladium overflader og sølvholdigt rustfrit stål. Det forventes at disse konstruktioner kan integreres i områder, hvor god hygiejne er et væsentligt krav.

De primære resultater af dette arbejde er beskrevet i en række tidsskriftsartikler, som er gengivet i bilagene. Artikel I og II omfatter undersøgelser af mikrostrukturer, elektrokemiske egenskaber og bakteriehæmmende effekter af sølv-palladium overflader. Desuden indgår en indledende diskussion af den eller de mekanismer, der ligger til grund for den bakteriehæmmende effekt. I artikel II indgår også en sammenligning af den bakteriehæmmende effekt ved Ag-holdigt ferritisk/austenittisk (duplex) rustfrit stål med den effekt fundet ved sølv-palladium overflader. I artikel III er fokus på hvorledes virkningsgraden af den biofilmhæmmende effekt udvikler sig, og heri indgår et studie af biofilmhæmning på sølv-palladium overflader under hhv. lav og høj koncentration af bakterier i flow-celle og batch opstillinger. I artikel IV er samlet undersøgelser af hvorledes tilsætning af sølv til austenittisk rustfrit stål af type 316 påvirker den bakteriehæmmende effekt, de mekaniske egenskaber og korrosionsbestandigheden af materialet. Der indgår tillige en diskussion af mulige mekanismer for afgivelse af sølv fra sølvholdige overflader. Artikel V omhandler hvorledes forøget sølvafgivelse kan foregå fra sølv-palladium overflader ved eksponering i specifikke miljøer.

De udførte forsøg har vist, at sølv-palladium overflader kan hæmme bakterier og biofilm ved at generere mikro-elektriske felter og elektrokemiske redox processer på overfladen. Forsøg med sølvholdigt rustfri stål har vist, at tilsætning af sølv til rustfri stål forbedrer materialet, da det får bakteriehæmmende egenskaber på grund af afgivelse af sølv i toksiske mængder tæt ved overfladen, men også at de mekaniske og korrosionsmæssige egenskaber kan forringes lidt i forhold til traditionelle rustfri stål. Bakterielle mikrokolonier kan dog opbygges, hvis de bakteriehæmmende overflader bliver dækket med et konditioneringslag af døde bakterier i kontakt med overfladen eller efter længere tids brug, hvorfor den bedste effekt af disse overflader vil kunne opnås under forhold, hvor passende rengøringsprocedurer kan anvendes.

Det er ikke overraskende, at kemiske stoffer, der er aggressive mod sølv og sølvforbindelser, kan accelerere sølvafgivelse fra overfladerne ved dannelse af sølvioner og sølvkomplexer. Men i dette arbejde er der fundet en direkte kobling mellem forøget sølvafgivelse og tilstedeværelsen af bakterier. Forsøgene viste, at bakterier, der befandt sig i tilknytning til overfladen, i høj grad forøgede sølvafgivelsen fra de sølvholdige overflader pga. vekselvirkninger mellem cellekomponenter og overfladerne, og at denne effekt blev forøget med stigende mængde bakterier ved overfladen. Selve tilstedeværelsen af bakterier kan således være en udløsende faktor for afgivelse af toksiske sølvioner, der kan give en bakteriel drabseffekt i medier, som ellers ikke forventes at være aggressive mod sølv.

# List of Publications (During the study at DTU)

1.  W. C. Chiang, W. C. Luu, and J. K. Wu: Effect of aluminum content on the passivation behavior of Fe-Al alloys in sulfuric acid solution. *Journal of Materials Science*, Vol. 41, No. 10, pp. 3041-3044, 2006.

2.  Y. F. Wu, W. C. Chiang, J. Chu, T. G. Nieh, Y. Kawamurad, and J.K. Wu: Corrosion resistance of amorphous and crystalline $Pd_{40}Ni_{40}P_{20}$ alloys in aqueous solutions. *Materials Letters*, Vol. 60, No. 19, pp. 2416-2418, 2006.

3.  Y. F. Wu, W. C. Chiang, and J. K. Wu: Effect of crystallization on corrosion behavior of $Fe_{40}Ni_{38}B_{18}Mo_4$ amorphous alloy in 3.5% sodium chloride solution. *Materials Letters*, Vol. 62, No. 10-11, pp. 1554-1556, 2008.

4.  W. C. Chiang, L. R. Hilbert, and P. Møller: Study of electroplated silver-palladium biofouling inhibiting coating. A conference paper presented at *14th Nordic Corrosion Congress*, Copenhagen, Denmark, May 2007.

5.  W. C. Chiang, L. R. Hilbert, T. Tolker-Nielsen, and P. Møller: Bacterial inhibiting surfaces caused by the effects of silver release and/or electrical field. A conference paper presented at *International Conference Biocorrosion of Materials*, Paris, France, June 2007.

6.  W. C. Chiang, L. R. Hilbert, C. B. Corfitzen, H. Albrechtsen, and P. Møller: Electrochemical properties and effects of new bacterial inhibiting surfaces in water. A conference paper presented at *European Corrosion Congress*, Freiburg im Breisgau, Germany, September 2007.

7.  W. C. Chiang, L. R. Hilbert, T. Tolker-Nielsen, and P. Møller: A new method to inhibit microbial and biofilm adhesion. A conference paper and a poster presented at *International Water Association Biofilm Technologies Conference*, Singapore, January 2008.

8.  <u>W. C. Chiang</u>, L. R. Hilbert, T. Tolker-Nielsen, and P. Møller: How can silver-palladium surfaces inhibit silver-resistant bacteria. A conference paper presented at *39th R3 Nordic Symposium*, Helsingør, Denmark, May 2008.

9.  <u>W. C. Chiang</u>, L. R. Hilbert, C. Schroll, T. Tolker-Nielsen, and P. Møller: Study of electroplated silver-palladium biofouling inhibiting coating. *Corrosion Engineering, Science and Technology*, Vol. 43, No. 2, pp. 142-148, 2008 **(included as Appendix I)**.

10. <u>W. C. Chiang</u>, L. R. Hilbert, C. Schroll, T. Tolker-Nielsen, and P. Møller: Bacterial inhibiting surfaces caused by the effects of silver release and/or electrical field. *Electrochimica Acta*, Vol. 54, No. 1, pp. 108-115, 2008 **(included as Appendix II)**.

11. <u>W. C. Chiang</u>, C. Schroll, L. R. Hilbert, P. Møller, and T. Tolker-Nielsen: Anti-biofilm properties of a silver-palladium surface. *Applied and Environmental Microbiology*, Vol. 75, No. 6, pp. 1674-1678, 2009 **(included as Appendix III)**.

12. <u>W. C. Chiang</u>, I. S. Tseng, P. Møller, L. R. Hilbert, T. Tolker-Nielsen, and J. K. Wu: Influence of silver additions to type 316 stainless steels on bacterial inhibition, mechanical properties, and corrosion resistance. *Materials Chemistry and Physics*, Vol. 119, No. 1, pp. 123-130, 2010 **(included as Appendix IV)**.

13. <u>W. C. Chiang</u>, L. R. Hilbert, C. Schroll, T. Tolker-Nielsen, and P. Møller: Influence of bacteria on silver dissolution from silver-palladium surfaces. A conference paper presented at *European Corrosion Congress*, Nice, France, September 2009. **(included as Appendix V)**.

# Paper Award



*Paper Award*

*on*

A new method to inhibit microbial and biofilm adhesions

*awarded to*

**Chiang Wen-Chi**

*at the*

## IWA Biofilm Technologies Conference

8-10 January 2008, Singapore

*Organised by*

Nanyang Technological University
National University of Singapore

**Dr Volodymyr Ivanov**
Chairman, Local Organising Committee

**Dr Ng How Yong**
Co-Chairman, Local Scientific Committee

# Contents

# 1. Introduction

## 1.1. Bacterial contamination in human life

Bacterial contamination is a major concern in many areas, such as food industries, water distributing systems, and hospitals, because they may harbor pathogens, causing hygienic risks or diseases in humans, and may also cause other adverse effects, such as causing microbially influenced corrosion of materials and reducing heat transfer [1-16]. An essential pre-requisite in hygienic-related areas is therefore to ensure that undesired bacterial adhesion and proliferation do not occur, or that these bacteria can be efficiently removed. However, the efficient removal of bacterial adhesion can sometimes be difficult. Some sites in food processing factories and water distributing systems, such as dead ends, joints, and bends in pipes, are vulnerable points where bacteria may well live because of difficult cleaning or disinfecting access [9,14,15]. In hospitals, all reusable devices, such as surgical instruments, theater tables, and kidney dishes, must be decontaminated between clinical uses and between patients. However, hospital-acquired infections can be transmitted via some inadequately decontaminated or re-contaminated devices. Patients in hospitals and people in general could also be infected via transient contacts with surfaces and objects that have been touched or used by someone carrying pathogenic bacteria, such as taps and door handles [5,6]. In the past few decades, studies on the transmission of infections have mostly focused on hospitals and schools, and only have paid little attention to the home. Recent studies have helped to give people a better understanding of the relationship between home hygiene and health. Studies have shown that areas in the home environment can serve as reservoirs for bacterial colonization, especially at some 'critical points', such as kitchen, where efficient rinsing is not feasible, and that bacterial contamination can be

widely spread via these specific areas [3,7,17].

## 1.2. Bacteria and biofilm

Biofilms (Fig. 1.1) are surface-associated bacterial communities that include cells of one or of many species. These bacterial communities are surrounded by the slime that bacteria produce, and may be attached to an inert or living surface. Bacteria in natural, industrial and clinical settings most often live in biofilms. It has been reported that when a clean material comes in contact with a non-sterile aquatic environment, the attachments of planktonic bacteria on surfaces will start and result in biofilm formation [4,11,18]. People are already familiar with biofilms in daily life, for examples, slippery film on river stones.
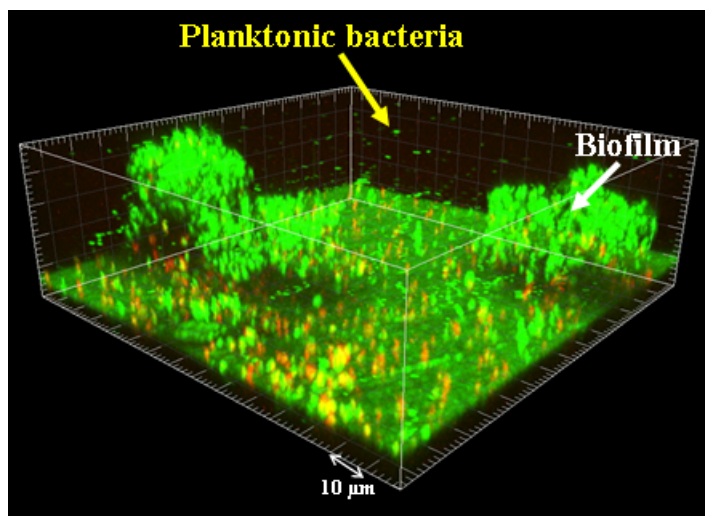


**Fig. 1.1.** Micrograph of biofilms.

Biofilm consists of approximately 10-25 % cells and 75-90 % extracellular polymeric substances (EPS), depending upon the bacterial species involved and environmental conditions. EPS is a chemically complex that surround the bacteria and constitute the biofilm matrix. The composition of EPS varies depending upon the bacterial species

and environmental conditions, but in general EPS contains polysaccharides, proteins, humic substances, and nucleic acids. Recent studies also indicate that some species of bacteria [4,11,18-20], such as *Pseudomonas aeruginosa* (*P. aeruginosa*), extracellular deoxyribonucleic acid (eDNA) is one of the major matrix components in biofilms.

In general, biofilm formation can be divided into 5 stages [4,18]:

1. Conditioning of the surface by adsorption of organic molecules.

2. Reversible attachment of pioneer planktonic bacteria to the surface.

3. Irreversible attachment by production of EPS which allow bacteria to become surface-associated (sessile) bacteria.

4. Growth of surface-associated bacteria, and maturation of the biofilm.

5. Release of bacteria from the biofilm.

The main benefits of the biofilm mode of growth to bacteria are nutrient capturing and the development of protection against antibacterial agents and cleaning, enabling bacteria to survive inside biofilm, and causing the release of new bacteria to surroundings [4,18]. Therefore, biofilm bacteria are more tolerant to cleaning, disinfecting operations, and antibiotic therapies than planktonic bacteria, making these treatments less effective or ineffective [2,4,9-13]. It has been reported that biofilm bacteria are resistant to antibacterial agents at levels 500 to 5000 times higher than those needed to kill planktonic bacteria of the same species [10]. It may raise some problems, such as environmental pollution, by using antibacterial agents at these high levels. Also for patients with biofilm-related infections, it becomes impossible to treat them safely.

In health care environment, it has been reported that more than 60 % of bacterial infections are caused by biofilms, including both device-related infections and non-device-related infections [21]. Infections caused by biofilms on medical implants can cause considerable problems because of requiring a longer period of antibiotic therapy and repeated surgical procedures, and currently the only effective method for curing implant-associated biofilm infections involves replacement of the implant [13,16].

On the other hand, in practice in water distributing systems and food industries, the number of planktonic bacteria is the index which is monitored and attempted minimized, while biofilm formations are rarely controlled [22]. The presence of biofilms may cause sudden increases in planktonic bacteria, and lead to serious problems of the hygienic management [4,22].

Previous study indicated that substrate material and surface topography have some effects on the rate of biofilm formation, but no direct biofilm inhibiting effect can be found in any simple substrate material [15]. It is of high priority to develop methods or chemical compounds for directly combating biofilms. Small molecules that may affect the bacteria and inhibit critical steps in biofilm formation, as well as different surface modifications that may inhibit biofilm formation are among the strategies that are actively pursued [23,24]. Different kinds of physical treatments have also been investigated as potential means of inhibiting bacteria and biofilm formation. For example, recent studies have shown that the efficacy of antibacterial agents against biofilm bacteria can be enhanced if these agents are given in combination with an

applied electric field [10,25-29]. However, in many areas, applying electric potential or current on a setting (requiring an external voltage, electrical contacts, etc.,) is not feasible, and the release of chemicals in high concentration is undesired.

## 1.2. Bacterial inhibition by silver-palladium surface

In view of these considerations, a silver-palladium (Ag-Pd) surface has been designed to form a bacteria inhibiting effect by generating micro-electric fields and electrochemical redox processes from the surface, and it is also desired that the release of chemicals from the surface is minimal. It is expected that this design can be applied on the surfaces of conducting materials, such as stainless steels, and non-conducting materials, such as ceramics and polymers, with conventional techniques. The purpose of this work during my Ph.D. study was to investigate the bacteria inhibiting mechanism and electrochemical properties of Ag-Pd surfaces, and examine their inhibiting effects. The main results of thermodynamic calculations, electrochemical tests, and antibacterial activities of Ag-Pd surfaces have been published (in appended papers I, II, III).

## 1.3. Bacterial inhibition by silver-bearing stainless steel

It is well-known that stainless steels, such as type 304, 316, and 430, have been widely used in areas where hygiene is a major requirement because of their good corrosion resistance and cleanability [14,15,30,31]. Hygienic quality is linked to cleanability of selected steels to ensure that bacterial contamination may not occur [15]. However, stainless steels themselves do not have indigenous bacteria inhibiting properties. However, stainless steels themselves do not have indigenous bacteria inhibiting properties. Different kinds of treatments, such as surface coatings [22,32,33]

and alloying modifications [34-37], have been studied as potential means of inhibiting bacteria on stainless steel surfaces. The inhibiting effects provided by surface coatings may deteriorate because of friction, processing, cleaning, or daily use. In view of these considerations, it was decided to investigate the method of alloying modification to improve their bacteria inhibiting properties by using Ag addition to type 316 stainless steels. The main results of bacterial inhibition (in appended papers II and IV), corrosion resistance, and mechanical properties of the Ag-bearing stainless steels, and the mechanism of Ag dissolution from these steel surfaces have been published (in appendix paper IV).

## 1.4. Microbiologically influenced silver dissolution

Metal dissolution is sometimes recognized as a result of corrosion or deterioration in materials [38]. This phenomenon is undesired and will reduce the lifetime of materials and contaminate the surroundings. It has been recently reported that metallic gold (Au) on medical implants can be dissolved by cells, which is called ''dissolucytosis'' [39,40]. These studies demonstrated that whenever metallic Au surfaces are attacked by membrane-bound dissolucytosis, Au ions are dissolved by surrounding cells or cells growth on metallic Au surfaces. These observations indicated that even indigestible noble metals can experience the phenomenon of microbiologically influenced dissolution. For bacteria inhibiting Ag-Pd surfaces, it is desired that the release of any metal will be at low concentration. However, the phenomenon of undesired metal dissolution from the Ag-Pd surface could happen under a bacterial condition. In this work, the correlation between solution contents, and bacteria, and metal dissolution of Ag-Pd surfaces was investigated, with the prospect of decreasing the risk of contamination to a surrounding environment due to metal dissolution. The

mechanism of metal dissolution behind the effect is also discussed based on thermodynamic considerations and experiments carried out in this work. The main results and discussions of this work are described in appended paper V.

# 2. Bioelectric effect

As mentioned in chapter 1, the concentrations of antibacterial agents needed for killing biofilm bacteria can be much higher than those for killing planktonic bacteria. Recent studies have showed that the efficacies of some antibacterial agents against biofilm bacteria can be enhanced if these agents are given in combination with an applied electric current field on a setting. This phenomenon of electric enhancement of biofilm bacteria killing during the application of antibacterial agents is so called "bioelectric effect" [10], and some studies [10,25-29] have shown that the concentrations of antibacterial agents needed for killing biofilm bacteria can be reduced to levels very close to those needed for killing planktonic bacteria of the same species. These studies have also showed that the bioelectric effect alone does not influence biofilm bacteria killing. Most of the studies about this phenomenon are focused on medical applications. This technique may also have potential to be applied in industries to increase effectiveness of disinfecting operations against biofilms. However, the application in industries may be limited on or near conductive surfaces [26].

Although many studies have provided evidences in support of the electric enhancement of biofilm bacteria killing, the real mechanisms of this phenomenon are unknown. The mechanisms of bioelectric effect may be related to the transportation of antibacterial agents into biofilms by an electrophoretic process, local changes in pH, and the generation of additional inhibiting ions and oxygen ($O_2$). An applied electric field may behave as a pumping system and increase the mass transport of antibacterial agents into biofilms. Local changes in pH (changing acidic and basic conditions) may increase the effectiveness of antibacterial agents against biofilm bacteria [10,25-29].

The electrolytic $O_2$ generation, which can potentially increase the local $O_2$ concentration in biofilms, may also explain the electric enhancement of antibacterial efficiency. It has been hypothesized that the bioelectric effect results from increased metabolic and replicative activity associated with increased $O_2$ tensions within the biofilm bacteria which make them more susceptible to antibacterial agents. It is well established that antibacterial agents are much more effective against rapidly metabolizing and dividing bacteria than they are to metabolically quiescent bacteria, and one of the limiting nutrients within the core of the biofilm is $O_2$. It has been shown that the provision of $O_2$ deep within the biofilm results in greatly increased metabolism [28].

The bioelectric effect also has the effect that the membranes of bacteria become more permeable in the presence of an applied electrical field. In some practical applications of the researches of molecular biology, this bioelectric effect is well-known for the practice of electroporation. The effect of electroporation is theoretically explained as a process that introduces very small openings (pores) in the cell membrane, which increase the permeability. Here an electrical field is applied as a technique and an effective way of introducing different substances inside a cell, such as drugs or as sophisticated as a piece of coding DNA [22].

# 3. Silver-palladium surface

In this project, the biofilm inhibiting properties of a silver-palladium (Ag-Pd) surface were investigated. The results of thermodynamic calculations, electrochemical tests, and antibacterial activity have been published (appended papers I, II, and III). The bacteria inhibiting mechanisms of Ag-Pd surface is summarized as follows:

## 3.1. Bacterial inhibition by micro-electric field

This design is based on Ag coatings applied to stainless steels (or ceramic and polymers) that can be micro/ nano-structured by a treatment with Pd. In this way, a Ag-Pd surface can form an electrical field on the surface by itself. Due to the potential difference between Ag and Pd while contacting with an electrolyte, the surface can form numerous discrete anodic and cathodic areas. It is desired that when live bacteria pass or approach the electrical field between the anode and cathode, they will be inhibited in growth (Fig. 3.1). In order to ensure a high local strength of electrical field, the surface should be micro or nano structured. The characterization of this structure is that one of electrodes is appropriately distributed in small discrete areas, either as micro-clusters upon the surface or as micro-holes within the surface. The distance between two adjacent electrodes should be preferably small because potential difference over a short distance can give a high field strength (100 mV $\mu$m$^{-1}$ = 100 V mm$^{-1}$). This inhibiting reaction is in popular terms referred to as the "electric chair effect". In this design, it is desired that the release of chemicals from the surface is minimal and that the materials are corrosion resistant.
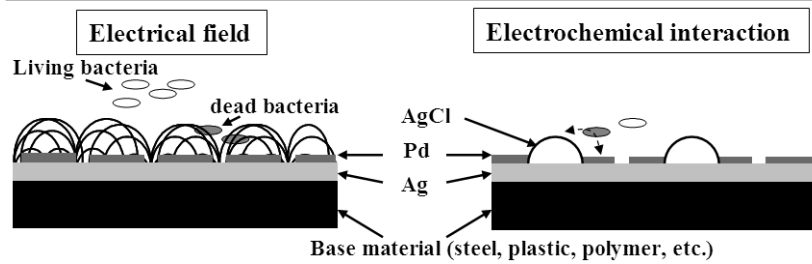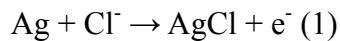
**Fig. 3.1.** Ag-Pd surface and its desired bacterial inhibiting methods.

## 3.2. Bacterial inhibition by electrochemical interactions (redox)

When Ag immerses in a chloride-containing solution, anodic polarization of Ag will immediately form an adherent AgCl layer on surfaces, according to the reaction below:

$$Ag + Cl^- \rightarrow AgCl + e^- \quad (1)$$

The reaction can convert Ag to low soluble AgCl on surfaces. Ag ions release from the surface is insignificant because of the low solubility product of AgCl ($1.8 \times 10^{-10}$) [41] even at potentials over the equilibrium potential for the reaction. In drinking water, AgCl will be in equilibrium with only 2 μg l$^{-1}$ Ag$^+$ at 10 °C.

According to the Pourbaix diagram in Fig. 3.2, at pH=7, there is a potential difference of 200 mV between Pd and Ag, and AgCl can easily and stably be formed even in water with low Cl$^-$ concentration of 50 mg l$^{-1}$ (typical Cl$^-$ concentration in Danish drinking water). This can explain the formation of AgCl, even in water with low Cl$^-$ concentration, if Ag is coupled to Pd.
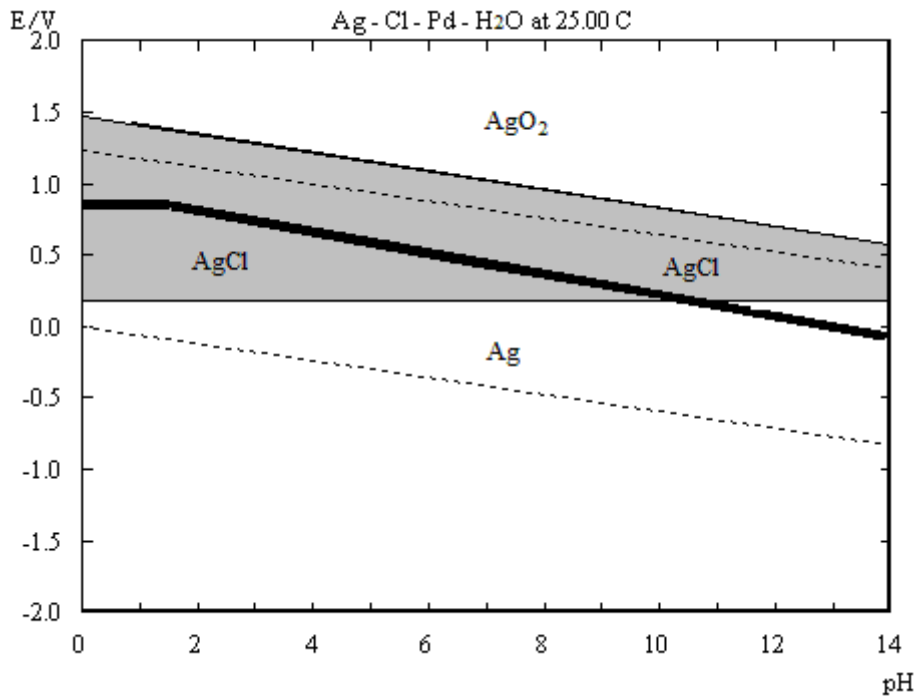
**Fig. 3.2.** Pourbaix diagram of Ag-Cl-Pd-H$_2$O system. It was calculated from Cl$^-$ concentration of $1.4 \times 10^{-3}$ M (50 mg l$^{-1}$) and the metal ions concentration of $10^{-6}$ M. The diagram was superimposed by the immune area of Pd (the area below the bold line).

It has been reported that AgCl can be reduced to Ag by oxidation of hydroxyl groups in organic compounds [42], which means that organic species, such as bacteria, can interact in an oxidation process with AgCl. These reactions are in good agreement with thermodynamic calculations where ethanol or reducing sugars (such as fructose and glucose) are used for the verifications [22]. Thus, bacterial metabolisms can be inhibited (Fig. 3.1) through the reaction as follows:

AgCl + live bacteria → Ag + Cl$^-$ + dead bacteria (2)

After the oxidation process of the organic species, AgCl can only be regenerated in the presence of oxygen (aerobic condition), where Ag is easily oxidized in connection

to the reduction of oxygen on the Pd cathode, if the Ag is coupled to Pd.

Anodic partial reaction: $4Ag + 4Cl^- \rightarrow 4AgCl + 4e^-$ (3)

Cathodic partial reaction: $2H_2O + O_2 + 4e^- \rightarrow 4OH^-$ (4)

Organic species, such as bacteria, can be oxidized on the Ag surface with an accompanying reduction of oxygen or other species on the Pd surface [41]. These reactions simply demonstrate the reactions of Ag converting to AgCl and AgCl converting to Ag back and forth, which can continuously happen if hydroxyl groups in organic compounds, such as bacteria, are supplied to the surface. This reaction can also be regarded as a micro or nano fuel cell system.

The microstructure of the Ag-Pd surface (Fig. 3.3) has been described in appended papers I and II. Pd was incompletely deposited as a microhole-structured layer upon Ag. Ag was partially exposed through these microholes. In these microholes, some Ag can react to form silver chloride (AgCl) during Pd deposition. The calculated reaction of AgCl formation at room temperature during Pd deposition is as follows [43-45]:
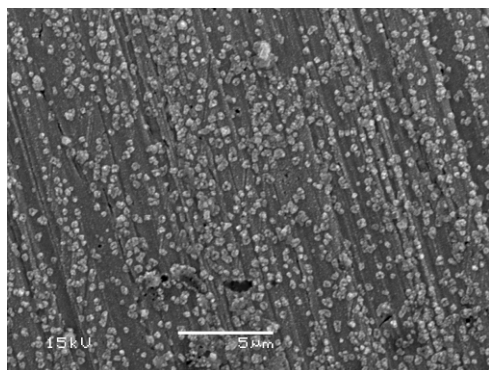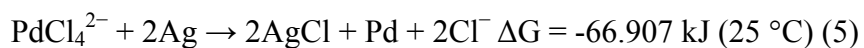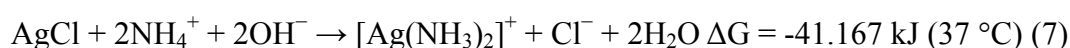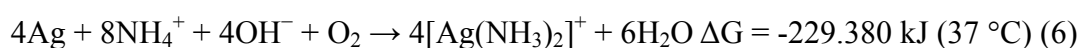
$PdCl_4^{2-} + 2Ag \rightarrow 2AgCl + Pd + 2Cl^-$ $\Delta G$ = -66.907 kJ (25 °C) (5)



**Fig. 3.3.** Micrograph of Ag-Pd surface (White particles are AgCl).

## 3.3. Silver dissolution from silver-palladium surfaces

The stability and acceptable lifetime of Ag-containing surfaces must be considered, if the bioelectric effect is to be active. Furthermore the release of silver from the surface is desired to be as low as possible to minimize environmental impact.

If $NH_4^+$ is present in the media, the process of increased Ag dissolution can occur by Ag complex (diamminesilver ion) formations. The calculated reactions are as follows [46,47]:

$$4Ag + 8NH_4^+ + 4OH^- + O_2 \rightarrow 4[Ag(NH_3)_2]^+ + 6H_2O \ \Delta G = -229.380 \text{ kJ } (37 \text{ °C}) \ (6)$$

$$AgCl + 2NH_4^+ + 2OH^- \rightarrow [Ag(NH_3)_2]^+ + Cl^- + 2H_2O \ \Delta G = -41.167 \text{ kJ } (37 \text{ °C}) \ (7)$$

Since the Gibbs free energy ($\Delta G$) for these reactions is negative, these calculated reactions are thermodynamically favorable.

The influence of surface-associated bacteria on the increased rate of Ag dissolution can be explained by the interactions between cell components and Ag-Pd surface. It is well-known that Ag can react with amino acids ($H_2NCHRCOOH$, where R is an organic substituent) or amino groups ($-NH_2$) of membranes or enzymes inside bacteria, [48-50]. When surface-associated bacteria were present, these above reactions can lead to increased rate of Ag dissolution from the surface by Ag complex formations.
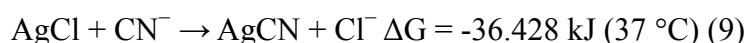
On the other hand, in some specific environments (not above-mentioned test conditions), a number of bacterial species, e.g. *Escherichia coli* (*E. coli*), can perform

respiratory reduction of nitrate ($NO_3^-$) to nitrite ($NO_2^-$) and of nitrite to ammonia ($NH_3$) under an anaerobic condition [51,52]. If Ag-Pd surfaces are applied in these environments, these $NH_3$ or $NH_4^+$ ions can cause Ag and AgCl to form Ag complexes (Eq. 6 and Eq. 7). It also has been reported that microbial cyanide biosynthesis, so called microbial cyanogenesis, can occur in some species of bacteria, e.g. *Pseudomonas aeruginosa* (*P. aeruginosa*) [53,54]. Cyanide produced by bacteria or already presented in an environment can cause Ag and AgCl to form Ag complexes (dicyanoargentate ion). For Ag dissolution, the calculated reaction is as follows [55,56]:

$$4Ag + 8CN^- + O_2 + 4H^+ \rightarrow 4[Ag(CN)_2]^- + 2H_2O \quad \Delta G = \text{-626.809 kJ (37 °C) (8)}$$
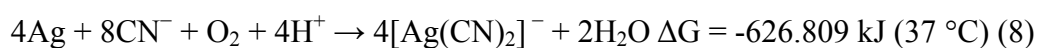
For AgCl dissolution, a series of reactions can occur, and these calculated reactions are as follows [44,46]:

$$AgCl + CN^- \rightarrow AgCN + Cl^- \quad \Delta G = \text{-36.428 kJ (37 °C) (9)}$$

$$AgCN + CN^- \rightarrow AgCN^{2-} \quad \Delta G = \text{-23.375 kJ (37 °C) (10)}$$

Since the Gibbs free energy ($\Delta G$) for these reactions is negative, these calculated reactions are thermodynamically favorable.

This study indicated that it is important to select applicative environments to avoid the degradation of Ag-Pd surfaces. In some specific environments, an undesired increased Ag dissolution can occur and add to the bacteria inhibiting effect when chemicals aggressive to Ag and AgCl, such as $NH_4^+$ ions, are present. Surface-associated

bacteria can increase Ag dissolution from Ag-Pd surfaces due to the interactions between cell components and the surfaces, and the amount of surface-associated bacteria can improve this effect.

# 4. Silver as an antibacterial agent

Ag has been used for bacterial inhibition for 2500 years [57]. Ag is a metallic element well-known for inhibiting bacterial activities. Therefore, Ag and its compounds have been introduced into many commercial products to obtain bacteria inhibiting effects, and are considered to have a potential to reduce the risk of infection in many investigations in recent years [48,57-60]. It also has been suggested that Ag can be used as a potential surface for certain hospital and healthcare applications, especially in the areas where problems of hospital-acquired infections are seen [48,60]. Furthermore, from the hygienic point of view, Ag has lower toxicity to human cells and tissues as compared with other metal, such as Cu [58].

Metallic state of Ag is inert but it can react with some specific surrounding environment and become ionized Ag. The antibacterial activity of Ag is related to the amount of Ag release. The detailed mechanism of bacterial inhibition of Ag is still unknown but the possible mechanisms have been suggested [61]. Ag ions are highly reactive inside bacteria, and can react with amino acid residues in proteins, and can attach to the amino, sulphydryl, imidazole, phosphate and carboxyl groups of membrane or enzyme proteins which can lead to protein denaturation. Ag ions can also inhibit the oxidative enzymes and respiratory process of bacteria, which can cause metabolite efflux and inhibit bacterial replication. Ag can also bind to the surface of bacterial cell wall and membrane, which can damage the membrane function and cause cell distortion [49,61]. Clement and Jarrett suggested that Ag binds to bacterial surface and damages to membrane function are the most important mechanisms for inhibiting bacteria [58].

# 5. Silver-bearing stainless steel

Although there is no known official classification of food grade stainless steels, type 316 stainless steel is often referred to as the food grade. Type 316 stainless steel is also one of the most commonly used medical grade materials [31]. In view of these considerations, we decided to investigate the effect of Ag addition to type 316 stainless steels in bacterial inhibition. If effective, these Ag-bearing 316 stainless steels could substitute commonly commercial stainless steels in areas where hygiene is a major requirement. In this study, austenitic Ag-bearing 316 stainless steels were prepared, and influence of Ag addition on their bacterial inhibition, corrosion resistance, and mechanical properties were investigated.

Some studies have shown that Ag has extremely low solubility in steel and precipitates as small particles [62-63]. Therefore, the Ag-bearing 316 steel can be regarded as a two-phase alloy (Ag and austenitic phases).

When pure Ag is in contact with normal drinking water, it can be thermodynamically calculated that there is equilibrium with 2 $\mu$gl$^{-1}$ Ag$^{+}$ at 10 °C to 33 $\mu$gl$^{-1}$ Ag$^{+}$ at 40 °C (calculated from average Cl$^{-}$ concentration of 70 mgl$^{-1}$ in Lyngby, Denmark). However, when chemical compounds aggressive to Ag are present in an environment, such as ammonium (NH$_4^{+}$) and cyanide (CN$^{-}$) ions, as well as the galvanic effect of Ag and 316 austenitic matrix, the process of increased Ag dissolution can occur by Ag complex formations. These Ag complexes can be effective and have a wide spectrum of bacterial inhibition [50]. The proposed mechanisms are visualized in Fig 5.1. As shown in Fig. 5.1 (a), the Ag-bearing 316 surface releases small amounts of Ag ions in bacteria-free solution, but in general this content should not cause any or only a slight

inhibiting effect because of low Ag concentration. In Fig. 5.1 (b), when bacteria are present and produce some chemical compounds through their metabolism, the effect of increased Ag dissolution can occur and furthermore improve the bacterial inhibition of the Ag-bearing 316 surfaces. The detailed discussions of these reactions can be found in Chapter 3.3 and appendix paper IV.

As shown in the mechanism in Fig. 5.1 (c), when bacteria attach to Ag particles on a Ag-bearing 316 surface, they are killed because of interactions with chemical groups inside cells, and furthermore increase Ag dissolution, which can enhance the bacterial inhibition.
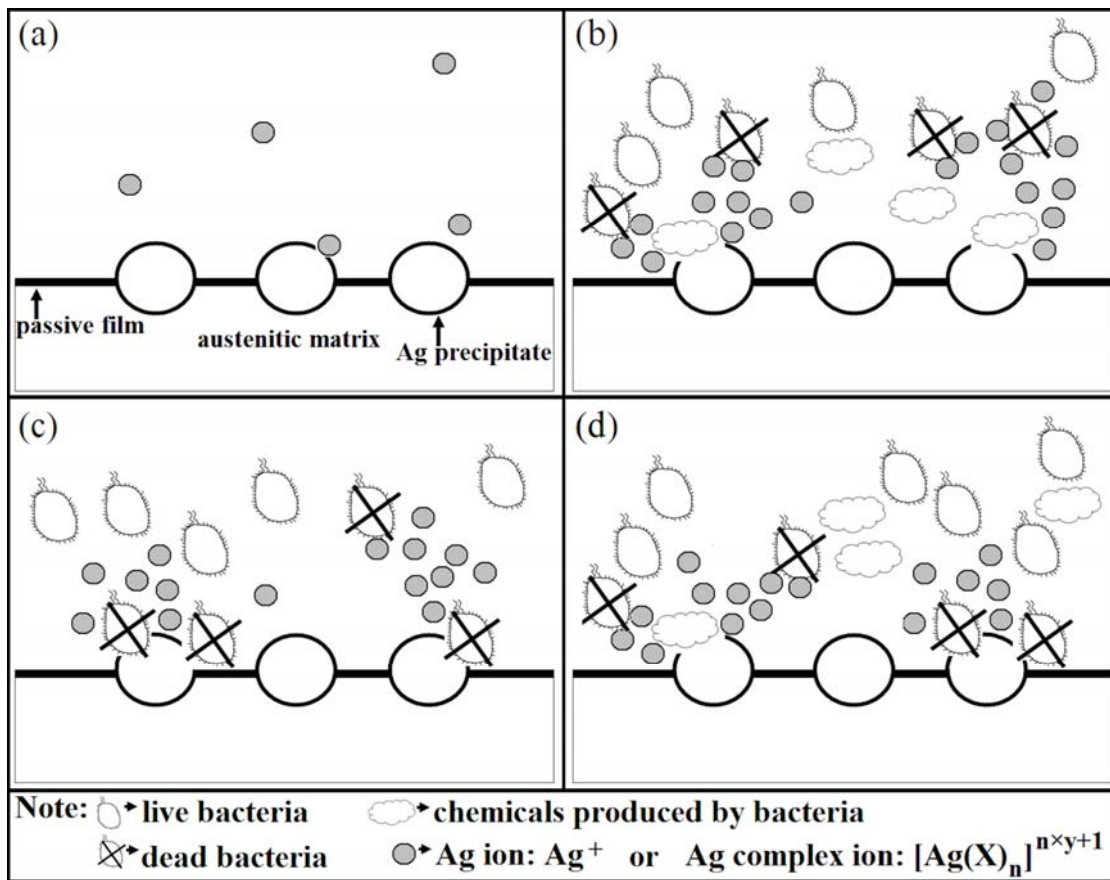
**Fig. 5.1.** Schematic illustrations of possible mechanisms of Ag dissolution from Ag-bearing 316 surfaces. (a) Mechanism 1: bacteria are not present, and the surface releases small amount of Ag ions. (b) Mechanism 2: bacteria are present, and chemicals produced by bacteria increase Ag dissolution. (c) Mechanism 3: bacteria are present, attach to the surface, and increase Ag dissolution because of the interactions with chemical groups inside bacteria cells. (d) Mechanism 2 + 3. (Ag complex ions $[Ag(X)n]^{n \times y+1}$, where X is $NH_3$, $CN^-$, etc., and y is the charge of X)

# 6. Experimental methods

The experimental methods used in the appended papers I-V are described in this chapter. All the results shown in this thesis are representative of three independent experiments at least.

## 6.1. Ag-Pd surface

### 6.1.1 Surface preparation

In order to obtain desired surface structures, the Ag surface was treated by the immersion plating in palladium chloride solution at ambient temperature. The palladium chloride solution was prepared from 5 vol. % of the stock solution which is prepared from 0.5 $gl^{-1}$ $PdCl_2$ and 4 $gl^{-1}$ NaCl dissolved in water. The surfaces were immersed for a few minutes. The reaction of this plating is as follows:
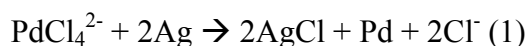
$$PdCl_4^{2-} + 2Ag \rightarrow 2AgCl + Pd + 2Cl^- \quad (1)$$

A JEOL 5900 scanning electron microscope (SEM) equipped with an INCA 400 energy dispersive X-ray (EDX) system were applied to characterize the appearance and compositions of the surfaces.

### 6.1.2. Galvanic current measurement

The purpose of this test was to investigate whether the coupling of Ag and Pd, and Ag and 316 stainless steel electrodes, can electrochemically oxidize organic compounds or not. Therefore, the couplings were tested to measure the faradaic current introduced by the addition of organic compounds to simulate bacteria in an electrolyte. The electrodes were connected through a zero resistance ammeter (ZRA). The area ratio

was about 2.5: 1 for Ag to Pd, and was about 1:1 for Ag to 316. These tests used 1 M sodium acetate pH 7 containing 3.0 wt. % NaCl solutions, and were carried out in a cell with 400 ml volumes, stirred with oxygen (purity$\geq$ 99.99%) at ambient temperature. After stabilization of the measured current, 0.04 moles of paraformaldehyde (HCHO) to simulate bacteria or organic species were added. If HCHO can be oxidized on the surfaces of electrodes, an increased faradaic current will be measured.

### 6.1.3. Potentiodynamic polarization and chronoamperometric tests

Cylindrical Ag samples were treated in palladium chloride solution to obtain Ag-Pd surface. The tests were carried out in a typical three-electrode cell with 400 ml volumes, with platinum (Pt) as a counter electrode and a saturated calomel electrode (SCE) as a reference electrode. The exposed area of the working electrode was 3.98 cm$^2$. 1 M sodium acetate buffer pH 7 containing 250 mgl$^{-1}$ Cl$^-$ solution and ABTG medium (the detailed compositions are listed in appendix paper I) were used, and stirred with oxygen (purity$\geq$ 99.99%) during the tests at ambient temperature. Before potentiodynamic polarization, all samples were equilibrated for 1 hour to obtain an open-circuit potential. The curves were recorded at a scan rate of 0.5 mVsec$^{-1}$ from the initial potential of -250 mV versus open-circuit potential to the final potential of 900 mV versus SCE.

In the chronoamperometric test, the applied overpotential of 5 mV was referred to the open-circuit potential. 1 M sodium acetate buffer pH 7 containing 250 mgl$^{-1}$ Cl$^-$ solution and ABTG medium were used, and stirred with oxygen (purity$\geq$ 99.99%) during the tests at ambient temperature. Before tests, all samples were equilibrated for

1 hour to obtain an open-circuit potential. After the tests, Ag ion concentration in the solutions was analyzed by inductively coupled plasma optical emission spectrometry (ICP-OES).

### 6.1.4. Analysis of Ag concentration in solutions

After the microbiological investigations, the spent bacterial ABTG media taken from the tests of Ag, CF-3M-Ag, and Ag-Pd were diluted, acidified (nitric acid), and then boiled on a heating plate to make a clear solution for Ag concentration analyses. Total Ag in media were analyzed by a JOBIN YVON JY38S inductively coupled plasma optical emission spectrometry (ICP-OES) and a PERKIN ELMER SIMA 6000 graphite furnace atomic absorption spectrometry (GFAAS).

### 6.1.5. Microbiological investigations

**Bacteria and growth conditions:** *Escherichia coli* J53 [64] and *E. coli* J53[pMG101] [65] were used as the silver sensitive and silver resistant model organisms in this study. Batch cultivation of *E. coli* was carried out at 37°C in AB minimal medium (the detailed information is listed in appendix paper III) supplemented with glucose (6.25 g/l), methionine (25 mg/l), proline (25 mg/l), and thiamin (2.5 mg/l). Flow-chamber cultivation of *E. coli* was carried out at 37°C in FAB medium (the detailed information is listed in appendix paper III) supplemented with glucose (0.125 g/l), methionine (2 mg/l), proline (2 mg/l), and thiamin (0.2 mg/l).

**Coupon preparation:** To obtain Ag-Pd coupons, Ag (99.9% Ag) plates were treated by an immersion plating in palladium chloride solution, which was prepared from 0.5 g l$^{-1}$ PdCl$_2$ and 4 g l$^{-1}$ NaCl dissolved in water. The coupons of stainless steel grade

AISI 316L (approximately 68.7% Fe, 16.9% Cr, 10.16% Ni, and 2.02% Mo) and Ag (99.9% Ag) were used as controls. The sizes of the coupons of Ag-Pd, steel, and Ag were 4 mm × 7 mm × 0.5 mm (for batch assays), and 2 mm × 14 mm × 0.5 mm (for flow-chamber assays).

**Cultivation of biofilms in batch assays:** The batch assays (Fig. 6.1) for biofilm cultivation were performed in multiwell dishes. Each coupon was placed in a well of a multiwell dish, 5 ml 100-fold diluted *E. coli* overnight cultures were transferred to each well, and the multiwell plates were incubated at 37 °C with shaking at 20 rpm for 72 hours. For the determination of colony forming units in the 72-hour-old multiwell cultures, serial dilutions of cell suspensions were plated on LB (the detailed information is listed in appendix paper III) agar plates, and colonies were counted after 30 hours incubation at 37 °C.
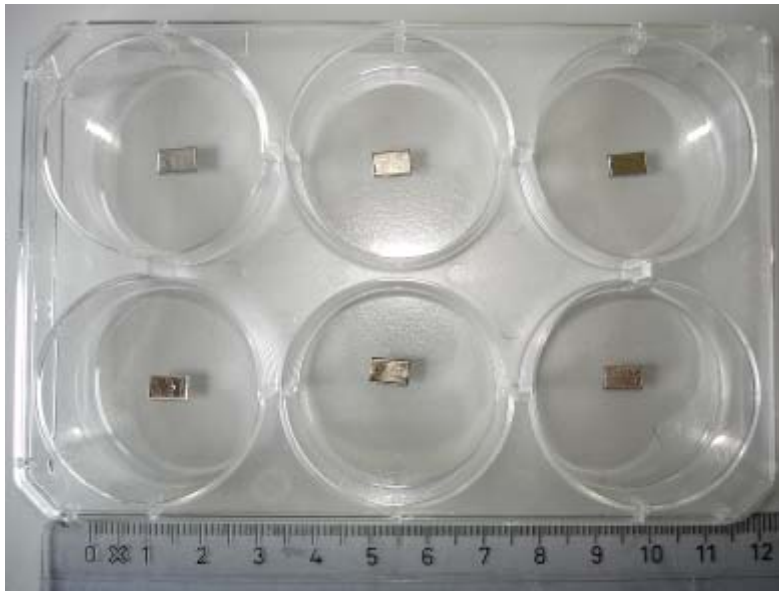


Fig. 6.1. A photograph of a 6-well multi dish with a coupon of dimension 4x7 mm in each well.

**Cultivation of biofilms in continuous flow-chamber assays:** The flow-chamber systems (Fig. 6.2) for biofilm cultivation were assembled and prepared as described previously (66). Each coupon was installed in a flow-chamber that was subsequently inoculated by injecting 250 µl 100-fold diluted *E. coli* overnight culture using a small syringe. After inoculation, adhesion of cells to the coupon surfaces was allowed for 1 hour without flow, and afterwards FAB medium was started to flow through the chambers at a mean flow velocity of 0.2 mm/s, corresponding to laminar flow with a Reynolds number of 0.02, using a Watson Marlow 205S peristaltic pump at 37 °C for 72 hours.
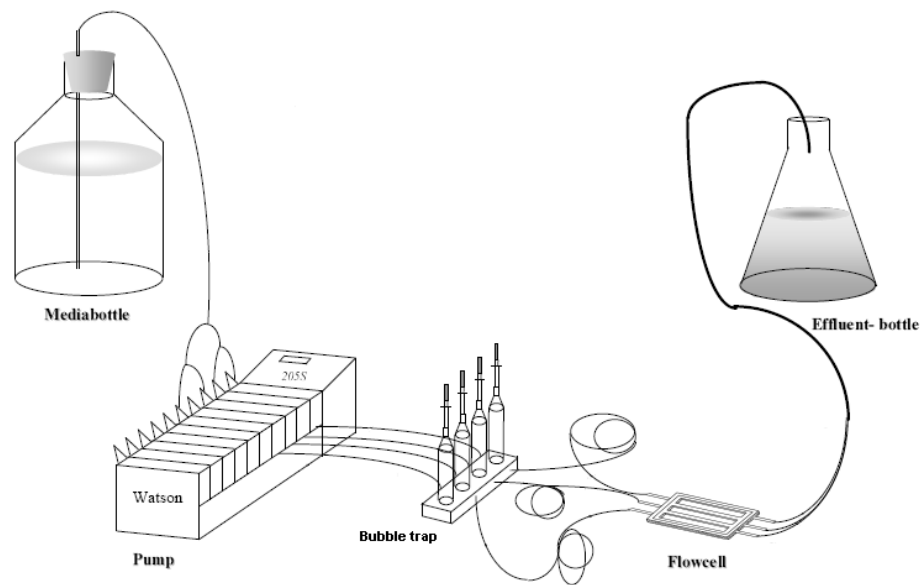


Fig. 6.2. The set-up of continuous flow-chamber assays. The flow direction is from the media bottle, through the pump, the bubble trap and the flowcell, and finally into the effluent-bottle. The tested coupons are in the flowcells [66].

**Microscopy and image acquisition:** Biofilms on the coupon surfaces were observed by the use of a ZEISS LSM 510 META confocal laser scanning microscope (CLSM), and staining with the LIVE/DEAD BacLight Bacterial Viability Assay (Molecular

Probes, Eugene, Oregon, USA), which utilizes the green fluorescent SYTO 9 (Molecular Probes, USA) for staining of live cells (5 μM and for batch-grown biofilms, and 5 μM for flow-chamber-grown biofilms), and the red fluorescent propidium iodide (Sigma, Germany) for staining of dead cells (40 μM for batch-grown biofilms, and 20 μM for flow-chamber-grown biofilms). Simulated 3-D images were generated by the use of IMARIS software (Bitplane, Switzerland).

## 6.2. Ag-bearing stainless steel

### 6.2.1. Steel preparation

Ingots with nominal compositions 316 stainless steel, containing 0, 0.03, and 0.09 wt. % Ag respectively, were prepared by repeated melting in a vacuum induction melting (VIM) furnace, and then drop casting to form ingots. The cast ingots, with 6.5 cm diameter and 15 cm height, were forged at 1150 ∘C to reduce their thickness from 15 to 5 cm, and followed by solution treatment at 1050 ∘C for 5 min. The treated steel samples were prepared for the investigations of microstructure, mechanical properties, corrosion resistance, and bacterial inhibition. As-received pure Ag (99.9 % Ag) plates and type 304 stainless steels were also prepared to use as comparisons for the investigations of properties of bacterial inhibition and corrosion resistance respectively. The chemical analysis compositions for the investigated steels were determined by an SPECTRO X-LAB 2000 X-ray fluorescence spectroscopy (XRF) and a PERKIN ELMER AAnalyst 300 flame atomic absorption spectroscopy (FAAS) (for Ag analysis). A Jeol 5900 scanning electron microscope (SEM) equipped with an INCA 400 energy dispersive X-ray (EDX) system were applied to microstructural investigations. Aqua regia solution (1 $HNO_3$:3 HCl) was used to etch the samples for 10 s before microstructural investigations.

**6.2.2. Mechanical properties**

The effect of Ag addition of type 316 stainless steel on mechanical properties was studied by tensile and hardness tests. The tensile samples with gauge dimensions of 3.2 cm × 0.4 cm × 0.5 cm (thickness) were prepared by electrical discharge machine (EDM), and then polished with SiC paper to a final grit size of 1000. Tensile tests were performed at room temperature in a MTS 810 tensile machine at a strain rate of $10^{-2}$ $s^{-1}$. After tensile tests, the fracture surfaces were examined by SEM. The hardness tests were performed by using a Vickers hardness testing machine using 1 kg load.

**6.2.3. Corrosion properties**

The effect of Ag addition of type 316 stainless steel on corrosion properties was studied by electrochemical polarization tests. As-received type 304 stainless steels were also prepared to use as comparisons for corrosion resistance because 304 steels are also widely used in many areas where hygiene is a major requirement. For materials with active-passive properties, such as stainless steels, pitting potential measurements are used for ranking the aggressiveness of different media or the corrosion resistance of different alloys in specific solution. A Gill ACM Instrument potentiostat was used for potentiodynamic polarization tests. All samples were polished with SiC paper to a final grit size of 1000 before tests. The tests were performed in a typical three-electrode cell setup with platinum (Pt) as a counter electrode and a saturated calomel electrode (SCE) as a reference electrode. The exposed area of the working electrode was 1.25 $cm^2$. 1 M sodium acetate buffer pH 7 containing 3.5 wt. % NaCl solution was used. The experiments were performed under nitrogen gas purging during the tests at room temperature. The polarization curves

were recorded at a scan rate of 0.5 mVsec$^{-1}$ from the initial potential of -0.4 V versus open-circuit potential, which was recorded after 1.5 hours immersion before tests, to the final current density of 1 mAcm$^{-2}$. In this paper, all potentials were reported with respect to saturated hydrogen electrode (SHE). Pitting potential was defined as the potential at which current density exceeded $10^{-2}$ mAcm$^{-2}$ [15].

### 6.2.4. Determination of bacterial inhibiting effect

The purpose of this test was to determinate the bacterial inhibiting effect of Ag-bearing 316 in comparison with 316 and pure Ag in a bacteria-contaminated environment. The test was performed by using bacteria-containing solutions (suspensions) held in close contact with test surfaces. 316, 316-0.03Ag, 316-0.09Ag, and pure Ag were used as test samples with dimensions 5 cm × 5 cm × 0.05 cm (thickness), and were polished with SiC paper to a final grit size of 1000 before tests. *Escherichia coli* (*E. coli*) BCRC11634 were used as test organisms in this study. *E. coli* are commonly used as indicator microorganisms of an environmental monitoring parameter in many areas where hygiene is a requirement [67]. Cultivation of *E. coli* was carried out at 37 °C in nutrient broth solution, and the initial bacterial concentration was approximately $10^5$ CFU ml$^{-1}$. 0.4 ml of this nutrient broth solution inoculated with *E. coli* was then dripped and spread on each sample in order to obtain a contaminated surface (Fig. 6.3).



Fig. 6.3. Experimental set-up of bacterial inhibiting test.

Each inoculated sample was covered by a sterilized polyethylene film (4 cm × 4 cm) to hold in close contact, and then incubated for 24 hours at 37 °C. After 24-hour incubation, each test surface was rinsed by 10 ml of SCDLP (soybean-casein digest broth with lecithin and polysorbate) solution for counting the numbers of live bacteria on each surface. Then, for the determination of bacterial inhibiting effect, collected SCDLP solutions were used for plating serial dilutions on agar plates to count the colony numbers of live *E. coli* (CFU cm$^{-2}$), and to calculate the bacterial inhibiting rate of each sample. The inhibiting rate can be calculated from:

$$\text{Inhibiting rate (\%)} = \frac{\text{CFU}_{\text{Ag-free sample}} - \text{CFU}_{\text{Ag-bearing sample}}}{\text{CFU}_{\text{Ag-free smaple}}} \quad (2)$$

### 6.2.5. Analysis of Ag concentration in solutions

The determinations of Ag release from Ag-bearing surfaces in bacteria-containing and bacteria-free solutions were performed by immersion tests. Ag-bearing 316 and pure Ag were used as test samples with dimensions 2 m × 2 m × 0.05 cm (thickness), and were polished with SiC paper to a final grit size of 1000 before tests. *E. coli* were used as test organisms in this study. Cultivation of *E. coli* was carried out at 37 °C in nutrient broth solution, and the initial bacterial concentration was approximately $10^5$ CFU ml$^{-1}$. Test Samples were placed into 15 ml bacterial and bacterial-free nutrient broth solutions respectively. After 24-hour immersion tests, the solutions were collected for Ag analyses. Total Ag determinations were analyzed by a Perkin Elmer SCIEX ELAN 5000 inductively coupled plasma-mass spectrometer (ICP-MS). Before ICP-MS analysis, a microwave-assisted digestion in acidic solution (1 HNO$_3$:1 test

solution) was performed.

**6.2.6. Observation of bacterial activities associated with surfaces in solutions**

he purpose of this study is to use microscopic techniques to directly observe bacterial activities associated with the sample surfaces in solutions, and furthermore study the inhibiting mechanism. *E. coli* were used as test organisms in this study. Cultivation of *E. coli* was carried out at 37 °C in ABTG solution, and the initial bacterial concentration was approximately $10^6$ CFU $ml^{-1}$ (colony forming units). 316, Ag-bearing 316, and pure Ag were used as test samples with dimensions 0.7 cm × 0.4 cm × 0.05 cm (thickness), and were polished with SiC paper to a final grit size of 1000 before tests. Samples of 316 and pure Ag were included as controls along with Ag-bearing 316. Each sample was placed in a dish, 5 ml ABTG solution inoculated with *E. coli* were transferred to each dish, and the dishes were incubated at 37 °C with shaking at 60 rpm for 24 hours.

After 24-hour incubation, the bacterial activities on surfaces in solution were observed by a Zeiss LSM 510 META confocal laser scanning microscope (CLSM), and staining with Molecular Probes LIVE/DEAD BacLight Bacterial Viability Assay, which utilizes the green fluorescent SYTO 9 for staining of live cells, and the red fluorescent propidium iodide for staining of dead cells. Simulated 3-D images were generated by the use of BITPLANE IMARIS software.

# 7. Summary of appended papers

1. **Appended papers I:** Study of electroplated silver-palladium biofouling inhibiting coating, and bacterial inhibiting surfaces caused by the effects of silver release and/or electrical field;

   **Appended papers II:** Bacterial inhibiting surfaces caused by the effects of silver release and/or electrical field

➢ The studies suggested that pure Ag surfaces can be structured by plating treatments with palladium for the formation of small catalytic areas, where a cathodic reaction can take place. The idea of electric field for bacteria inhibiting from Ag-Pd surface itself was demonstrated in both papers. The studies were shown that the Ag-Pd surface has an bacteria inhibiting effect in media. The inhibiting effect caused by Ag ions release cannot explain the effect found in these results because of the using of Ag-resistant bacteria in the tests. It was evident that the inhibiting effects can be caused by electrochemical interactions and/ or electrical field between the catalytic Pd and Ag combined with an organic and bacterial environment. In both studies, we also found that in some specific media with aggressive compounds like ammonium, undesired Ag ions release can occur and add to the inhibiting effect. In the appendix paper I, the optimized surface preparation conditions of desired Ag-Pd surfaces were studied, and the electrochemical properties of Ag-Pd surfaces were also studied. Based on the results of the appendix paper I, Ag-bearing stainless steels were was designed and introduced as a control to the study of inhibiting mechanism of Ag-Pd surface in the appendix paper II.

2.  **Appendix paper III:** Anti-biofilm properties of a silver-palladium surface.

➢   In this paper, experiments with Ag-sensitive and Ag-resistant *E. coli* strains showed that Ag-Pd surfaces can inhibit biofilm formation by killing the bacteria. Batch experiments provided evidence that biofilm formation of the silver-sensitive bacteria was inhibited on the Ag-Pd surface due to release of toxic levels of $Ag^+$ in addition to the killing effects of the surface, whereas biofilm formation of the silver-resistant bacteria occurred upon a layer of surface-associated dead bacteria on the Ag-Pd coupons. Unlike the batch setup, where high numbers of silver-resistant planktonic bacteria could continuously initiate biofilm formation, the flow-chamber system had a lower bacterial load, and in this system the Ag-Pd surfaces proved efficient in preventing biofilm formation by both silver-sensitive and silver-resistant bacteria.

3.  **Appendix paper IV:** Influence of silver additions to type 316 stainless steels on bacterial inhibition, mechanical properties, and corrosion resistance.

➢   Although the idea of Ag-bearing stainless steel has been patented by Japanese, the detail information of this stainless steel, such as corrosion and mechanical properties, is unclear. They are very important for the practical applications. Based on this motivation, the study of this stainless steel was carried out. In this paper, we indicated that the microstructural observation of Ag-bearing 316 stainless steels showed that Ag precipitates as small particles on the steel matrix surfaces because Ag has extremely low solubility in steel. The Ag additions to 316 stainless steels influenced both their strength and ductility properties. The

observation of fracture morphologies indicated that Ag additions to steels did not change the deformation behavior. Ag remained as a second phase in the passive film of 316 stainless steels and therefore affected the stability of passive film, resulting in a discontinuous passive film. Therefore, Ag-bearing 316 stainless steels had a lower corrosion resistance than that of 316 stainless steels in chloride-containing solutions. The experiments provided evidences that the Ag addition to type 316 stainless steels can improve their bacteria inhibiting properties, and bacteria can be inhibited on the surfaces of Ag-bearing 316 stainless steels due to the release of toxic levels of Ag ions from their surfaces. Dispersive Ag precipitates on the surfaces of 316 stainless steels played an important role on bacterial inhibition. Good inhibiting properties were obtained already at 0.03 wt. % of Ag additions to 316 stainless steels, but 0.09 wt. % of Ag additions improved the effect. When bacteria were present in solutions, an increased Ag ion release rate was found in this study due to the chemical interactions between Ag phases on 316 surfaces and bacteria.

4.  **Appendix paper V:** Silver dissolution from silver-palladium surfaces under conditions of bacterial load.

➢   The undesired Ag ions release from Ag-Pd surface can occur as described in appended papers I and II. In this paper based on the observations of Ag release from appended papers I and II, we described the possible mechanisms of Ag dissolution from Ag-Pd surfaces under conditions of bacterial load. This study indicated that it is important to select applicative environments to avoid the degradation of Ag-Pd surfaces. In some specific environments, an undesired

increased Ag dissolution can occur and add to the bacteria inhibiting effect when chemicals aggressive to Ag and AgCl, such as $NH_4^+$ ions, are present. Surface-associated bacteria can increase Ag dissolution from Ag-Pd surfaces due to the interactions between cell components and the surfaces, and the amount of surface-associated bacteria can improve this effect. Biofilm formation evidently can occur if the Ag-Pd surface becomes covered with a conditioning layer of dead bacteria. Highest bacteria inhibiting efficiency and lowest Ag-dissolved rate of an Ag-Pd surface may be achieved under conditions where appropriate cleaning processes can be applied.

# 8. Conclusion and outlook

People traditionally use chemicals to inhibit bacteria activities. However, biofilm can provide a protection for bacteria against environmental impacts, and therefore these bacteria in biofilms are more resistant to disinfectants than planktonic bacteria, making disinfecting operations less effective or ineffective. It may raise some problems by using chemicals at higher levels to inhibit biofilm formation. Also for patients with biofilm-related infections, it becomes impossible to treat them safely. The use of applied potential or electrical current can reduce or inhibit the bacterial activities. However, in some conditions, applying electrical potential or current on surfaces is unpractical.

The Ag-Pd surface designed and investigated in this study provides an alternative way to inhibit bacterial activity by generating electric fields and electrochemical redox processes. It may be beneficial to coat for example the vulnerable parts of medical implants, medical equipment, water distribution systems, or food producing facilities with biofilm inhibiting Ag-Pd surfaces. However, as biofilm formation evidently can occur if the antimicrobial surface becomes covered with a conditioning layer, highest efficiency of an Ag-Pd surface may be achieved under conditions where appropriate cleaning practices can be applied. The field test of this Ag-Pd surface has not been done during my Ph.D. study. The further study about the real applications in human life should be tested in the future.

There is no detail information for practical applications of the Ag-bearing stainless steel. My Ph.D. study suggested that Ag-bearing 316 stainless steels could be used in place of traditional stainless steels to help reduce the occurrence of bacterial

contamination giving primarily an inhibiting effect close to the surface, however, the mechanical and corrosion properties are slightly poorer than those of 316 stainless steels. The field test of this steel has not been done during my Ph.D. study. The further study about the real applications in human life should be tested in the future.

The methods mentioned in this study to achieve bacteria inhibiting effect are involved in the use of noble metals. Some people may argue that it will be expensive to apply these methods. However, the value of the life of every person is so great that it cannot be measured in terms of money.

# 9. References

1. H.A. Videla, W. G. Characklis, Int. Biodeter. Biodegr. 29 (1992) 195.
2. E.A. Zottola, K.C. Sasahara, Int. J. Food Microbiol. 23 (1994) 125.
3. M.V. Jones, Int. Biodeter. Biodegr. 41 (1998) 191.
4. J.W. Costerton, Int. J. Antimicrob. Ag. 11 (1999) 217.
5. S.J. Dancer, J. Hosp. Infect. 43 (1999) 85.
6. A. Rampling, S. Wiseman, L. Davis, A.P. Hyett, A.N. Walbridge, G.C. Payne, A.J. Cornaby, J. Hosp. Infect. 49 (2001) 109.
7. L.J. Kagan, A.E. Aiello, E. Larson, J. Comm. Health 27 (2002) 247.
8. J.R. Flanders, F.H. Yildiz, in: M. Ghannoum, G.A. O'Toole (Ed.), Microbial Biofilms. ASM Press, Washington, DC, 2004, p.314-331.
9. T. Mattila-Sandholm, G. Wirtanen, Food Rev. Int. 8 (1992) 573.
10. J.W. Costerton, B. Ellis, K. Lam, F. Johnson, A.E. Khoury, Antimicrob. Agents Chemother. 38 (1994) 2803.
11. J.W. Costerton, Z. Lewandowski, D.E. Caldwell, D.R. Korber, H.M. Lappin-Scott, Annu. Rev. Microbiol. 49 (1995) 711.
12. P.S. Stewart, P.K. Mukherjee, M.A. Ghannoum, in: M. Ghannoum, G.A. O'Toole (Ed.), Microbial Biofilms. ASM Press, Washington, DC, 2004, p.250-268.
13. R.O. Darouiche, New Engl. J. Med. 350 (2004) 1422.
14. M. Hjelm, L.R. Hilbert, P. Møller, L. Gram, J. Appl. Microbiol. 92 (2002) 903.
15. L.R. Hilbert, D. Bagge-Ravn, J. Kold, L. Gram L, Int. Biodeter. Biodegr. 52 (2003) 175.
16. A.S. Lynch, G.T. Robertson, Annu. Rev. Med. 59 (2008) 415.
17. E. Scott, Am. J. Infect. Control 27 (1999) S22.
18. J.W. Costerton, in: M. Ghannoum, G.A. O'Toole (Ed.), Microbial Biofilms. ASM Press, Washington, DC, 2004, p.4-19.
19. I.W. Sutherland, Arch. Microbiol. 9 (2001) 222.
20. C.B. Whitchurch, T. Tolker-Nielsen, P.C. Ragas, J.S. Mattick, Science 295 (2002) 1487.
21. K. Lewis, Antimicrob. Agents Chemother. 455 (2001) 999.
22. P. Møller, L.R. Hilbert, C.B. Corfitzen, H.J. Albrechtsen, J. Appl. Surf. Finish. 2 (2007) 149.
23. H.C. Flemming, T. Griebe, G. Schaule, Water Sci. Technol. 34 (1996) 517.
24. I. Francolini, G. Donelli, P. Stoodley, Rev. Environ. Sci. Biotechnol. 2 (2003) 307.
25. N. Wellman, S.M. Fortun, B.R. McLeod, Antimicrob. Agents Chemother. 40 (1996) 2012.
26. P. Stoodley, D. deBeer, H.M. Lappin-Scott, Antimicrob. Agents Chemother. 41 (1997) 1876.
27. B.R. McLeod, S. Fortun, J.W. Costerton, P.S. Stewart, Method. Enzymol. 310 (1999) 656.
28. P.S. Stewart, W. Wattanakaroon, L. Goodrum, S.M. Fortun, B.R. McLeod, Antimicrob. Agents Chemother. 43 (1999) 292.
29. J.L. del Pozo, M.S. Rouse, J.N. Mandrekar, M.F. Sampedro, J.M. Steckelberg, R. Patel, Antimicrob. Agents Chemother. 53 (2009) 35.
30. P. Marshall, Austenitic Stainless Steels: Microstructure and Mechanical Properties, Elsevier Applied Science Publishers, London, 1984, p.410.
31. J.A. Disegi, L. Eschbach, Injury 31 (2000) D2.

32. Y. Ohko, S. Saitoh, T. Tatsuma, A. Fujishima, J. Electrochem. Soc. 148 (2001) B24.
33. J.C. Yu, W. Ho, J. Lin, H. Yip, P.K. Wong, Environ. Sci. Technol. 37 (2003) 2296.
34. S. Nakamura, S. Suzuki, N. Okubo, M. Hasegawa, K. Miyakusu, CAMP-ISIJ 11 (1998) 1147.
35. S. Suzuki, S. Nakamura, N. Ookubo, M. Hasegawa, K. Miyakuso, CAMP-ISIJ 12 (1999) 518.
36. K.R. Sreekumari, K. Nandakumar, K. Takao and Y. Kikuchi, ISIJ Int. 43 (2003) 1799.
37. I.T. Hong, C.H. Koo, Mater. Sci. Eng. A 393 (2005) 213.
38. D.A. Jones, Principles and Prevention of Corrosion, 2$^{nd}$ ed., Prentice Hall, Upper Saddle River, NJ, 1996.
39. G. Danscher, Histochem. Cell Biol. 117 (2002) 447.
40. A. Larsen, M. Stoltenberg, G. Danscher, Histochem. Cell Biol. 128 (2007) 1.
41. T.E. Graedel, J. Electrochem. Soc. 139 (1992) 1963.
42. M.V. ten Kortenaar, J.J.M. de Goeij, Z.I. Kolar, G. Frens, P.J. Lusse, M.R. Zuiddam, E. van der Drift, J. Electrochem. Soc. 148 (2001) C28.
43. Thermodynamic Tables for Nuclear Waste Isolation. Prepared by S.L. Philips, F.V. Hale, L.F. Silvester, Lawrence Berkely Laboratory M. D. Siegel, Sandia National Laboratories, 182, 1988.
44. Landolt-Börnstein: Thermodynamic Properties of Inorganic Material, Scientific Group Thermodata Europe (SGTE), Springer-Verlag, Berlin-Heidelberg, Part 1, 1999.
45. Barin I: Thermochemical Data of Pure Substances, VCH Verlags Gesellschaft, Weinheim, 1989.
46. E.L. Shock, H.C. Helgeson, Geochim. Cosmochim. Acta 52 (1988) 2009.
47. Landolt-Börnstein: Thermodynamic Properties of Inorganic Material, Scientific Group Thermodata Europe (SGTE), Springer-Verlag, Berlin-Heidelberg, Part 1, 1999.
48. J.M. Schierholz, L.J. Lucas, A. Rump, G. Pulverer, J. Hosp. Infect. 40 (1998) 257.
49. S.L. Percival, P.G. Bowler, D. Russell, J. Hosp. Infect. 60 (2005) 1.
50. N.C. Kasuga, M. Sato, A. Amano, A. Hara, S. Tsuruta, A. Sugie, K. Nomiya, Inorg. Chim. Acta 361 (2008) 1267.
51. H. Neubauer, F. Goetz, Arch. Microbiol. 154 (1990) 349.
52. H. Neubauer, F. Götz, J. Bacteriol. 178 (1996) 2005.
53. C.J. Knowles, Bacteriol. Rev. 40 (1976) 652.
54. P.A. Castric, J. Bacteriol. 130 (1977) 826.
55. D.D. Wagman, W.H. Evans, V.B.Parker, R.H. Schumm, I. Halow, S.M. Bailey, K.L. Churney, R.L. Nuttall, J. Phys. Chem. Ref. Data 11 (1982).
56. E.L. Shock, D.C. Sassani, M. Willis, D.A. Sverjensky, Geochim. Cosmochim. Acta 61 (1997) 907.
57. R.L. Davies, S.F. Etris, Catal. Today 36 (1997) 107.
58. J.L. Clement, P.S. Jarrett, Met. Based Drugs 1 (1994) 467.
59. N. Silvestry-Rodriguez, E.E. Sicairos-Ruelas, C.P. Gerba, K.R. Bright, Rev. Environ. Contam. Toxicol. 191 (2007) 23.
60. P.D. Bragg, D.J. Rainnie, Can. J. Microbiol. 20 (1974) 883.
61. M. Rai, A. Yadav, A. Gade, Biotechnol. Adv. 27 (2009) 76.
62. W.B. Morrison, Mater. Sci. Technol. 1 (1985) 954.
63. K. Cho, J. Gurland, Metall. Trans. 19A (1988) 2027.
64. A. Gupta, M. Maynes, S. Silver, Appl. Environ. Microb. 64 (1998) 5042.

65. A. Gupta, K. Matsui, J. F. Lo, S. Silver, Nat. Med. 5 (1999) 183.

66. C. Sternberg, T. Tolker-Nielsen, 2005. Growing and analyzing biofilms in flow cells, p. 1B2.1–1B2.15. In R. Coico, T. Kowalik, J. Quarles, B. Stevenson, R. Taylor (eds.), Current protocols in microbiology. John Wiley & Sons, New York, NY, 2005.

67. World Health Organization, Guidelines for Drinking-water Quality vol. 1, WHO, Geneva, 2006.

Appendix I

# Study of electroplated silver-palladium biofouling inhibiting coating

# Study of electroplated silver–palladium biofouling inhibiting coating

## W.-C. Chiang*[1], L. R. Hilbert[1], C. Schroll[2], T. Tolker-Nielsen[2] and P. Møller[1]

Biofouling can cause many undesirable effects in industrial and medical settings. In this study, a new biofouling inhibiting Ag–Pd surface was designed to form an inhibiting effect by itself. This design was based on silver combined with nobler palladium, both with catalytic properties. Owing to the potential difference between silver and palladium while contacting with an electrolyte, the surface can form numerous discrete anodic and cathodic areas, so that an inhibiting reaction can occur. In this paper, a series of electrochemical and biological investigations were conducted to study the properties and biofouling inhibiting mechanism of these surfaces. In this study, the evidence is presented that the inhibiting effect can be caused by the electrochemical interactions and/or electric field between Pd and Ag/AgCl combined with an organic environment.

## Introduction

Bacteria in natural, industrial and clinical settings most often live in surface associated communities known as biofilms. Undesired biofouling can cause many adverse effects, such as materials corrosion and human diseases. The main benefits of the biofilm mode of growth to bacteria are nutrient capturing and the development of protection against antimicrobials, disinfectants and cleaning, enabling bacteria to survive inside biofilm, and causing the release of new bacteria to solutions. Most bacteria in water systems are likely to be in biofilms.[1–3] Removal of existing biofilm or inhibition of biofilm formation on the surfaces of water systems can be difficult. To improve the biofouling inhibiting properties of materials, many methods have been studied.[4–17] However, under some specific conditions, the release of chemicals at high concentration is undesired, and applying electrical potential or current on surfaces is unpractical.

### Biofouling inhibiting mechanism: electrical field

In view of these considerations, a new biofouling inhibiting silver–palladium (Ag–Pd) surface has been designed to form an inhibiting effect by itself. This design is based on Ag combined with relatively nobler Pd, both with catalytic properties. In this way, it is desired that the release of any matter will be at low concentration. Owing to the potential difference between Ag and Pd while contacting with an electrolyte, the surface can form numerous discrete anodic and cathodic areas. It is desired that when living bacteria pass or approach the electrical field between anode and cathode, they will be inhibited in growth (Fig. 1). To ensure a high local strength of electrical field, the distance between two adjacent electrodes should preferably be small because potential difference over a short distance can give high field strength ($100 \text{ mV } \mu\text{m}^{-1} = 100 \text{ V mm}^{-1}$).

### Biofouling inhibiting mechanism: electrochemical interaction

Anodic polarisation of Ag in chloride containing solutions will immediately form an adherent AgCl layer on surfaces, according to the reaction below

$$Ag + Cl^- = AgCl + e^- \qquad (1)$$

The reaction can convert Ag to insoluble AgCl on surfaces. The Ag ion release from the surface is insignificant because of the low solubility product of AgCl ($1 \cdot 8 \times 10^{-10}$)[18] even at potentials over the equilibrium potential for the reaction.

According to the Pourbaix diagram in Fig. 2, at pH = 7, there is a potential difference of 200 mV between Pd and Ag, and AgCl can be easily and stably formed even in water with low $Cl^-$ concentration of 50 mg $L^{-1}$ (typical $Cl^-$ concentration in Danish drinking water), if Ag is coupled to Pd.

AgCl can be reduced to Ag by oxidation of hydroxyl groups in organic compounds,[19] which means that organic species, such as bacteria, can interact in an oxidation process with AgCl. Thus, bacteria can be inhibited through this reaction
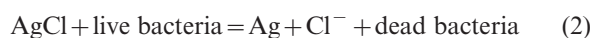
$$AgCl + \text{live bacteria} = Ag + Cl^- + \text{dead bacteria} \qquad (2)$$

After the oxidation process of the organic species, AgCl can only be regenerated in the presence of oxygen (aerobic condition), where Ag is easily oxidised in connection to the reduction of oxygen on the Pd cathode, when the Ag is coupled to Pd
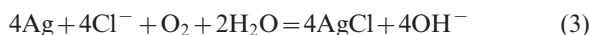
[1]Department of Manufacturing Engineering and Management, Technical University of Denmark, 2800 Kgs. Lyngby, Denmark
[2]BioCentrum, Technical University of Denmark, 2800 Kgs. Lyngby, Denmark

*Corresponding author, email wcc@ipl.dtu.dk
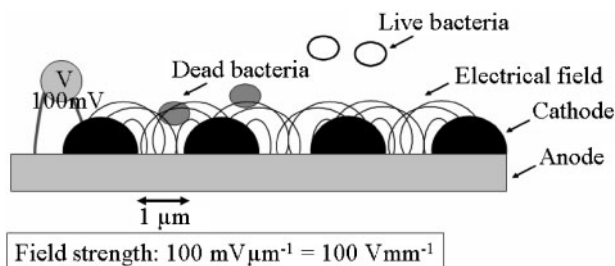
**1 Inhibiting surface and its electrical field**

$$4Ag + 4Cl^- + O_2 + 2H_2O = 4AgCl + 4OH^- \quad (3)$$

The above reaction can also be separated in an anodic and a cathodic partial reaction.

$$\text{Anodic partial reaction}: 4Ag + 4Cl^- = 4AgCl + 4e^- \quad (4)$$

$$\text{Cathodic partial reaction}: 2H_2O + O_2 + 4e^- = 4OH^- \quad (5)$$

These reactions simply demonstrate the reactions of Ag converting to AgCl and AgCl converting to Ag back and forth, which can continuously happen if hydroxyl groups in organic compounds, such as bacteria, are supplied to the surface.

## Experimental

### Ag–Pd surface preparation

The details of the Ag–Pd surface preparation are described previously.[20] In order to obtain desired surface structures, the Ag surface was treated by the immersion plating in palladium chloride solution at ambient temperature. The palladium chloride solution was prepared from 5 vol.-% of the stock solution which is prepared from $0.5$ g L$^{-1}$ PdCl$_2$ and 4 g L$^{-1}$ NaCl dissolved in water. The surfaces were immersed for one and three minutes. 'Ag–Pd5/1' and 'Ag–Pd5/3' respectively were used as the symbols for the representation in this report. The reaction of this plating is as follows

$$PdCl_4^{2-} + 2Ag \rightarrow 2AgCl + Pd + 2Cl^- \quad (6)$$

A JEOL 5900 scanning electron microscope (SEM) equipped with an INCA 400 energy dispersive X-ray (EDX) system were applied to characterise the appearance and compositions of the surfaces.

### Microbiological investigations

The samples chosen for the microbiological investigations were AISI 316 stainless steel, Ag, Ag–Pd5/1 and Ag–Pd5/3 with dimensions $7 \times 4 \times 0.5$ mm. To distinguish the inhibiting effect from Ag release, electrical field, or other reactions, the bacterial strain used in this study was Ag resistant *Escherichia coli (E. coli) J53 [pMG101]*.[21] ABTG medium (Table 1) was used to cultivate biofilms and planktonic bacteria. Each test was carried out in an incubation plate with 5 mL ABTG medium at 37°C, and slowly shaken for 24 h. The sample surface/volume (S/V) ratio in the incubation plate was 13·4 m$^{-1}$.

The test for the Ag toleration concentration of this *E. coli* was conducted in ABTG medium with adding AgNO$_3$.
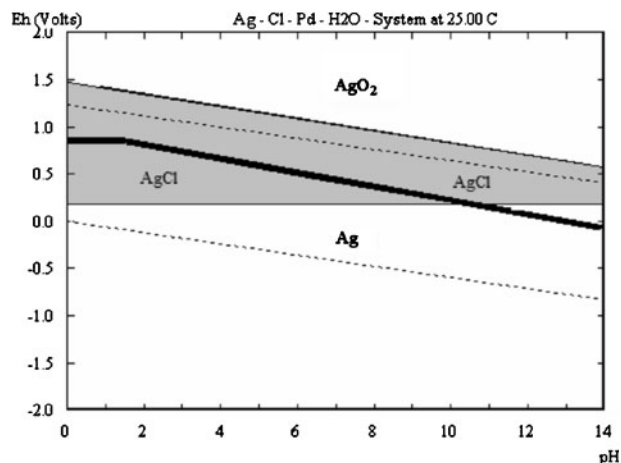


**2 Pourbaix diagram of Ag–Cl–Pd–H$_2$O system: it is calculated from Cl$^-$ concentration of $1.4 \times 10^{-3}$M (50 mg L$^{-1}$) and the metal ions concentration of $10^{-6}$M; diagram is superimposed by immune area of Pd (area below bold line)**

Biofilm formation on surfaces was investigated by the use of a ZEISS LSM 510 META confocal laser scanning microscope (CLSM),[22] and the LIVE/DEAD BacLight bacterial viability assay (molecular probes), which utilises the green fluorescent SYTO 9 for staining of live cells, and the red fluorescent propidium iodide for staining of dead cells. To evaluate the inhibiting effect on planktonic bacteria, tests were conducted by the plain plate dilute method to count the numbers of live planktonic bacteria (colony forming units, CFU mL$^{-1}$) in the medium.

After the tests, the spent bacterial ABTG media were diluted, acidified (nitric acid), and then boiled on a heating plate to make a clear solution. The total dilution was 10 times. Total Ag in media were analysed by JOBIN YVON JY38S inductively coupled plasma optical emission spectrometry (ICPOES).

### Electrochemical investigations

#### Galvanic current measurement

The purpose of this test is to investigate whether the coupling of Ag and Pd electrodes can electrochemically oxidise organic compounds or not. Therefore, the coupling was tested to measure the faradaic current introduced by the addition of organic compounds to simulate the bacteria in an electrolyte. The electrodes were connected through a zero resistance ammeter (ZRA). The area ratio is about 1 : 2·29 for Ag to Pd (Ag: 0·7 cm$^2$; Pd: 1·6 cm$^2$). The test used 5·0 wt-%NaCl solution, and was carried out in a cell with 400 mL volumes, stirred with oxygen (purity≥99·99%) at ambient temperature. After stabilisation of the current, to simulate bacteria or organic species, 0·5 moles of paraformaldehyde (HCHO) was added. If HCHO can

**Table 1 Compositions of ABTG medium**

| | | |
|---|---|---|
| 100 mL A-10 | 900 mL BT | 25 mL 20% glucose |
| 20 g (NH$_4$)$_2$SO$_4$ | 1 mL 1M MgCl$_2$ | 200 g glucose |
| 60 g Na$_2$HPO$_4$ | 1 mL 0·1M CaCl$_2$ | 800 mL H$_2$O |
| 30 g KH$_2$PO$_4$ | 1 mL 0·01M FeCl$_3$ | |
| 30 g NaCl | 2·5 mL 1 g L$^{-1}$ thiamin | |
| 1000 mL H$_2$O | 900 mL H$_2$O | |
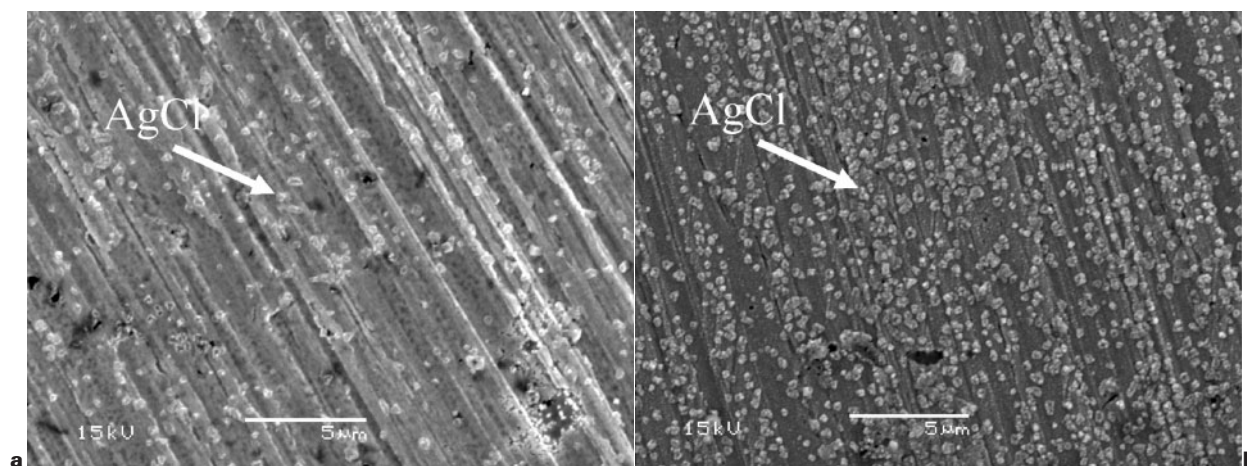
**3** Images (SEM) of *a* Ag–Pd5/1 and *b* Ag–Pd5/3

be oxidised on the surfaces of electrodes, an increased faradaic current will be measured.

### Potentiodynamic polarisation and chronoamperometric tests

Cylindrical Ag samples were treated in palladium chloride solution to obtain Ag–Pd surface. The samples of Ag–Pd5/1 and Ag–Pd5/3 were used in these tests. The tests were carried out in a typical three electrode cell with 400 mL volumes, with platinum (Pt) as a counter electrode and a saturated calomel electrode (SCE) as a reference electrode. The exposed area of the working electrode was 3·98 cm$^2$. Sodium acetate buffer (pH 7) of 1M containing 250 mg L$^{-1}$ Cl$^-$ solution and ABTG medium were used, and stirred with oxygen (purity$\geqslant$ 99·99%) during the tests at ambient temperature. Before potentiodynamic polarisation, all samples were equilibrated for 1 h to obtain an open circuit potential. The curves were recorded at a scan rate of 0·5 mV s$^{-1}$ from the initial potential of −250 mV versus open circuit potential to the final potential of 900 mV versus SCE.

In the chronoamperometric test, the applied overpotential of 5 mV was referred to the open circuit potential. Sodium acetate buffer (pH 7) of 1M containing 250 mg L$^{-1}$ Cl$^-$ solution and ABTG medium were used, and stirred with oxygen (purity$\geqslant$99·99%) during the tests at ambient temperature. Before tests, all samples were equilibrated for 1 h to obtain an open circuit potential. After the tests, Ag concentration in the solutions was analysed by ICP.

## Results and discussion

### Characterisation of Ag–Pd surfaces

The SEM images of the Ag–Pd samples (Fig. 3) show the surfaces were formed with numerous discrete areas, where the distance between two adjacent areas is less than 5 μm, and there was a tendency to form bright clusters when increasing the contact times of immersion plating.

The EDX analyses of the Ag–Pd surfaces are shown in Table 2. It can be found that Pd was deposited in a very thin layer with microholes on top of Ag, and AgCl was formed as the light microclusters during the deposition of Pd.

## Microbiological investigations

The maximum concentration of Ag ion that can be tolerated by the Ag resistant *E. coli J53 [pMG101]* was found to be about 5000 μg L$^{-1}$.

Figure 4 shows the ability of the *E. coli J53 [pMG101]* strain to form biofilm on the different surfaces. Figure 4*a* and *b* shows that microcolonies which mainly consisted of live bacteria (green fluorescence) were formed on 316 steel and Ag surfaces. Only few dead bacteria (red fluorescence) were observed. These experiments suggest that there was no direct inhibiting effect on these surfaces.

Figure 4*c* and *d* shows that Ag–Pd5/1 and Ag–Pd5/3 had an inhibiting effect when bacteria attached to the surface. Especially on the Ag–Pd5/3 surface, there was a significant reduction of the formation of microcolonies, and presence of dead bacteria on the surfaces.

Table 3 shows that the planktonic *E. coli* can still grow up at least two log increases in the medium surrounding each of the samples. It suggests that there was no significant inhibiting effect on planktonic *E. coli* for all samples.

Table 4 shows that the Ag–Pd had higher Ag release than Ag. It was also found that the surface with more Pd contents obtained higher Ag release. This undesired effect can be explained by the aggressive ammonium to Ag and AgCl in ABTG medium.

The planktonic *E. coli* can still grow, even in an environment with 600 μg L$^{-1}$ Ag concentrations. However, the biofilm formation was inhibited on the Ag–Pd surfaces. It suggests that the inhibiting effect cannot be attributed to Ag release, but probably can be explained from the electrochemical interaction or/and electric field between Ag–Pd surfaces and bacteria. However, at present it can not be excluded that the

**Table 2** Compositions of Ag–Pd surfaces, wt-%

| | Ag–Pd5/1 | | Ag–Pd5/3 | |
|---|---|---|---|---|
| | Light cluster | Dark area | Light cluster | Dark area |
| Ag | 97·8 | 98·6 | 95·4 | 94·2 |
| Cl | 2·2 | 0·6 | 2·5 | 1·2 |
| Pd | 0·1 | 0·8 | 2·0 | 4·7 |
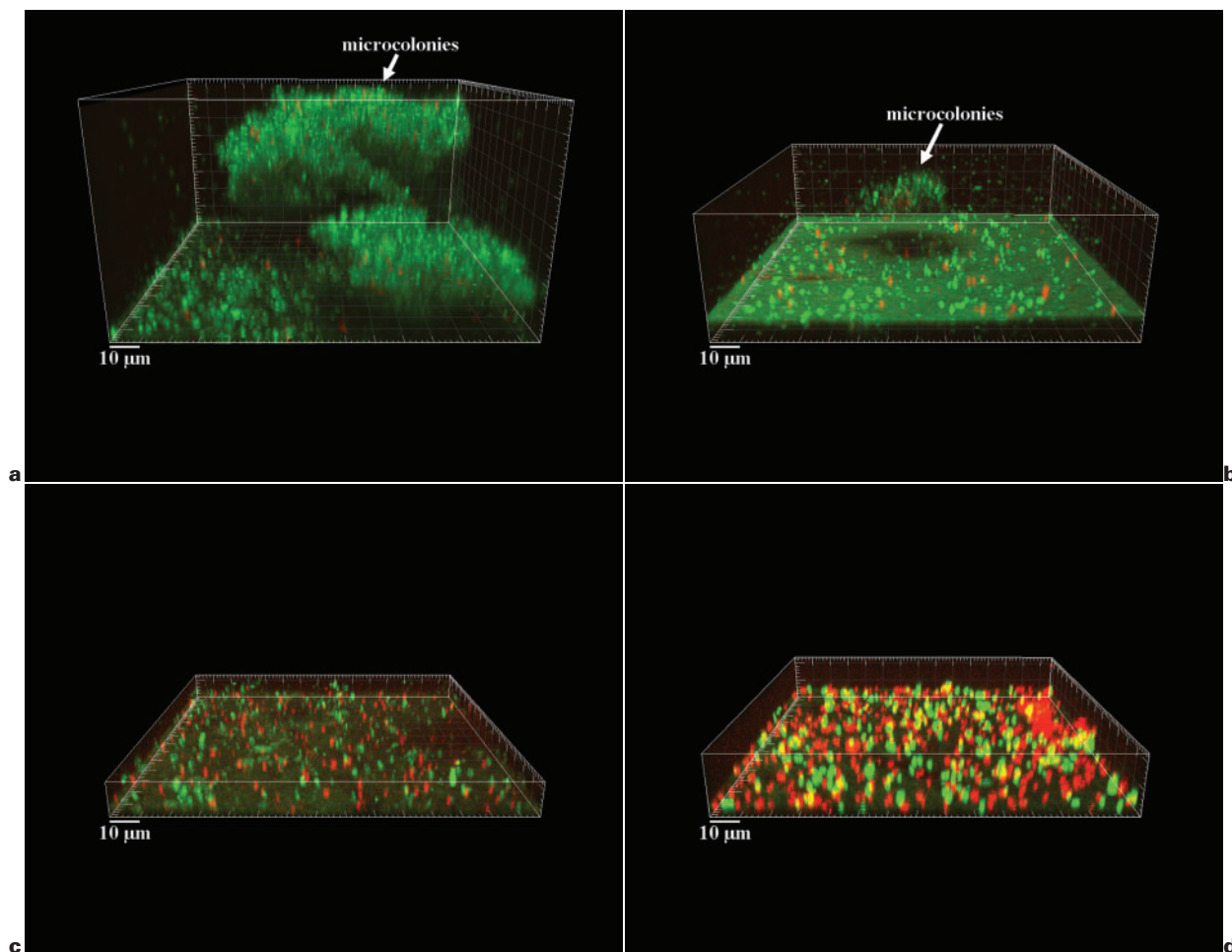
**4 Images (CLSM) of surfaces of *a* 316 stainless steel, *b* Ag, *c* Ag–Pd5/1 and *d* Ag–Pd5/3 after 24 h in bacterial ABTG medium**

observed inhibiting effect of bacteria on Ag–Pd surfaces may be caused by higher local Ag concentrations.

## Electrochemical test

### Galvanic current measurement

For galvanic current measurement, the current flow direction was determined by the relative polarity between two electrodes, and the connecting method of positive and negative sides of a ZRA to two electrodes. As shown in Fig. 5, if electrode W1 is connected to the negative side of the ZRA and positive current is measured, then W1 is anode relatively to W2, and vice versa.

In this measurement, Ag was connected to the negative side of the ZRA, and then positive current was measured. This indicated that Ag was anode relatively to Pd in 5 wt-%NaCl solution. Figure 6 shows

that the galvanic current from the coupling of Ag and Pd electrodes. The initial current could be due to AgCl being developed on Ag surfaces by the coupling with Pd that will increase the potential. Then the current stabilised at approximately $0.6 \ \mu A$. After 17 h, $0.5$ moles HCHO was added, and the current gradually increased to the highest values of $1.6 \ \mu A$, and then gradually decreased. The decrease in current to a nearly steady state indicated the formation of AgCl. After this test, a white layer of deposit was on the surface of Ag electrode, and its composition was confirmed to be AgCl showing a strong Cl signal by EDX.

This current increase after HCHO added to the solution can be explained by a number of reactions as follows. On the Ag/AgCl surface, AgCl was reduced to Ag, and HCHO was oxidised to formic acid or formate
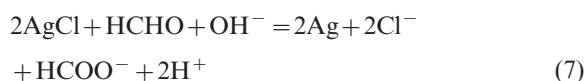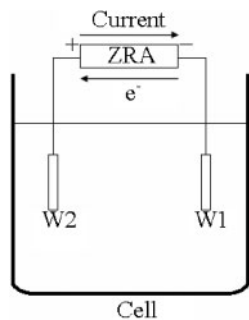
$$2AgCl + HCHO + OH^{-} = 2Ag + 2Cl^{-}$$
$$+ HCOO^{-} + 2H^{+} \qquad (7)$$

**Table 3 Colony forming numbers of planktonic *E. coli* after 24 h in medium with each of samples**

|  | CFU mL$^{-1}$ |
|---|---|
| Before test | $6.9 \times 10^5$ |
| After 24 h |  |
| 316 | $3.3 \times 10^8$ |
| Ag | $4.6 \times 10^8$ |
| Ag–Pd5/1 | $1.8 \times 10^8$ |
| Ag–Pd5/3 | $2.7 \times 10^7$ |

**Table 4 Concentration and release rate of Ag after 24 h in bacterial ABTG medium**

|  | Ag | Ag–Pd5/1 | Ag–Pd5/3 |
|---|---|---|---|
| [Ag], μg L$^{-1}$ | 103 | 365 | 626 |
| Ag release rate, μg cm$^{-2}$ h$^{-1}$ | 0.03 | 0.11 | 0.19 |

**5 Schematic diagram of cell for galvanic current measurement**

Equation (7) can also be separated in an anodic and a cathodic partial reaction as follows.

Anodic partial reaction : $HCHO + OH^- =$

$$HCOO^- + 2H^+ + 2e^- \tag{8}$$

Cathodic partial reaction : $2AgCl + 2e^- =$

$$2Ag + 2Cl^- \tag{9}$$
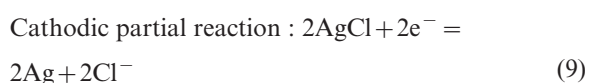
Then, due to the galvanic coupling between Ag and Pd electrodes, the regeneration of AgCl (on the Ag electrode) after the oxidation of HCHO can be formed immediately in the presence of $O_2$ and $Cl^-$ (equation (3)), and provide an increased galvanic current. The reduction of $O_2$ can be carried out on the Pd electrode (equation (5)). Thus, the addition of an organic compound, such as HCHO, can work as a fuel source to provide the generation of current on surfaces. In this test, it evidenced that the biofouling inhibiting reaction caused by $Ag \rightleftharpoons AgCl$ can continuously happen if bacteria, acting as organic compounds, are supplied to the surface.

On the other hand, the galvanic current increase could also be explained by the reaction of HCHO oxidation that directly takes place on the Ag surface without any interaction with AgCl. The reduction of $O_2$ can be carried out on the Pd electrode (equation (5)).

$$2HCHO + O_2 = 2HCOO^- + 2H^+ \tag{10}$$
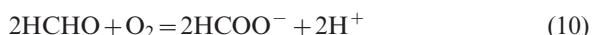
In this case, the anodic partial reaction of equation (10) is as follows
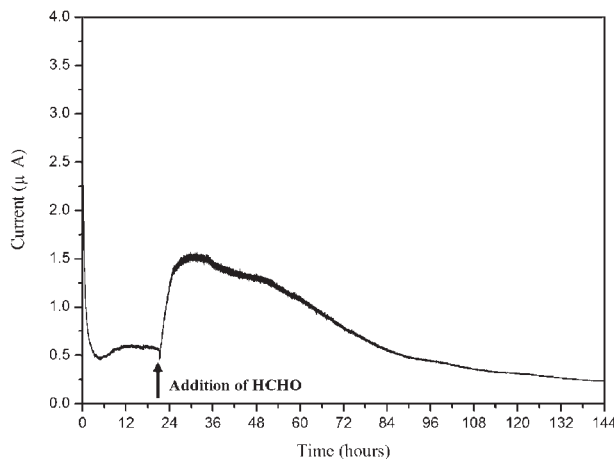


**6 Galvanic current from coupling of Ag and Pd electrodes, before and after addition of 0·5M HCHO**

$$2HCHO + 4OH^- =$$
$$2HCOO^- + 2H^+ + 2H_2O + 4e^- \tag{11}$$
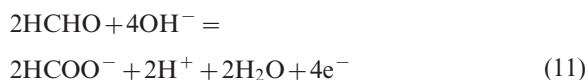
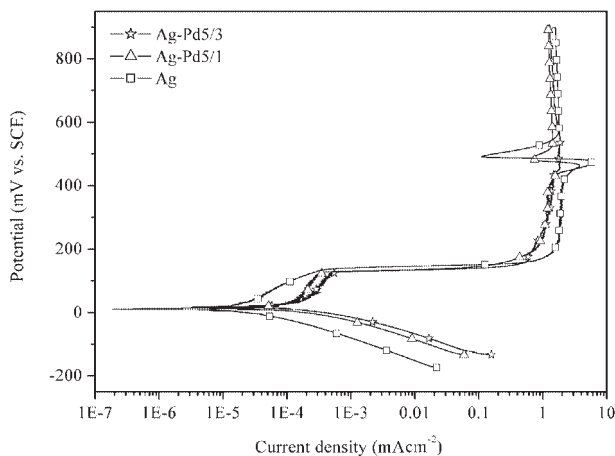### Potentiodynamic polarisation and chronoamperometric tests

The polarisation curves (Fig. 7) show that the presence of Pd can cause more increased rates on the cathodic reaction both in ABTG and 1M sodium acetate buffer (pH 7) containing 250 mg $L^{-1}$ $Cl^-$ solution. Both in these two solutions, Ag, Ag–Pd5/1, and Ag–Pd5/3 showed a sharp anodic behaviour at low anodic overpotential region, and then followed by a limiting current density at higher anodic overpotential region. In chloride containing environments, the formation of AgCl layers on Ag and Ag-Pd surfaces was observed at anodic overpotential region in these studies, and was reported previously.[23–25] However, because there was an aggressive compound ($NH_4^+$) to AgCl in ABTG medium (equation (12)), the presence of Pd did not obviously change anodic reaction electrochemically. AgCl was chemically dissolved by ammonium.

$$AgCl + 2NH_4^+ + 2OH^- =$$
$$Ag(NH_3)_2^+ + Cl^- + 2H_2O \tag{12}$$
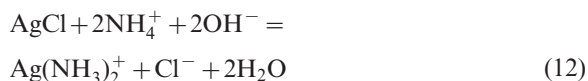
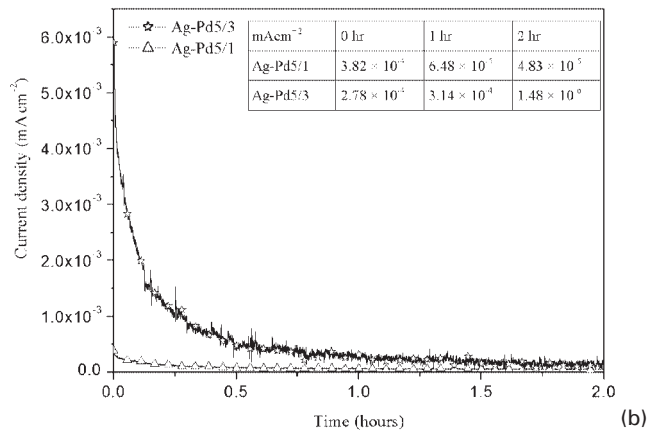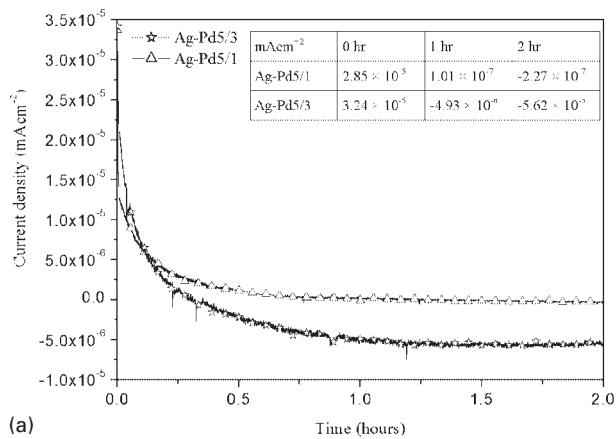For the chronoamperometric tests shown in Fig. 8, the
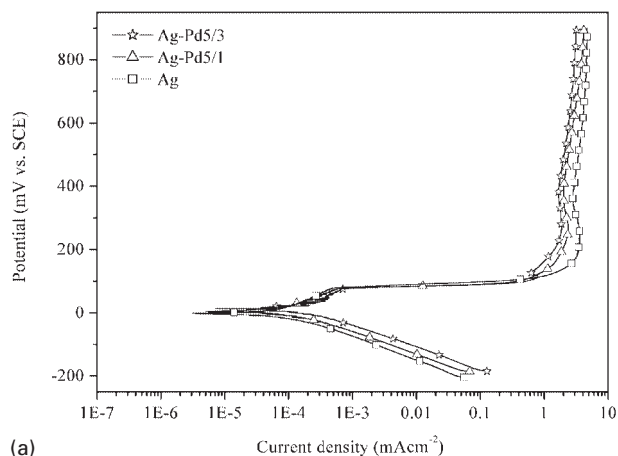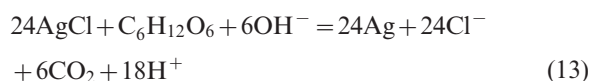


(a)



(b)

**7 Potentiodynamic polarisation curves in *a* ABTG medium and *b* 1M sodium acetate buffer (pH 7) containing 250 mg $L^{-1}$ $Cl^-$ solution**

**8 Chronoamperometric tests in *a* ABTG medium and *b* 1M sodium acetate buffer (pH 7) containing 250 mg L$^{-1}$ Cl$^-$ solution**

initial current densities were lower than those in potentiodynamic polarisation at the same potential. In spite of the slow potential scan selected in potentiodynamic polarisation, it indicated that the polarisation curves did not correspond to steady state conditions. The chronoamperometric curves were followed by a decrease in the current densities in positive current densities region. It can be due to the formation of AgCl on the Ag–Pd surfaces. More Pd on the surfaces can cause more increased positive anodic current densities, which means more AgCl can be formed on the surfaces. In Fig. 8*a* for the chronoamperometry in ABTG medium, negative current densities can be observed both in Ag–Pd5/1 and Ag–Pd5/3, because the applied overpotential obviously was close to the open circuit potential, so AgCl reduction (equation (9)) and oxygen reduction (equation (5)) can occur on these heterogeneous surfaces.

Furthermore, there were organic compounds, such as glucose (reducing sugar), in ABTG medium, and these compounds can be oxidised (equation (13)) on Ag/AgCl surfaces by reducing AgCl. AgCl can be regenerated in connection to the O$_2$ reduction on Pd surfaces

$$24AgCl + C_6H_{12}O_6 + 6OH^- = 24Ag + 24Cl^-$$
$$+ 6CO_2 + 18H^+ \qquad (13)$$

More AgCl and Pd on surfaces seem to cause more increased negative cathodic current densities in the test, which means more AgCl reduction and O$_2$ reduction happened on the surfaces. In Fig. 8*b* for the chronoamperometry in 250 mg L$^{-1}$ Cl$^-$ solution, only positive current densities can be observed. There was no organic compound in this solution, and therefore only AgCl formation on Ag–Pd surfaces occurred.

**Table 5  Concentrations and release rates of Ag in chronoamperometric tests in *a* ABTG medium and *b* 1M sodium acetate buffer (pH 7) containing 250 mg L$^{-1}$ Cl$^-$ solution**

| (a) | Ag–Pd5/1 | Ag–Pd5/3 |
|---|---|---|
| [Ag], µg L$^{-1}$ | 99 | 157 |
| Ag release rates, µg cm$^{-2}$ h$^{-1}$ | 5·32 | 8·42 |
| (b) | Ag–Pd5/1 | Ag–Pd5/3 |
| [Ag], µg L$^{-1}$ | 27 | 45 |
| Ag release rates, µg cm$^{-2}$ h$^{-1}$ | 1·45 | 2·38 |

Table 5 shows that an accelerated rate of Ag release was observed on Ag–Pd surfaces in ABTG medium, and it was also found that Ag–Pd surfaces with more Pd contents can obtain higher Ag release. This can be explained by chemical dissolution of Ag and AgCl by ammonium as combined with a galvanic effect between Ag and Pd.

## Conclusion

The biofilm inhibiting properties and electrochemical characteristics of Ag–Pd surfaces were investigated in this study. The desired inhibiting surface can be designed with conventional techniques easily. It was shown that the Ag–Pd surface had an inhibiting effect on biofilm formation of Ag resistant *E. coli* in organic solutions, i.e. growth medium. The ammonium component of the growth medium promoted undesired Ag release, but the Ag content in the medium did not kill planktonic bacteria. At present it can not be excluded that the observed inhibiting effect of bacteria on Ag–Pd surfaces may be caused by higher local Ag concentrations. However, the available evidences from galvanic current measurements and microbiological tests suggest that the inhibiting effect was caused by the electrochemical interactions and/or electric field between Pd and Ag/AgCl combined with an organic environment. More work is required to fully elucidate the mechanisms for inhibiting bacterial growth on these surfaces.

## References

1. J. W. Costerton, Z. Lewandowski, D. E. Caldwell, D. R. Korber and H. M. Lappin-Scott: *Ann. Rev. Microbiol.*, 1995, **49**, 711–745.
2. J. W. Costerton: *Int. J. Antimicrob. Ag.*, 1999, **11**, 217–221.
3. M. Ghannoum and G. A. O'Toole: 'Microbial biofilms'; 2004, DC, American Society for Microbiology Press.
4. L. R. Hilbert, D. Bagge-Ravn, J. Kold and L. Gram: *Int. Biodeter. Biodegr.*, 2003, **52**, 175–185.
5. T. J. Berger, J. A. Spadaro, S. E. Chapin and R. O. Becker: *Antimicrob. Agents Chemother.*, 1976, **9**, 357–358.
6. N. Grier: in 'Disinfection, sterilization and preservation', (ed. S. S. Block), 3rd edn, 375–389; 1983, Philadelphia, PA, Lea & Febiger.
7. P. Stoodley, D. de Beer and H. M. Lappin-Scott: *Antimicrob. Agents Chemother.*, 1997, **41**, 1876–1879.
8. R. L. Davies and S. F. Etris: *Catal. Today*, 1997, **36**, 107–114.
9. J. M. Schierholz, L. J. Lucas, A. Rump and G. Pulverer: *J. Hosp. Infect.*, 1998, **40**, 257–262.
10. A. Kerr, T. Hodgkiess, M. J. Cowling, C. M. Beveridge, M. J. Smith and A. C. S. Parr: *J. Appl. Microbiol.*, 1998, **85**, 1067–1072.

11. B. R. McLeod, S. Fortun, J. W. Costerton and P. S. Stewart: *Methods Enzymol.*, 1999, **310**, 656–670.
12. P. S. Stewart, W. Wattanakaroon, L. Goodrum, S. M. Fortun and B. R. McLeod: *Antimicrob. Agents Chemother.*, 1999, **43**, 292–296.
13. M. Hjelm, L. R. Hilbert, P. Møller and L. Gram: *J. Appl. Microbiol.*, 2002, **92**, 903–911.
14. I. Alvarez, R. Virto, J. Raso and S. Condon: *Innovat. Food Sci. Emerging Technol.*, 2003, **2**, 195–202.
15. I. T. Hong and C. H. Koo: *Mater. Sci. Eng. A*, 2005, **A393**, 213–222.
16. S. L. Percivala, P. G. Bowlera and D. Russell: *J. Hosp. Infect.*, 2005, **60**, 1–7.
17. S. Y. Tseng: 'Pulsed electric field generators for food sterilization', PhD thesis, National Chung Cheng University, Chiayi, Taiwan, 2005.
18. T. E. Graedel: *J. Electrochem. Soc.*, 1992, **139**, 1963–1970.
19. M. V. ten Kortenaar, J. J. M de Goeij, Z. I. Kolar, G. Frens, P. J. Lusse, M. R. Zuiddam and E. van der Drift: *J. Electrochem. Soc.*, 2001, **148**, C28–C33.
20. P. Møller, E. O. Jensen and L. R. Hilbert: US Patent, 2006, US2006003019.
21. A. Gupta, L. T. Phung, D. E. Taylor and S. Silver: *Microbiology*, 2001, **147**, 3393–3402.
22. B. R. Masters: in 'Handbook of coherent domain optical methods: biomedical diagnostics, environmental and material science', (ed. V. V. Tuchin), Vol. 2, 363–402; 2004, Boston, MA, Kluwer.
23. T. K. Vaidyanathan and K. Mukherjee: *Metall. Trans. A*, 1982, **13A**, 313–317.
24. D. W. Berzins, I. Kawashima, R. Graves and N. K. Sarkar: *Dent. Mater.*, 2000, **16**, 266–273.
25. L. Joska, M. Marek and J. Leitner: *Biomaterials*, 2005, **26**, 1605–1611.

Appendix II

# Bacterial inhibiting surfaces caused by the effects of silver release and/or electrical field

Electrochimica Acta, 2008

# Bacterial inhibiting surfaces caused by the effects of silver release and/or electrical field

Wen-Chi Chiang [a,*], Lisbeth Rischel Hilbert [a], Casper Schroll [b], Tim Tolker-Nielsen [b], Per Møller [a]

[a] *Department of Manufacturing Engineering and Management, Building 204, Technical University of Denmark, 2800 Kgs. Lyngby, Denmark*
[b] *BioCentrum, Building 227, Technical University of Denmark, 2800 Kgs. Lyngby, Denmark*

## ARTICLE INFO

## ABSTRACT

In this study, silver–palladium surfaces and silver-bearing stainless steels were designed and investigated focusing on electrochemical principles to form inhibiting effects on planktonic and/or biofilm bacteria in water systems. Silver-resistant *Escherichia coli* and silver-sensitive *E. coli* were used for the evaluation of inhibiting effects and the inhibiting mechanism. For silver–palladium surfaces combined with bacteria in media, the inhibiting effect was a result of electrochemical interactions and/or electrical field, and in some specific media, such as ammonium containing, undesired silver ions release can occur from their surfaces. For silver-bearing stainless steels, the inhibiting effect can only be explained by high local silver ions release, and can be limited or deactivated dependent on the specific environment.

## 1. Introduction

### 1.1. Bacteria and biofilm

Bacterial adhesion and biofilm on surfaces in water systems are familiar. These formations can cause many undesired effects, such as materials corrosion and human diseases. It has been reported that when a clean material comes in contact with a non-sterile aquatic environment, the attachments of planktonic bacteria on surfaces will start and result in biofilm formation. Biofilm is bacteria attached to either inert or living surfaces and surrounded by a matrix of slime. The main benefits obtained by biofilm are easier capture of nutrients and protection against disinfectants and cleaning, enabling bacteria to survive inside biofilm, and causing the release of new live bacteria to aquatic environment. Most bacteria in water systems are likely to be in biofilms. Therefore, the presence of biofilm can cause sudden increasing numbers of planktonic bacteria, and lead to serious problems of the hygienic management. In practice, the number of planktonic bacteria is the index which is monitored and attempted minimized, while biofilm formations are rarely controlled [1–3].

### 1.2. Bacterial inhibition in water and food industries

Until now, there are few non-toxic treatments available to inhibit bacterial growth and biofilm. The use of silver (Ag) and its compounds to obtain bacterial inhibiting effects has been applied since 1000 BC [4]. In recent years, it is well known that Ag and its compounds have been introduced into many commercial products. The method of Ag ions release is effective to inhibit bacterial activities [5–10]. However, in some specific conditions, the release of chemicals in high concentration is undesired. The material and topography of the substrate also have some effects on the rate of biofilm formation, but there is no direct inhibiting effect that can be found in any simple substrate material [11]. Metallic Ag only has slight inhibiting effects because of its chemical stability [5], and laboratory studies have recently shown that pure Ag surfaces do not have a significantly inhibiting effect on bacterial adhesion as compared to standard stainless steel [6]. Free Ag ions in halide-containing solutions may be formed as inactive Ag halides, such as silver chloride (AgCl), and these compounds also have the property of low solubility [5,7]. Therefore, the inhibiting effect will be lowered in saline environment [5,7,12]. It also has been reported that the use of applied potential or electrical current can reduce or inhibit bacterial activities [13–20]. However, in some specific conditions, applying electrical potential or current on surfaces is unpractical.
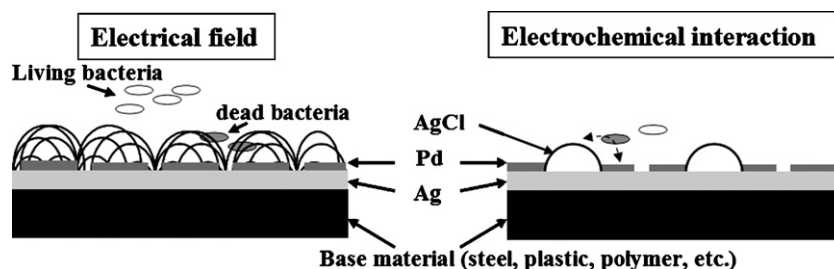
**Fig. 1.** Ag–Pd surface and its desired bacterial inhibiting methods.

Stainless steels have been widely used in water and food industries because of their good corrosion resistance, weldability, cleanability, etc. [6,11]. However, stainless steels do not have indigenous bacterial inhibiting properties, and removal of existing biofilm or inhibition of biofilm formation on the surfaces of stainless steels can be difficult in the facilities of water and food industries. The purpose of this study was to design a silver–palladium (Ag–Pd) coating (surface) and a Ag-bearing stainless steel (bulk) for improving the bacterial inhibiting activities of stainless steels, and examine their inhibiting effects. If effective, these inhibiting surfaces can be integrated into the facilities of water and food industries where disinfection or cleaning is difficult.

### 1.3. Ag–Pd surface

#### 1.3.1. Inhibition by electrical field

This design is based on Ag coatings applied to stainless steels (or ceramic and polymers) that can be micro/nanostructured by a treatment with Pd. In this way, a Ag–Pd surface can form an electrical field on the surface by itself. Due to the potential difference between Ag and Pd while contacting with an electrolyte, the surface can form numerous discrete anodic and cathodic areas. It is desired that when live bacteria pass or approach the electrical field between the anode and cathode, they will be inhibited in growth (Fig. 1). In order to ensure a high local strength of electrical field, the surface should be micro- or nanostructured. The characterization of this structure is that one of electrodes is appropriately distributed in small discrete areas, either as microclusters upon the surface or as micro-holes within the surface. The distance between two adjacent electrodes should be preferably small because potential difference over a short distance can give a high field strength ($100 \, \text{mV} \, \mu\text{m}^{-1} = 100 \, \text{V} \, \text{mm}^{-1}$). This inhibiting reaction is called the "electric chair effect" [21]. In this design, it is desired that the release of chemicals from the surface is minimal and that the materials are corrosion resistant.

#### 1.3.2. Inhibition by electrochemical interactions

When Ag immerses in a chloride-containing solution, anodic polarization of Ag will immediately form an adherent AgCl layer on surfaces, according to the reaction below:

$$Ag + Cl^- \rightarrow AgCl + e^- \tag{1}$$

The reaction can convert Ag to low soluble AgCl on surfaces. Ag ions release from the surface is insignificant because of the low solubility product of AgCl ($1.8 \times 10^{-10}$) [22] even at potentials over the equilibrium potential for the reaction. In drinking water, AgCl will be in equilibrium with only $2 \, \mu\text{g} \, \text{l}^{-1}$ Ag$^+$ at 10 °C.

According to the Pourbaix diagram in Fig. 2, at pH 7, there is a potential difference of 200 mV between Pd and Ag, and AgCl can easily and stably be formed even in water with low Cl$^-$ concentration of $50 \, \text{mg} \, \text{l}^{-1}$ (typical Cl$^-$ concentration in Danish drinking

water). This can explain the formation of AgCl, even in water with low Cl$^-$ concentration, if Ag is coupled to Pd.

It has been reported that AgCl can be reduced to Ag by oxidation of hydroxyl groups in organic compounds [23], which means that organic species, such as bacteria, can interact in an oxidation process with AgCl. These reactions are in good agreement with thermodynamic calculations where ethanol or reducing sugars (such as fructose and glucose) are used for the verifications [21]. Thus, bacterial metabolisms can be inhibited (Fig. 1) through the reaction as follows:
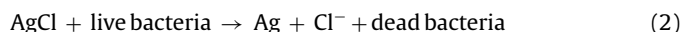
$$AgCl + live \, bacteria \rightarrow Ag + Cl^- + dead \, bacteria \tag{2}$$
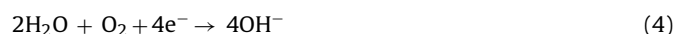
After the oxidation process of the organic species, AgCl can only be regenerated in the presence of oxygen (aerobic condition), where Ag is easily oxidized in connection to the reduction of oxygen on the Pd cathode, if the Ag is coupled to Pd.

Anodic partial reaction:

$$4Ag + 4Cl^- \rightarrow 4AgCl + 4e^- \tag{3}$$

Cathodic partial reaction:

$$2H_2O + O_2 + 4e^- \rightarrow 4OH^- \tag{4}$$

Organic species, such as bacteria, can be oxidized on the Ag surface with an accompanying reduction of oxygen or other species on the Pd surface [21]. These reactions simply demonstrate the reactions of Ag converting to AgCl and AgCl converting to Ag back and forth, which can continuously happen if hydroxyl groups in organic compounds, such as bacteria, are supplied to the surface.
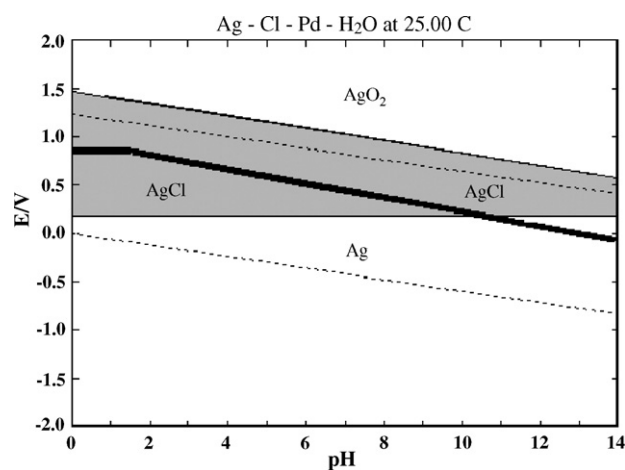


**Fig. 2.** Pourbaix diagram of Ag–Cl–Pd–H$_2$O system. It was calculated from Cl$^-$ concentration of $1.4 \times 10^{-3}$ M ($50 \, \text{mg} \, \text{l}^{-1}$) and the metal ions concentration of $10^{-6}$ M. The diagram was superimposed by the immune area of Pd (the area below the bold line).

This reaction can also be regarded as a micro- or nano-fuel cell system.

### 1.4. Ag-bearing stainless steel

Copper (Cu)-bearing stainless steels have been investigated widely for the purpose of bacterial inhibition [24–26]. However, there are few studies about Ag-bearing stainless steels [27]. From the hygienic point of view, Cu is more toxic than Ag. Therefore, in this study, Ag-bearing stainless steel was prepared, and its bacterial inhibiting effect was evaluated.

## 2. Experimental

### 2.1. Preparation of samples

To obtain a desired Ag–Pd surface, Ag surface was treated by an immersion plating in palladium chloride solution at ambient temperature for 3 min [28]. The palladium chloride solution was prepared from 5 vol.% of the stock solution which is prepared from $0.5\,g\,l^{-1}$ $PdCl_2$ and $4\,g\,l^{-1}$ NaCl dissolved in water. Pd metal can be easily deposited on the Ag surface by this immersion plating using tetrachloropalladate (II)$^{2-}$ ions ($PdCl_4^{2-}$). The reaction of this plating is as follows:

$$PdCl_4^{2-} + 2Ag \rightarrow 2AgCl + Pd + 2Cl^- \tag{5}$$
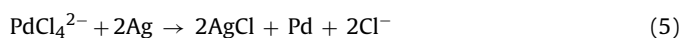
Stainless steel grade, CF-3M, is the cast equivalent of AISI 316 stainless steel. Ag-bearing CF-3M (CF-3M-Ag) steel was melted in a vacuum induction-melting furnace (VIM), and remelted in a vacuum arc remelting furnace (VAR) to ensure homogeneity and cleanliness, and then cast into a round ingot. There was no further heat treatment and rolling process after casting ingots received.

Optical microscopes (OM) and a Jeol 5900 scanning electron microscope (SEM) equipped with an INCA 400 energy dispersive X-ray (EDX) system were applied to characterize the appearance and compositions of surfaces. The compositions of CF-3M-Ag were determined by an SPECTRO X-LAB 2000 X-ray fluorescence spectroscopy (XRF) and a PerkinElmer AAnalyst 300 flame atomic absorption spectroscopy (FAAS).

### 2.2. Microbiological investigations

The samples chosen for the microbiological investigations were AISI 316 stainless steel, pure Ag, CF-3M-Ag, and Ag–Pd. Each sample was cut into a rectangular form with dimensions $7\,mm \times 4\,mm \times 0.5\,mm$.

In order to distinguish the bacterial inhibiting effect from Ag ions release, electrical field, or other electrochemical interactions, the bacterial strains used in this study were Ag-resistant *E. coli J53 [pMG101]* [29] and Ag-sensitive *E. coli SAR18 [R1drd19]*. ABTG medium (Table 1) was used to cultivate biofilms and planktonic bacteria. Each bacterial culture (Ag-resistant *E. coli* and Ag-sensitive *E. coli*) was initially controlled at $10^6$ to $10^7$ CFU ml$^{-1}$ (colony forming units) and incubated together with test samples in an incubation plate with 5 ml ABTG medium at 37 °C, and slowly shaken for 24 h.

**Table 1**
Composition of ABTG medium

| 100 ml A-10 | 900 ml BT-media | 25 ml 20% Glucose |
|---|---|---|
| 20 g $(NH_4)_2SO_4$ | 1 ml, 1 M $MgCl_2$ | 200 g glucose |
| 60 g $Na_2HPO_4$ | 1 ml, 0.1 M $CaCl_2$ | 800 ml $H_2O$ |
| 30 g $KH_2PO4$ | 1 ml, 0.01 M $FeCl_3$ | |
| 30 g NaCl | 2.5 ml, 1 g l$^{-1}$ thiamin | |
| 1000 ml $H_2O$ | 900 ml $H_2O$ | |

#### 2.2.1. Evaluation of inhibiting effects on biofilm cells

Biofilm formation on surfaces was investigated by the use of a ZEISS LSM 510 META confocal laser scanning microscope (CLSM), and the LIVE/DEAD® BacLight Bacterial Viability Assay (Molecular Probes), which utilizes the green fluorescent SYTO® 9 for staining of live cells, and the red fluorescent propidium iodide for staining of dead cells.

#### 2.2.2. Evaluation of inhibiting effects on planktonic cells

To evaluate the inhibiting effect of test samples on planktonic *E. coli* after 24 h incubation, a plain-plate dilute method was conducted to count the numbers of live planktonic *E. coli* (CFU ml$^{-1}$) in the ABTG medium. The bacterial medium from each test was diluted by 0.9% NaCl solution, and then spared on an agar plate. These agar plates were incubated at 37 °C for 24 h. After that, colony-forming units were measured.

#### 2.2.3. Analysis of Ag concentration in bacterial media

After the microbiological investigations, the spent bacterial ABTG media taken from the tests of Ag, CF-3M-Ag, and Ag–Pd were diluted, acidified (nitric acid), and then boiled on a heating plate to make a clear solution for Ag concentration analyses. Total Ag in media were analyzed by a JOBIN YVON JY38S inductively coupled plasma optical emission spectrometry (ICP-OES) and a PerkinElmer SIMA 6000 graphite furnace atomic absorption spectrometry (GFAAS).

### 2.3. Galvanic current measurements

The purpose of this test was to investigate whether the coupling of Ag and Pd, and Ag and 316 stainless steel electrodes, can electrochemically oxidize organic compounds or not. Therefore, the couplings were tested to measure the Faradic current introduced by the addition of organic compounds to simulate bacteria in an electrolyte. The electrodes were connected through a zero resistance ammeter (ZRA). The area ratio was about 2.5:1 for Ag to Pd, and was about 1:1 for Ag to 316. These tests used 1 M sodium acetate pH 7 containing 3.0 wt.% NaCl solutions, and were carried out in a cell with 400 ml volumes, stirred with oxygen (purity ≥99.99%) at ambient temperature. After stabilization of the measured current, 0.04 moles of paraformaldehyde (HCHO) to simulate bacteria or organic species were added. If HCHO can be oxidized on the surfaces of electrodes, an increased Faradic current will be measured.

## 3. Results and discussion

### 3.1. Characterization of samples

The SEM micrograph of the Ag–Pd surface (Fig. 3) shows that the surface was formed with numerous discrete areas, where the distance between two adjacent areas was less than 5 μm. Based on the EDX analysis (Table 2), Pd was deposited in a very thin layer with micro-holes on top of Ag, and Ag was formed as the light microclusters of AgCl during the deposition.

The CF-3M-Ag steel contained 0.09 wt.% Ag (Table 3). Fig. 4(a) shows that CF-3M-Ag had a duplex structure consisting of delta (δ) ferrite and austenite phases. The retained δ-ferrite was formed

**Table 2**
Average composition of Ag–Pd surface

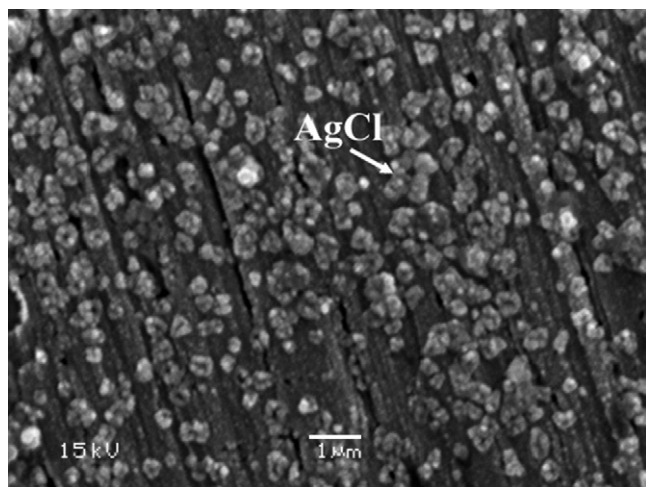| Wt.% | Light cluster | Dark area |
|---|---|---|
| Ag | 95.4 | 94.2 |
| Cl | 2.5 | 1.2 |
| Pd | 2.0 | 4.7 |

Fig. 3. SEM micrograph of Ag–Pd surface.

**Table 3**
Composition of CF-3M-Ag steel

|    | Wt.% |
|----|------|
| C  | 0.016 |
| Si | 0.35 |
| Mn | 1.40 |
| P  | 0.026 |
| S  | 0.002 |
| Ni | 12.70 |
| Cr | 17.10 |
| Mo | 2.12 |
| Ag | 0.092 |
| Fe | Bal. |



Fig. 4. Micrographs of CF-3M-Ag stainless steel: (a) optical microscope and (b) back-scattering electron images.

during solidification [30,31]. Because Ag precipitates on the passive film were too small to be observed by OM, back-scattering electron images (BEI) were applied as shown in Fig. 4(b). Since the atomic weight of Ag is larger than that of iron (Fe), bright particles of Fig. 4(b) indicate the positions where Ag particles precipitated. These Ag precipitates were confirmed by EDX. Ag can be mostly observed in δ-ferrite because the solubility of Ag in the δ-ferrite is lower than that in the austenite [32].

### 3.2. Microbiological investigations

#### 3.2.1. Inhibiting effects on biofilm E. coli

Figs. 5 and 6 show the ability of the *E. coli* strains to form biofilm on the different surfaces. Fig. 5(a–c) shows microcolonies (biofilm) which mainly consist of live Ag-resistant *E. coli* (brighter green fluorescence indicates live *E. coli*; darker green is background noise) that were formed on 316, Ag, and CF-3M-Ag surfaces, respectively. Only few dead Ag-resistant *E. coli* (red fluorescence) were observed. These experiments suggest that there was no direct bacterial inhibiting effect for Ag-resistant *E. coli* on these surfaces. Fig. 5(d) in contrast shows that Ag–Pd surface had a direct inhibiting effect that stopped the formation of microcolonies for Ag-resistant *E. coli* attaching to the surface.

Surprisingly high Ag concentrations were found after tests in the spent ABTG media of Ag-resistant *E. coli* compared to those from Ag-sensitive *E. coli* tests (Fig. 7). In the following discussion it was assumed that all Ag was present as Ag ions in media, although the analyses measured Ag compounds in total and not only dissolved ions. In Fig. 7 for Ag-resistant *E. coli*, it shows that Ag–Pd and CF-3M-Ag had higher Ag release than pure Ag. This effect of increased Ag release rate can be explained by the inter-
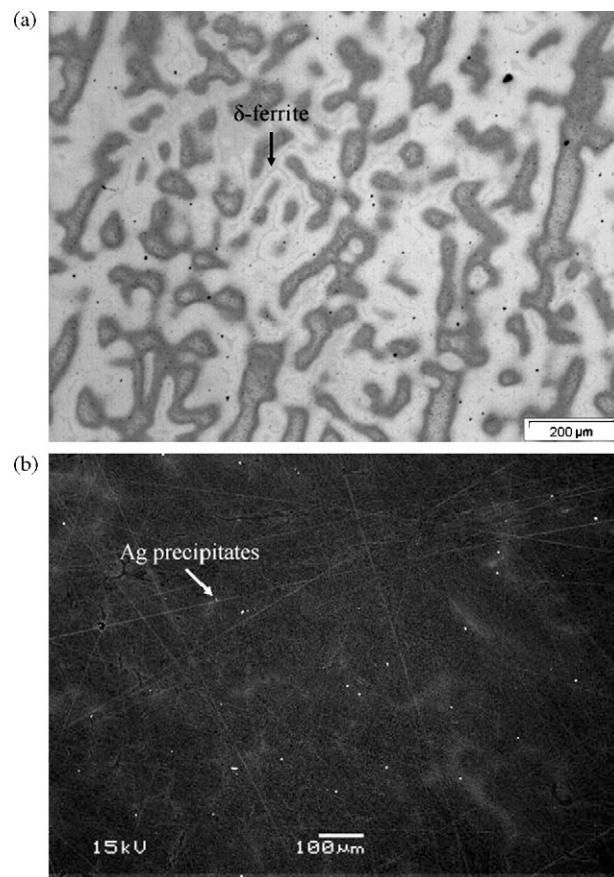
actions between bacterial metabolism and sample surfaces while Ag-resistant *E. coli* approached or attached to surfaces or microcolonies formed on surfaces (Fig. 5) which led to the formation of compounds aggressive to Ag as well as the galvanic effect of Ag/Pd and Ag/steel matrix couplings giving a risk of increased Ag release.

As shown in Fig. 7 for Ag-sensitive *E. coli*, it was also found that undesired high concentrations Ag release during the test of Ag–Pd. This undesired effect can be explained by aggressive ammonium ($NH_4^+$) in the ABTG medium in combination with the galvanic effect of Ag and Pd coupling as given in the following reaction:

$$AgCl + 2NH_4^+ + 2OH^- \rightarrow Ag(NH_3)_2^+ + Cl^- + 2H_2O \tag{6}$$
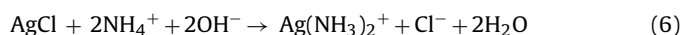
In the galvanic series between Ag and 316 stainless steel (passive), in saline environment [33], Ag is relatively nobler than 316 stainless steel, and therefore Ag of CF-3M-Ag is not expected to be released from the steel in that media. However, if compounds aggressive to Ag, such as ammonium, are formed through the bacterial metabolism or the interaction between bacterial microcolonies and metal surfaces, or these compounds are present in the environment, Ag can become relatively more active than the steel matrix, and then Ag can be released. This can explain a high Ag release rate from CF-3M-Ag as Ag becomes more active when microcolonies of Ag-resistant *E. coli* formed on its surface. On the other hand, the inhibiting effect of Ag-bearing steel caused by Ag ions release will then be limited or reduced in an aquatic environment with low concentration of compounds aggressive to Ag or low degree of bacterial activity near its surface.

Fig. 6 shows that microcolonies of Ag-sensitive *E. coli* only formed on the 316 surface. Fig. 6(b) and (c) shows the Ag-sensitive *E. coli* were inhibited, when they approached to Ag-bearing sur-
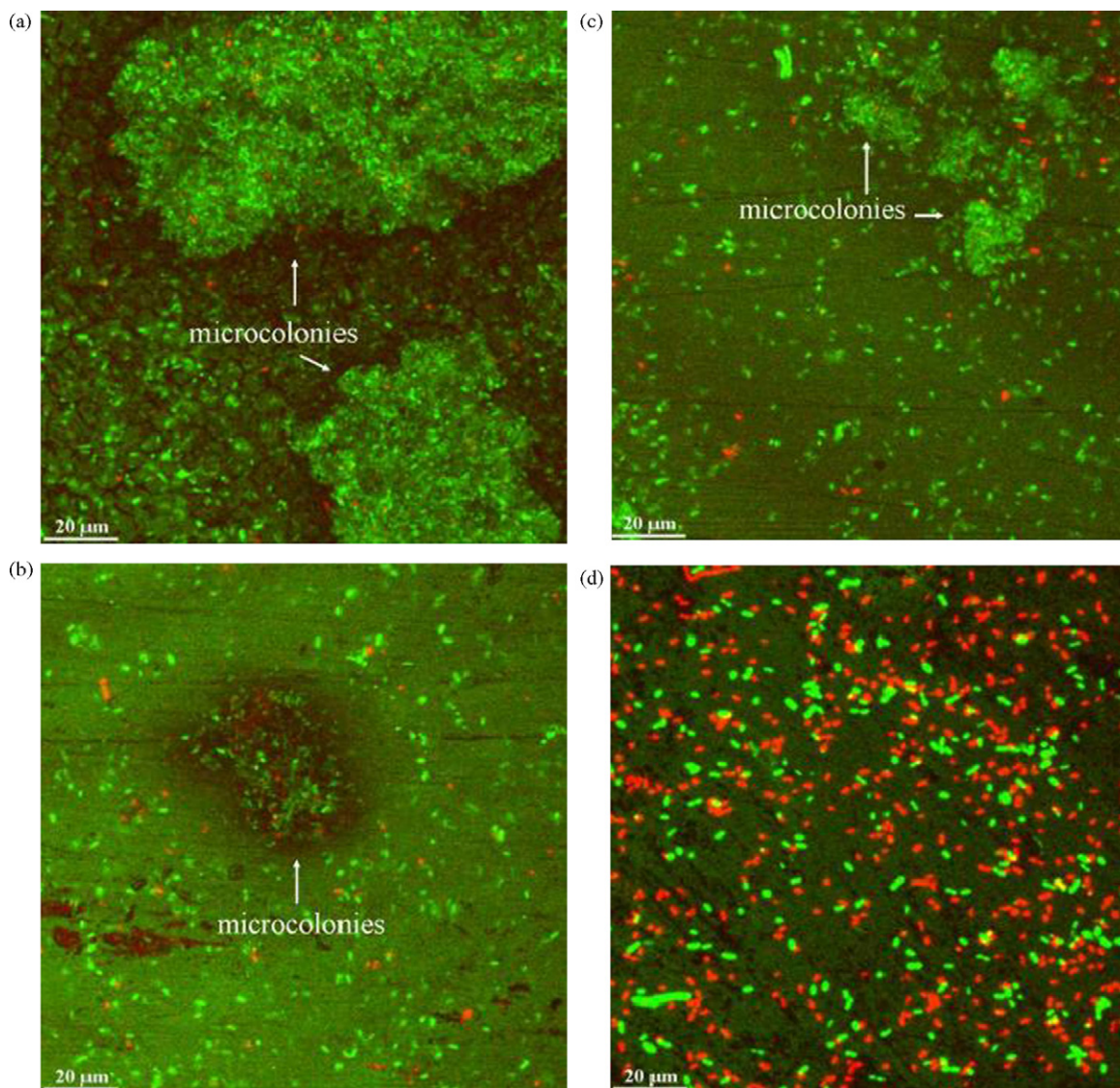
**Fig. 5.** CLSM micrographs for Ag-resistant *E. coli* on the surfaces of (a) 316 stainless steel, (b) Ag, (c) CF-3M-Ag, and (d) Ag–Pd after 24 h in the ABTG medium.

faces. Fig. 6(c) shows that the red patterns fitted the area where Ag precipitates were in the CF-3M-Ag surface (Fig. 4). In Fig. 6(b and c) and Fig. 7 (Ag-sensitive *E. coli*), the data indicate that the inhibiting effect for Ag-sensitive *E. coli* on pure Ag and CF-3M-Ag was even high local Ag ions concentration at their surfaces. On the Ag–Pd surface as shown in Fig. 6(d), there was no direct inhibiting effect in terms of killing bacteria, but only few live Ag-sensitive *E. coli* can be observed and no microcolonies formed. It can be explained by a high Ag concentration in the medium inhibiting planktonic Ag-sensitive *E. coli* before approaching to the Ag–Pd surface.

### 3.2.2. Inhibiting effects on planktonic E. coli

Fig. 8(a) shows that the planktonic Ag-resistant *E. coli* can still grow up at least two log increases on all tests, even in an environment with $700\,\mu g\,l^{-1}$ Ag concentration (Ag–Pd). The analytical techniques of ICP-OES and GFAAS gave the total concentration of Ag compounds and dissolved Ag ions in solution, so it cannot be determined from these analyses, if all $700\,\mu g\,l^{-1}$ were present as Ag ions. In any case the result suggests that Ag-resistant *E. coli* were quite silver tolerant and that inhibiting effect on biofilm (Fig. 5) cannot be attributed to Ag ions release, but probably can be explained from the electrochemical interaction and/or electrical field between Pd,

Ag/AgCl, and bacteria. As combined with the results as shown in Fig. 5, it can be evident that the reactions between the catalytic metals, Pd and Ag, combined with organic environment, can inhibit Ag-resistant *E. coli* by electrochemical interactions and/or electrical field. However, it could be argued that the inhibition of Ag-resistant *E. coli* on the Ag–Pd surface may be caused by an even higher local Ag ions concentration at the surface. In the previous investigations of Ag–Pd surfaces in cold tap water with naturally occurring bacteria (approximately $400\,\mathrm{CFU}\,\mathrm{ml}^{-1}$)[21], the toxic property of Ag ions could not explain the inhibiting effects found since the concentration of Ag was less than $10\,\mu g\,l^{-1}$. To obtain a bacterial inhibiting effect from Ag ions, a minimum content of $30$–$125\,\mu g\,l^{-1}$ is necessary [9]. The results from previous studies [21] and these studies indicate that the bacterial inhibiting effects can be obtained from electrochemical interactions and/or electrical field on Ag–Pd surfaces supplementary to than Ag ions release.

Fig. 8(b) shows that the planktonic Ag-sensitive *E. coli* can grow up in the tests of 316, Ag, and CF-3M-Ag. Combined with Fig. 7, this shows that either the concentration of Ag ions in the medium was not high enough to inhibit these planktonic Ag-sensitive *E. coli*, or that the Ag concentrations analyzed by ICP and GFAAS was not present as reactive Ag ions. In Fig. 6, it can be seen that Ag-sensitive
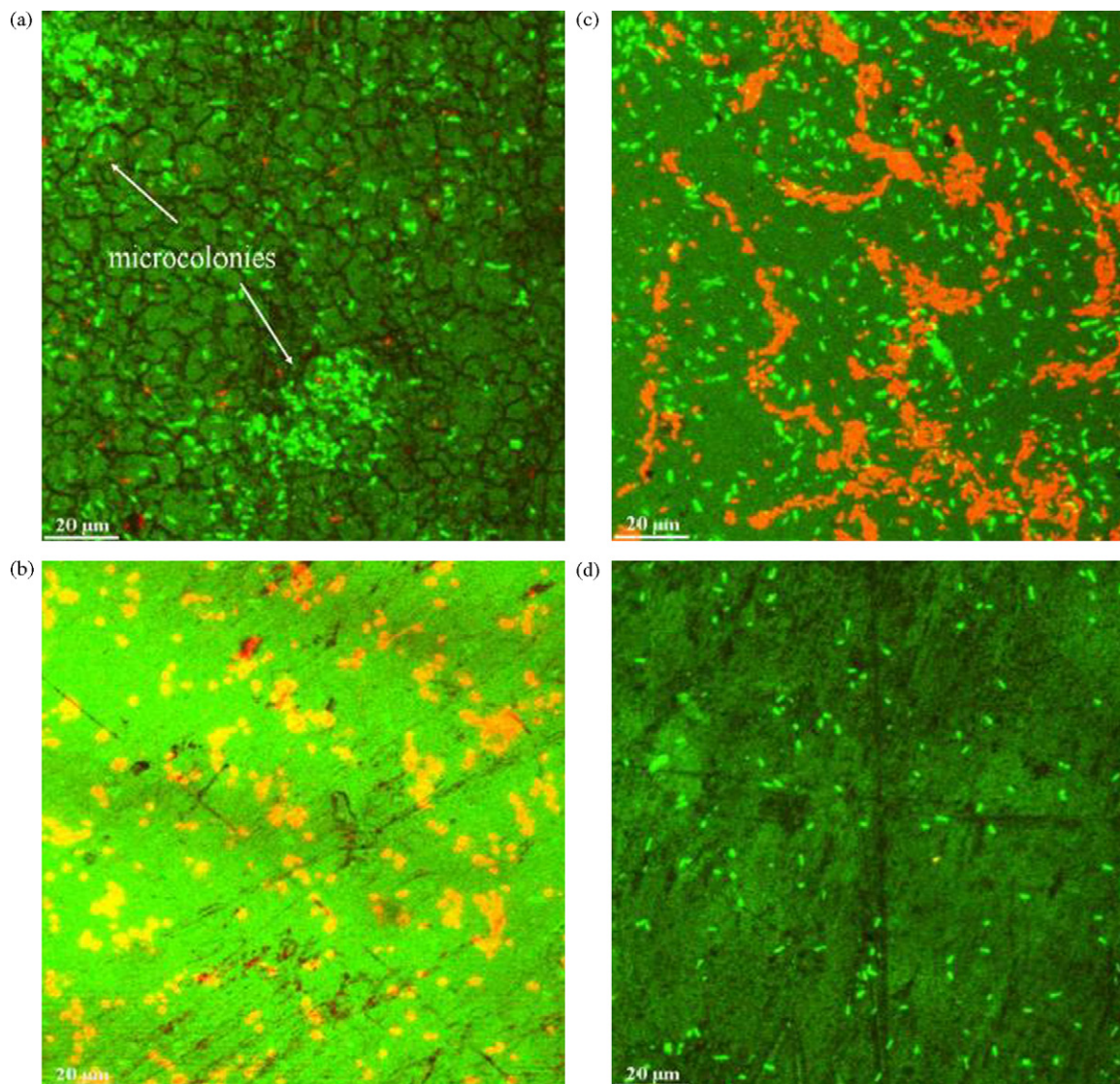
**Fig. 6.** CLSM micrographs for Ag-sensitive *E. coli* on the surfaces of (a) 316 stainless steel, (b) Ag, (c) CF-3M-Ag, and (d) Ag–Pd after 24 h in the ABTG medium.

*E. coli* in the tests of Ag and CF-3M-Ag can only be inhibited, when they approached to the surface, because of higher local Ag ions concentration at the surfaces.

### 3.3. Galvanic current measurements

For galvanic current measurement, the current flow direction was determined by the relative polarity between two electrodes, and the connecting method of positive and negative sides of a ZRA to two electrodes. Fig. 9(a) shows the galvanic current from the coupling of Ag and Pd electrodes. The initial current could be due to AgCl being developed on Ag surfaces by the coupling with Pd that will increase the potential. After 20 h, 0.04 mol HCHO were added, and the current gradually increased to the highest values of 0.7 μA, and then gradually reduced to the steady state again. Thus, the additions of organic compounds, such as HCHO, can work as a fuel source on surfaces. This current increase after HCHO added to the solution can be explained by the reactions as follows:
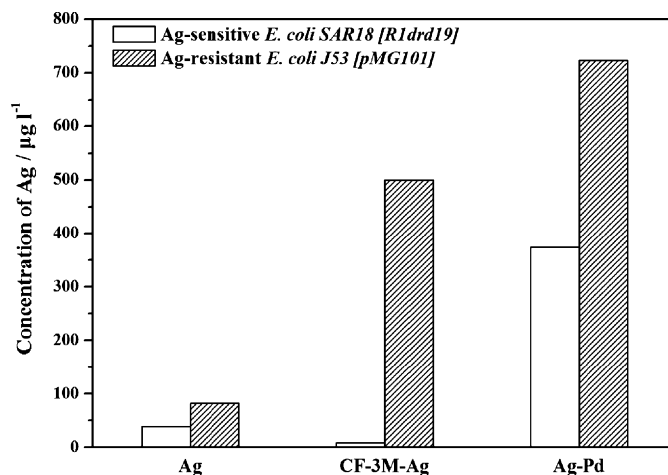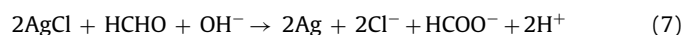
$$2AgCl + HCHO + OH^- \rightarrow 2Ag + 2Cl^- + HCOO^- + 2H^+ \qquad (7)$$



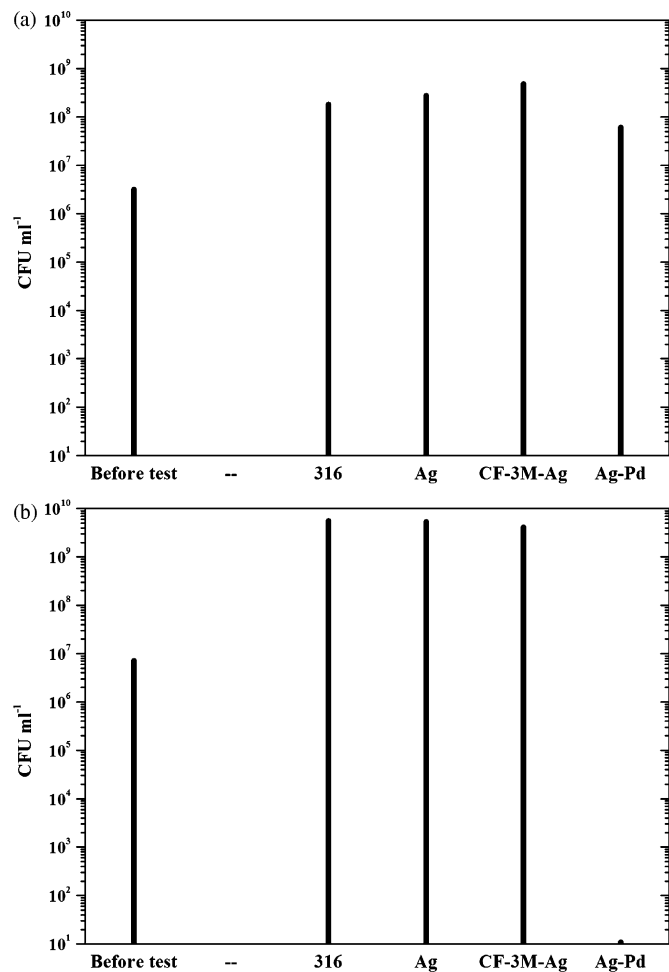**Fig. 7.** Concentration of Ag after 24 h in the ABTG medium.

(a)

(b)

**Fig. 8.** Colony forming numbers after 24 h in the ABTG medium: (a) planktonic Ag-resistant *E. coli* and (b) planktonic Ag-sensitive *E. coli*.



(a)

(b)

**Fig. 9.** Galvanic current from the couplings of (a) Ag and Pd electrodes and (b) Ag and 316 electrodes, before and after addition of 0.04 mol HCHO.

On the Ag/AgCl interface, AgCl was reduced to Ag, and HCHO was oxidized to formic acid or formate. Then, due to the galvanic coupling between Ag and Pd, AgCl can be regenerated on the Ag electrode, and provide an increased Faradic current (Eq. (3)). The reduction of $O_2$ can be carried out on the Pd electrode (Eq. (4)). In this test, it evidenced that the bacterial inhibiting reaction caused by Ag/AgCl electrochemical interactions can continuously happen if bacteria, acting as organic compounds, are supplied to the surface.

On the other hand, an increased Faradic current could also be explained by the reaction of HCHO oxidation directly on the Ag surface without any interaction with AgCl.

$$2HCHO + O_2 \rightarrow 2HCOO^- + 2H^+ \tag{8}$$

In this case, the reduction of $O_2$ (cathodic partial reaction) can be carried out on the Pd electrode (Eq. (4)), and the anodic partial reaction of Eq. (8) is as follows:

$$2HCHO + 4OH^- \rightarrow 2HCOO^- + 2H^+ + 2H_2O + 4e^- \tag{9}$$

For the coupling of Ag and 316 stainless steel electrodes, the current decreases and approaches zero. In this solution, the 316 stainless steel electrode was less noble and thus the anode, so this current decrease can be explained by passivation. There was no increased Faradic current that can be measured after HCHO was added as shown in Fig. 9(b). It means that this coupling cannot electrochemically oxidize organic compounds.
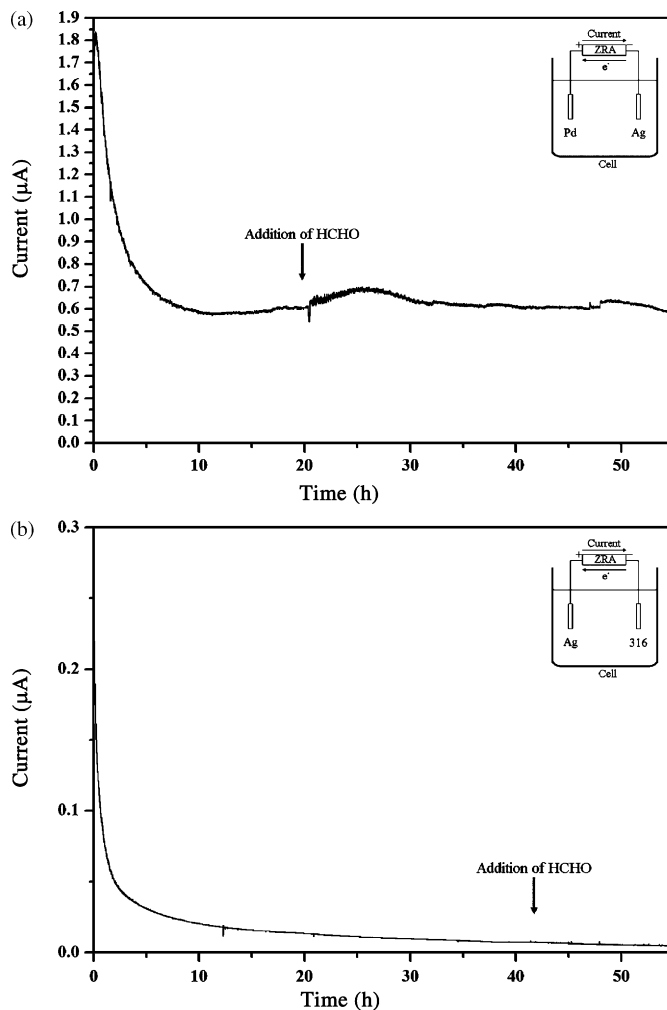
## 4. Conclusions

1. Ag surfaces can be structured by plating treatments with palladium for the formation of small catalytic areas, where a cathodic reaction can take place. It was shown that the Ag–Pd surface has an inhibiting effect on biofilm formation of Ag-resistant *E. coli* in ABTG media. The inhibiting effect caused by Ag ions release cannot explain the effect found in these results. It was evident that the inhibiting effects can be caused by electrochemical interactions and/or electrical field between the catalytic Pd and Ag combined with an organic and bacterial environment. However, the mechanisms for inhibiting bacterial growth on the Ag–Pd surface were also not fully clarified in this study. In some specific media, such as ABTG, with aggressive compounds like ammonium, undesired Ag ions release can occur and add to the inhibiting effect.

2. For Ag-bearing stainless steel as well as pure Ag surfaces investigated in this study, it was shown that the bacterial inhibiting effect can only be caused by a high local Ag ions release and that no effect was found on Ag-resistant *E. coli*. According to the galvanic series between Ag and 316 stainless steel in saline environment, Ag is nobler than 316 stainless steel, and therefore Ag should not be released from the Ag-bearing stainless steel. The galvanic current measurement also showed that the coupling of Ag and 316 stainless steel cannot electrochemically oxidize

organic compounds. However, if compounds aggressive to Ag are present, or are formed through the interaction of bacterial metabolism and metal surfaces, Ag ions can be released from the steel matrix. Therefore, the specific media and the organic loads are important parameters in evaluating the effectiveness of Ag-bearing stainless steels.

## References

[1] J.W. Costerton, Z. Lewandowski, D.E. Caldwell, D.R. Korber, H.M. Lappin-Scott, Annu. Rev. Microbiol. 49 (1995) 711.
[2] J.W. Costerton, Int. J. Antimicrob. Ag. 11 (1999) 217.
[3] J.W. Costerton, in: M. Ghannoum, G.A. O'Toole (Eds.), Microbial Biofilms, ASM Press, Washington, DC, 2004, Ch. 1.
[4] A.D. Russel, W.B. Hugo, Prog. Med. Chem. 31 (1994) 351.
[5] J.M. Schierholz, L.J. Lucas, A. Rump, G. Pulverer, J. Hosp. Infect. 40 (1998) 257.
[6] M. Hjelm, L.R. Hilbert, P. Møller, L. Gram, J. Appl. Microbiol. 92 (2002) 903.
[7] S.L. Percival, P.G. Bowler, D. Russell, J. Hosp. Infect. 60 (2005) 1.
[8] N. Grier, in: S.S. Block (Ed.), Disinfection, Sterilization, and Preservation, 3rd ed., Lea & Febiger, Philadelphia, PA, 1983, Ch. 18.
[9] T.J. Berger, J.A. Spadaro, S.E. Chapin, R.O. Becker, Antimicrob. Agents Chemother. 9 (1976) 357.
[10] K.H. Cho, J.E. Park, T. Osaka, S.G. Park, Electrochim. Acta 51 (2005) 956.
[11] L.R. Hilbert, D. Bagge-Ravn, J. Kold, L. Gram, Int. Biodeter. Biodegr. 52 (2003) 175.
[12] D.A. Webster, J.A. Spadar, S. Kramer, R.O. Becker, Clin. Orthop. 161 (1981) 105.
[13] P. Stoodley, D. deBeer, H.M. Lappin-Scott, Antimicrob. Agents Chemother. 41 (1997) 1876.
[14] A. Kerr, T. Hodgkiess, M.J. Cowling, C.M. Beveridge, M.J. Smith, A.C.S. Parr, J. Appl. Microbiol. 85 (1998) 1067.
[15] P.S. Stewart, W. Wattanakaroon, L. Goodrum, S.M. Fortun, B.R. McLeod, Antimicrob. Agents Chemother. 43 (1999) 292.
[16] B.R. McLeod, S. Fortun, J.W. Costerton, P.S. Stewart, Methods Enzymol. 310 (1999) 656.
[17] R.L. Davies, S.F. Etris, Catal. Today 36 (1997) 107.
[18] I. Alvarez, R. Virto, J. Raso, S. Condon, Innovat. Food Sci. Emerg. Technol. 4 (2003) 195.
[19] S.Y. Tseng, Pulsed electric field generators for food sterilization, Ph.D. Thesis, National Chung Cheng University, Chiayi, Taiwan, 2005.
[20] M.T. Madigan, J.M. Martinok, Brock Biology of Microorganisms, 11th ed., Prentice Hall, Upper Saddle River, NJ, 2005, p. 772.
[21] P. Møller, L.R. Hilbert, C.B. Corfitzen, H.J. Albrechtsen, J. Appl. Surf. Finish. 2 (2007) 149.
[22] T.E. Graedel, J. Electrochem. Soc. 139 (1992) 1963.
[23] M.V. ten Kortenaar, J.J.M. de Goeij, Z.I. Kolar, G. Frens, P.J. Lusse, M.R. Zuiddam, E. van der Drift, J. Electrochem. Soc. 148 (2001) C28.
[24] W.C. Liang, A study of the antibacterial property of the SUS430 stainless steel containing copper, Master Thesis, National Taiwan University, Taipei, Taiwan, 2000.
[25] I.T. Hong, C.H. Koo, Mater. Sci. Eng. A 393 (2005) 213.
[26] J. Yang, D. Zou, X. Li, J. Zhu, Mater. Sci. Forum 510/511 (2006) 970.
[27] K.R. Sreekumari, K. Nandakumar, K. Takao, Y. Kikuchi, ISIJ Int. 43 (2003) 1799.
[28] P. Møller, E.O. Jensen, L.R. Hilbert, US Patent US2,006,003,019 (2006).
[29] A. Gupta, L.T. Phung, D.E. Taylor, S. Silver, Microbiology 147 (2001) 3393.
[30] N. Suutala, T. Takalo, T. Moisio, Metall. Trans. A 11 (1980) 717.
[31] G.K. Allan, Ironmak. Steelmak. 22 (1995) 465.
[32] L.J. Swartzendruber, ASM Handbooks, vol. 3, ASM International, Materials Park, OH, 2003.
[33] D.A. Jones, Principles & Prevention of Corrosion, 2nd ed., Prentice Hall, Upper Saddle River, NJ, 1996, Ch. 1.

Appendix III

# Anti-biofilm properties of a silver-palladium surface

Applied and Environmental Microbiology, 2009

# Silver-Palladium Surfaces Inhibit Biofilm Formation[▽]

Wen-Chi Chiang,[1] Casper Schroll,[1] Lisbeth Rischel Hilbert,[1] Per Møller,[1] and Tim Tolker-Nielsen[2]*

*Department of Mechanical Engineering, Technical University of Denmark, DK-2800 Kongens Lyngby, Denmark,[1] and Department of International Health, Immunology and Microbiology, Faculty of Health Sciences, University of Copenhagen, DK-2200 Copenhagen N, Denmark[2]*

**Undesired biofilm formation is a major concern in many areas. In the present study, we investigated biofilm-inhibiting properties of a silver-palladium surface that kills bacteria by generating microelectric fields and electrochemical redox processes. For evaluation of the biofilm inhibition efficacy and study of the biofilm inhibition mechanism, the silver-sensitive *Escherichia coli* J53 and the silver-resistant *E. coli* J53[pMG101] strains were used as model organisms, and batch and flow chamber setups were used as model systems. In the case of the silver-sensitive strain, the silver-palladium surfaces killed the bacteria and prevented biofilm formation under conditions of low or high bacterial load. In the case of the silver-resistant strain, the silver-palladium surfaces killed surface-associated bacteria and prevented biofilm formation under conditions of low bacterial load, whereas under conditions of high bacterial load, biofilm formation occurred upon a layer of surface-associated dead bacteria.**

Undesired biofilm formation is a major concern in many areas, such as medical settings, water distribution systems, and the food industry. Bacteria in biofilms are more tolerant to disinfecting operations and antibiotic therapies than planktonic bacteria, making these treatments less effective or ineffective (5, 6, 7, 8, 19, 24, 28). Biofilm formation on medical implants causes significant problems, and currently the only effective method for curing implant-associated biofilm infections involves replacement of the implant (8, 18). Biofilms in food-processing plants and in water distribution systems may harbor pathogens, causing hygienic risks, and may cause other adverse effects, such as material corrosion (9, 15, 19, 26, 28).

It is of high priority to develop methods or compounds for combating biofilms. Small molecules that may affect the bacteria and inhibit critical steps in biofilm formation as well as different surface coatings that may inhibit biofilm formation are among the strategies that have been actively pursued (10, 11). Different kinds of physical treatments have also been investigated as potential means of inhibiting biofilm formation. For example, recent studies have shown that biofilm formation can be inhibited by applying an electric field or current on a particular surface (6, 27). It has also been reported that the efficacy of antibiotics against biofilm bacteria can be increased if the antibiotics are given in combination with an applied electric current (6, 27). However, in many areas, applying electric potential or current on a surface is not feasible.

In the present report we investigate biofilm-inhibiting properties of a silver-palladium (Ag-Pd) surface. The Ag-Pd surface has been described previously (20, 21), and preliminary results of thermodynamic calculations, electrochemical tests, and antimicrobial activity have been published (2, 3). The design of the Ag-Pd surface is based on Ag upon which Pd is incom-

pletely deposited as a microhole-structured layer, partially exposing Ag through the microholes (21). Due to the potential difference between Ag and Pd (200 mV in water) (21), Ag and Pd on the surface can be regarded as two discrete electrodes (anode and cathode), and the surface can have numerous discrete anodic and cathodic areas, generating numerous microelectric fields that may kill bacteria that approach the surface. The designed distance between Ag and Pd is less than 5 μm to ensure a high local strength of the microelectric fields because a potential difference over a short distance can give high field strengths (~100 mV/μm). In addition to the effects of the microelectric fields, the Ag-Pd surface can also kill bacteria via redox processes. Some Ag can react to form silver chloride (AgCl) during Pd deposition. Ag ions or AgCl can be reduced to Ag by oxidation of hydroxyl groups on organic species such as surface molecules on bacteria (21, 25). After the oxidation, AgCl can be regenerated in the presence of oxygen (under aerobic conditions), where Ag is oxidized in connection to oxygen reduction on Pd. These back-and-forth redox processes of Ag converting to AgCl and AgCl converting to Ag can continuously happen if hydroxyl groups on bacteria reach an Ag-Pd surface and undergo oxidation.

Here, we report experiments with silver-sensitive and silver-resistant *E. coli* strains which demonstrate that Ag-Pd surfaces can inhibit biofilm formation by killing the bacteria. Experiments in batch and flowthrough systems provide evidence that silver-sensitive bacteria are killed due to a combination of microelectric fields/redox processes on the Ag-Pd surface and release of toxic levels of Ag$^+$ from the Ag-Pd surface, whereas silver-resistant bacteria are killed due to microelectric fields/redox processes on the Ag-Pd surface. In addition, our experiments demonstrate an inherent weakness of antimicrobial surfaces, namely, that they allow biofilm formation upon a conditioning layer under some conditions.

## MATERIALS AND METHODS

**Bacteria and growth conditions.** *Escherichia coli* J53 (13) and *E. coli* J53[pMG101] (12) were used as the silver-sensitive and silver-resistant model

* Corresponding author. Mailing address: Department of International Health, Immunology and Microbiology, Faculty of Health Sciences, University of Copenhagen, DK-2200 Copenhagen N, Denmark. Phone: 45 35326656. Fax: 45 35327853. E-mail: ttn@sund.ku.dk.
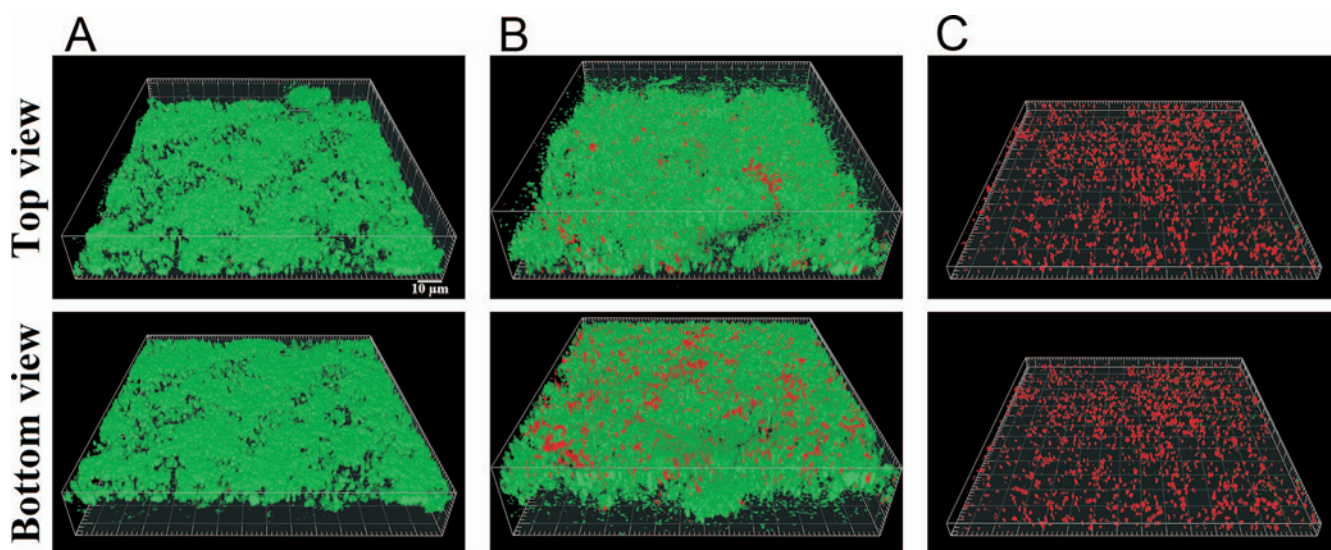▽ Published ahead of print on 16 January 2009.

FIG. 1. CLSM micrographs of batch-grown, 72-hour-old, Live/Dead-stained *E. coli* J53 biofilms on steel (A), Ag (B), and Ag-Pd (C). The top view shows the biofilms from the growth medium side, whereas the bottom view shows the biofilms from the metal coupon side. Green fluorescence indicates live cells, and red fluorescence indicates dead cells. The images are representative of three independent experiments. Bar, 10 μm.

organisms, respectively, in this study. Batch cultivation of *E. coli* was carried out at 37°C in AB minimal medium (4) supplemented with glucose (6.25 g/liter), methionine (25 mg/liter), proline (25 mg/liter), and thiamine (2.5 mg/liter). Flow chamber cultivation of *E. coli* was carried out at 37°C in FAB medium (14) supplemented with glucose (0.125 g/liter), methionine (2 mg/liter), proline (2 mg/liter), and thiamine (0.2 mg/liter).

**Coupon preparation.** To obtain Ag-Pd coupons, Ag (99.9% Ag) plates were treated by immersion plating in palladium chloride solution, which was prepared from 0.5 g/liter $PdCl_2$ and 4/g liter NaCl dissolved in water. The coupons of stainless steel grade AISI 316L (approximately 68.7% Fe, 16.9% Cr, 10.16% Ni, and 2.02% Mo) and Ag (99.9% Ag) were used as controls. The sizes of the coupons of Ag-Pd, steel, and Ag were 4 mm by 7 mm by 0.5 mm (for batch assays) and 2 mm by 14 mm by 0.5 mm (for flow chamber assays).

**Cultivation of biofilms in batch assays.** The batch assays for biofilm cultivation were performed in multiwell dishes. Each coupon was placed in a well of a multiwell dish; 5 ml of *E. coli* overnight cultures diluted 100-fold was transferred to each well, and the multiwell plates were incubated at 37°C with shaking at 60 rpm for 72 h. Prior to microscopic investigation, the spent medium was removed from the wells, and fresh AB minimal medium was added, after which Live/Dead stain was added as described below. For the determination of the number of CFU in the 72-h multiwell cultures, vigorously vortexed serial dilutions of cell suspensions were plated on LB (1) agar plates, and colonies were counted after 30 h of incubation at 37°C.

**Cultivation of biofilms in continuous flow chamber assays.** The flow chamber systems for biofilm cultivation were assembled and prepared as described previously (23). Each coupon was installed in a flow chamber that was subsequently inoculated by injecting 250 μl *E. coli* overnight culture diluted 100-fold using a small syringe. After inoculation, adhesion of cells to the coupon surfaces was allowed for 1 h without flow, and afterwards FAB medium was started to flow through the chambers at a mean flow velocity of 0.2 mm/s, corresponding to laminar flow with a Reynolds number of 0.02, using a Watson Marlow 205S peristaltic pump (Watson Marlow, United Kingdom). Biofilms were investigated microscopically after 24 and 72 h.

**Microscopy and image acquisition.** Biofilms on the coupon surfaces were observed by the use of a Zeiss LSM 510 META (Carl Zeiss, Germany) confocal laser scanning microscope (CLSM) and staining with the Live/Dead BacLight Bacterial Viability Assay (Invitrogen), which utilizes green fluorescent SYTO 9 (Invitrogen) for staining of cells (5 μM for batch-grown biofilms and 5 μM for flow chamber-grown biofilms), and red fluorescent propidium iodide (Sigma, Germany) for staining of membrane-compromised cells (40 μM for batch-grown biofilms and 20 μM for flow-chamber-grown biofilms). Although we cannot exclude that some propidium iodide-stained cells were membrane compromised but not dead, we have assumed in the following discussion that all propidium iodide-stained cells were dead. Images were obtained using a 63× objective with

a 0.95 numerical aperture for batch assays and a 40× objective with a numerical aperture of 1.30 for flow chamber assays. A 488-nm argon laser was used to excite the SYTO 9-stained cells, and a 543-nm helium/neon laser was used to excite the propidium iodide-stained cells. Simulated three-dimensional images were generated by the use of IMARIS software (Bitplane, Switzerland).

## RESULTS AND DISCUSSION

In order to study a potential biofilm-inhibiting effect of the Ag-Pd surface, metal coupons were placed in the wells of multiwell dishes, and diluted *E. coli* J53 overnight cultures were added to the wells; after incubation for 72 h, bacteria associated with the surface of the metal coupons were stained with the Live/Dead BacLight stain and visualized by the use of CLSM. Metal coupons with steel and Ag surfaces were included as controls along with the coupons with the Ag-Pd surface. As shown in Fig. 1A and B, the bacteria formed biofilms on both the steel surface and the Ag surface, the only apparent difference being that a few dead cells were present close to the Ag surface. In agreement with this finding is a report that metallic Ag has only a slight antimicrobial effect because of its chemical stability (22), and our previous studies have also demonstrated that pure Ag does not have a significant inhibiting effect on biofilm formation (16). Biofilm formation was inhibited, however, on the Ag-Pd coupons that had only a few dead bacteria scattered on the Ag-Pd surface (Fig. 1C). Because Ag-Pd surfaces were shown to release more $Ag^+$ to the surrounding liquid than Ag surfaces (2, 3, 17), we could not exclude the possibility that the bacteria in the wells with the Ag-Pd coupons were killed by the high $Ag^+$ levels. We therefore determined the number of live planktonic bacteria in the wells by plating serial dilutions on LB agar plates and determining the number of CFU after incubation. As shown in Fig. 2, the wells with the steel and Ag coupons contained approximately $10^8$ CFU/ml, whereas no live bacteria were found in the wells with the Ag-Pd coupons. From these experiments we therefore could not conclude whether the lack of biofilm for-
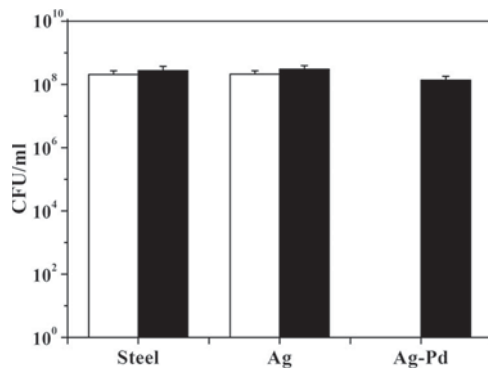
FIG. 2. Effect of steel, Ag, and Ag-Pd coupons on the number of CFU of planktonic *E. coli* cultures after 72 h of batch cultivation. Means and standard deviations (error bars) of three replicates are shown. White bars indicate *E. coli* J53, and black bars indicate *E. coli* J53[pMG101].

mation on the Ag-Pd surface was due to cell killing by microelectric field/redox processes or by $Ag^+$ toxicity.

In an attempt to separate the effects of microelectric field/redox processes from $Ag^+$ toxicity, we employed the silver-resistant strain *E. coli* J53[pMG101]. As shown in Fig. 3, the *E. coli* J53[pMG101] strain formed biofilm on the steel, Ag, and Ag-Pd surfaces. However, unlike the biofilms on the steel and Ag coupons (Fig. 3A and B), the biofilms on the Ag-Pd coupons had a layer of dead cells close to the Ag-Pd surface (Fig. 3C and D). Experiments with shorter incubation times than 72 h indicated that the bacteria were killed shortly after attaching to the Ag-Pd surfaces (Fig. 3E). Determinations of the numbers of CFU showed that the wells with steel, Ag, and Ag-Pd coupons all contained approximately $10^8$ CFU/ml of the *E. coli* J53[pMG101] bacteria (Fig. 2). Taken together, these experiments suggested that the bacteria close to the Ag-Pd
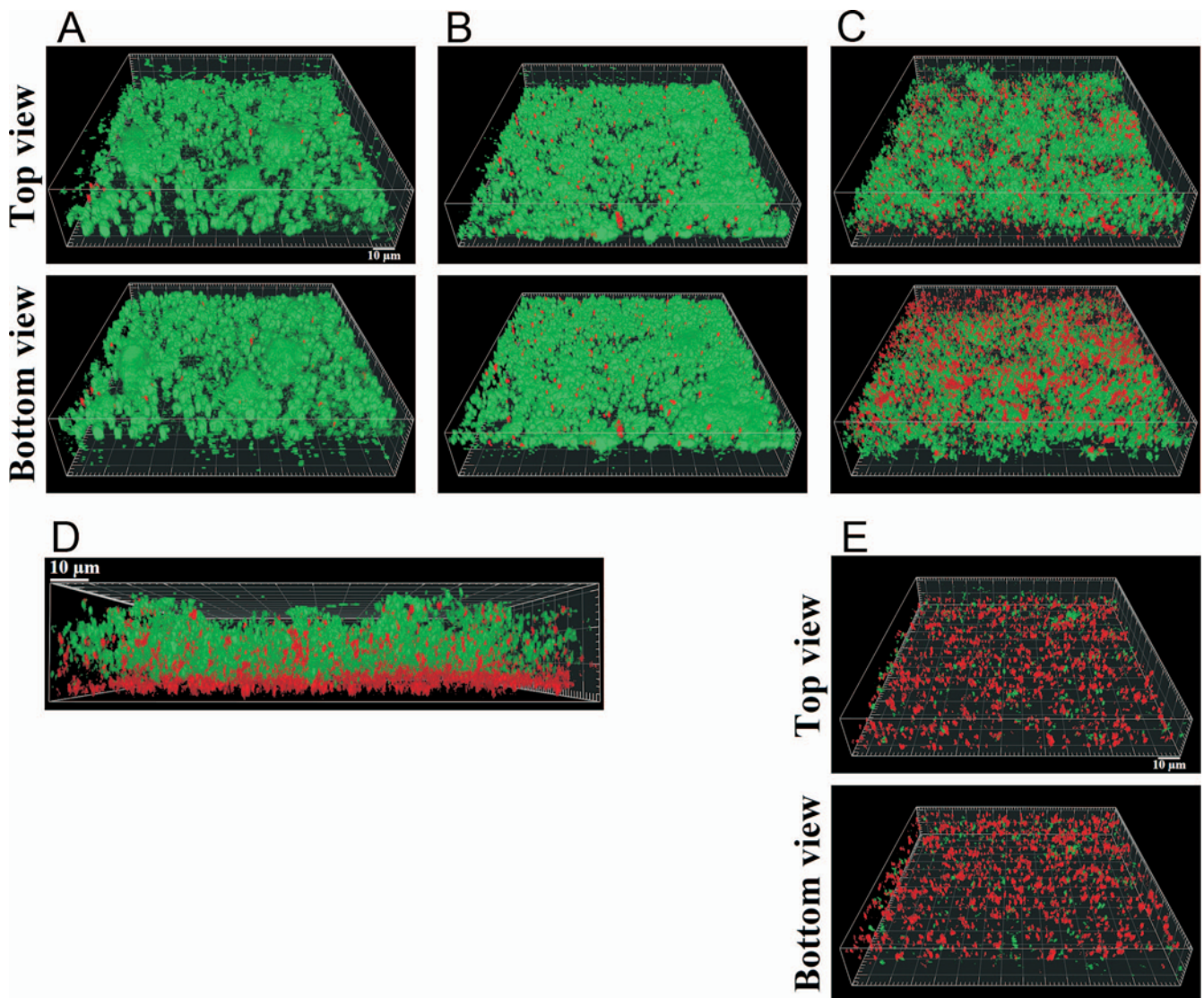


FIG. 3. CLSM micrographs of batch-grown, 72-h-old (A, B, C, and D) or 24-h-old (E), Live/Dead-stained *E. coli* J53[pMG101] biofilms on steel (A), Ag (B), and Ag-Pd (C, D, and E). The top views of A, B, C, and E show the biofilms from the growth medium side, whereas the bottom views of A, B, C, and E show the biofilms from the metal coupon side. Panel D shows a side view of a biofilm with the lower cell layer closest to the Ag-Pd surface. Green fluorescence indicates live cells, and red fluorescence indicates dead cells. The images are representative of three independent experiments. Bar, 10 μm.
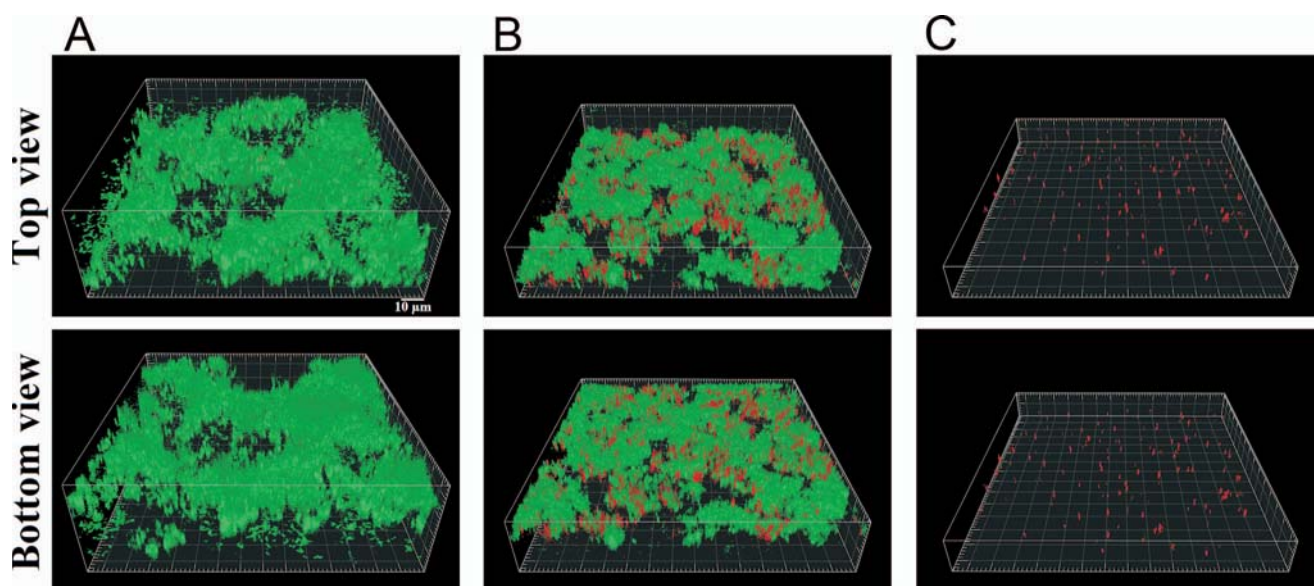
FIG. 4. CLSM micrographs of flow chamber-grown, 72-h-old, Live/Dead-stained *E. coli* J53 biofilms on steel (A), Ag (B), and Ag-Pd (C). The top view shows the biofilms from the growth medium side, whereas the bottom view shows the biofilms from the metal coupon side. Green fluorescence indicates live cells, and red fluorescence indicates dead cells. The images are representative of three independent experiments. Bar, 10 μm.

surface were killed due to the microelectric field/redox processes and that bacteria from the planktonic phase subsequently formed biofilm upon the layer of dead bacteria.

The number of planktonic bacteria in the wells of the multiwell dishes (approximately $10^8$ CFU/ml after 72 h of incubation) is much higher than in most relevant settings. In order to study the effects of the Ag-Pd surface on biofilm formation in a system with a lower bacterial load, we installed metal cou-

pons in flow chambers, inoculated the flow chambers with *E. coli* J53 or *E. coli* J53[pMG101], irrigated the flow chambers with growth medium for 72 h, stained the bacteria with Live/Dead BacLight, and visualized the bacteria by the use of CLSM. As shown in Fig. 4 and Fig. 5, the *E. coli* J53 and *E. coli* J53[pMG101] strains formed biofilms on both the steel and Ag surfaces although the biofilm formed by the *E. coli* J53 strain on the Ag coupon contained a few dead bacteria close to
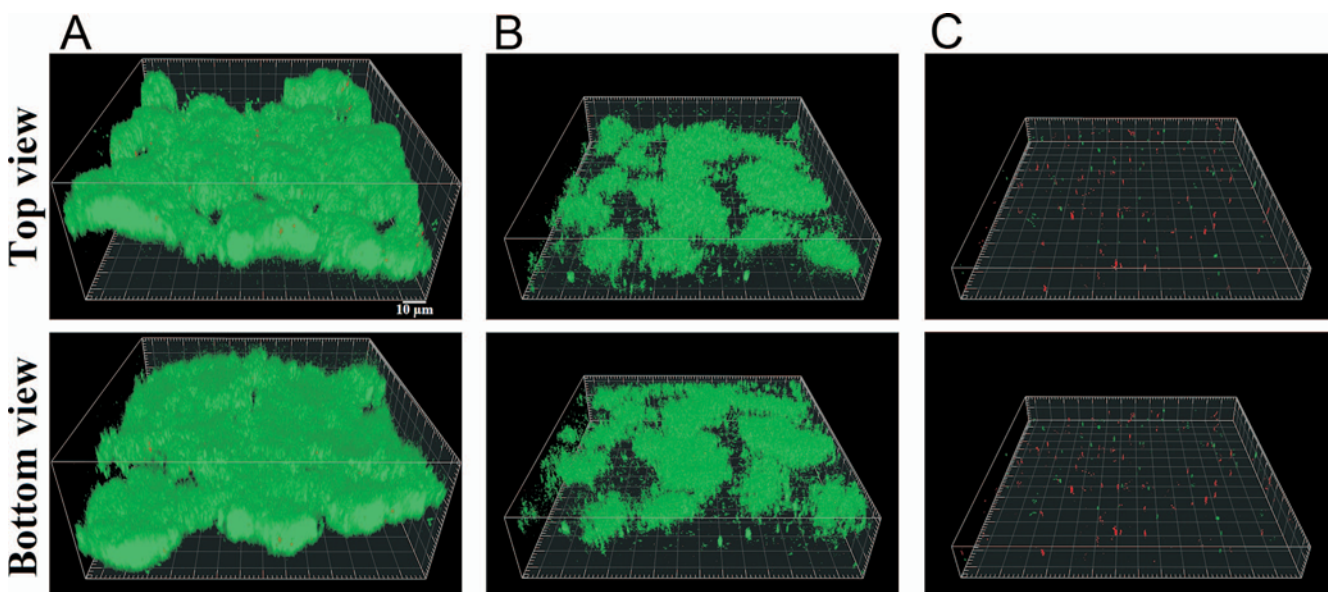


FIG. 5. CLSM micrographs of flow chamber-grown, 72-h-old, Live/Dead-stained *E. coli* J53[pMG101] biofilms on steel (A), Ag (B), and Ag-Pd (C). The top view shows the biofilms from the growth medium side, whereas the bottom view shows the biofilms from the metal coupon side. Green fluorescence indicates live cells, and red fluorescence indicates dead cells. The images are representative of three independent experiments. Bar, 10 μm.

the Ag surface. However, neither *E. coli* J53 nor *E. coli* J53[pMG101] could form biofilm on the Ag-Pd surfaces (Fig. 4C and Fig. 5C). The Ag-Pd coupons had only a few bacteria scattered on the surface. These experiments suggested that biofilm formation is inhibited on Ag-Pd surfaces under conditions where high numbers of bacteria from a planktonic phase cannot continuously initiate biofilm formation.

Although biofilm formation on the flow chamber-installed Ag-Pd coupons was inhibited in the case of both the silver-sensitive *E. coli* J53 strain and the silver-resistant *E. coli* J53[pMG101] strain, the outcomes of the Live/Dead BacLight staining were not identical. In the case of the silver-sensitive *E. coli* J53 strain, all the surface-attached bacteria were red (Fig. 4C) and supposedly dead, whereas in the case of the *E. coli* J53[pMG101] strain, the surface-attached cells were either red or green (Fig. 5C). The fact that some green-stained, and supposedly live, *E. coli* J53[pMG101] cells were present on the flow chamber-installed Ag-Pd coupons might reflect the microheterogeneity of the Ag-Pd surface. The surface may contain some sites where attached *E. coli* J53[pMG101] bacteria can live, but the daughter cells cannot establish on the surface close by and may be shed to the planktonic phase. This implies that the silver-sensitive *E. coli* J53 bacteria, present on the flow chamber-installed Ag-Pd coupons, were all killed either because of the microelectric field/redox processes or a local $Ag^+$ concentration that was higher than these silver-sensitive bacteria could tolerate.

In conclusion, experiments with silver-sensitive and silver-resistant *E. coli* strains showed that Ag-Pd surfaces could inhibit biofilm formation by killing the bacteria. Batch experiments provided evidence that biofilm formation of the silver-sensitive bacteria was inhibited on the Ag-Pd surface due to release of toxic levels of $Ag^+$ in addition to the killing effects of the surface, whereas biofilm formation of the silver-resistant bacteria occurred upon a layer of surface-associated dead bacteria on the Ag-Pd coupons. Unlike the batch setup, where high numbers of silver-resistant planktonic bacteria could continuously initiate biofilm formation, the flow chamber system had a lower bacterial load, and in this system the Ag-Pd surfaces proved efficient in preventing biofilm formation by both silver-sensitive and silver-resistant bacteria. We envision that it may be beneficial to coat, for example, the vulnerable parts of medical implants, medical equipment, water distribution systems, or food production facilities with biofilm-inhibiting Ag-Pd surfaces. However, as biofilm formation evidently can occur if the antimicrobial surface becomes covered with a conditioning layer, the highest efficiency of an Ag-Pd surface would be achieved under conditions where appropriate cleaning practices can be applied.

## REFERENCES

1. **Bertani, G.** 1951. Studies on lysogenesis. I. The mode of phage liberation by lysogenic *Escherichia coli*. J. Bacteriol. **62:**293–300.
2. **Chiang, W. C., L. R. Hilbert, C. Schroll, T. Tolker-Nielsen, and P. Møller.** 2008. Study of electroplated silver-palladium biofouling inhibiting coating. Corrosion Eng. Sci. Technol. **43:**142–148.
3. **Chiang, W. C., L. R. Hilbert, C. Schroll, T. Tolker-Nielsen, and P. Møller.** 2008. Bacterial inhibiting surfaces caused by the effects of silver release and/or electrical field. Electrochim. Acta **54:**108–115.
4. **Clark, D. J., and O. Maaløe.** 1967. DNA replication and the division cycle in *Escherichia coli*. J. Mol. Biol. **23:**99–112.
5. **Costerton, J. W.** 1999. Introduction to biofilm. Int. J. Antimicrob. Agents **11:**217–221.
6. **Costerton, J. W., B. Ellis, K. Lam, F. Johnson, and A. E. Khoury.** 1994. Mechanism of electrical enhancement of efficacy of antibiotics in killing biofilm bacteria. Antimicrob. Agents Chemother. **38:**2803–2809.
7. **Costerton, J. W., Z. Lewandowski, D. E. Caldwell, D. R. Korber, and H. M. Lappin-Scott.** 1995. Microbial biofilms. Annu. Rev. Microbiol. **49:**711–745.
8. **Darouiche, R. O.** 2004. Treatment of infections associated with surgical implants. N. Engl. J. Med. **350:**1422–1429.
9. **Flanders, J. R., and F. H. Yildiz.** 2004. Biofilms as reservoirs for disease, p. 314–331. *In* M. Ghannoum and G. A. O'Toole (ed.), Microbial biofilms. ASM Press, Washington, DC.
10. **Flemming, H. C., T. Griebe, and G. Schaule.** 1996. Antifouling strategies in technical systems—a short review. Water Sci. Technol. **34:**517–524.
11. **Francolini, I., G. Donelli, and P. Stoodley.** 2003. Polymer designs to control biofilm growth on medical devices. Rev. Environ. Sci. Biotechnol. **2:**307–319.
12. **Gupta, A., K. Matsui, J. F. Lo, and S. Silver.** 1999. Molecular basis for resistance to silver cations in *Salmonella*. Nat. Med. **5:**183–188.
13. **Gupta, A., M. Maynes, and S. Silver.** 1998. Effects of halides on plasmid-mediated silver resistance in *Escherichia coli*. Appl. Environ. Microb. **64:**5042–5045.
14. **Heydorn, A., A. T. Nielsen, M. Hentzer, C. Sternberg, M. Givskov, B. K. Ersbøll, and S. Molin.** 2000. Quantification of biofilm structures by the novel computer program COMSTAT. Microbiology **146:**2395–2407.
15. **Hilbert, L. R., D. Bagge-Ravn, J. Kold, and L. Gram.** 2003. Influence of surface roughness of stainless steel on microbial adhesion and corrosion resistance. Int. Biodeterior. Biodegradation **52:**175–185.
16. **Hjelm, M., L. R. Hilbert, P. Møller, and L. Gram.** 2002. Comparison of adhesion of the food spoilage bacterium *Shewanella putrefaciens* to stainless steel and silver surfaces. J. Appl. Microbiol. **92:**903–911.
17. **Jones, D. A.** 1996. Galvanic and concentration cell corrosion, p. 168–198. *In* D. A. Jones (ed.), Principles and prevention of corrosion. Prentice Hall, Upper Saddle River, NJ.
18. **Lynch, A. S., and G. T. Robertson.** 2008. Bacterial and fungal biofilm infections. Annu. Rev. Med. **59:**415–428.
19. **Mattila-Sandholm, T., and G. Wirtanen.** 1992. Biofilm formation in the industry: a review. Food Rev. Int. **8:**573–603.
20. **Møller, P., E. O. Jensen, and L. R. Hilbert.** January 2006. Biologically inhibiting material a method of producing said material as well as the use of said material for inhibiting live cells. U.S. patent 2006003019A1.
21. **Møller, P., L. R. Hilbert, C. B. Corfitzen, and H. J. Albrechtsen.** 2007. A new approach for biologically inhibiting surfaces. J. Appl. Surf. Finishing **2:**149–157.
22. **Schierholz, J. M., L. J. Lucas, A. Rump, and G. Pulverer.** 1998. Efficacy of silver-coated medical devices. J. Hosp. Infect. **40:**257–262.
23. **Sternberg, C., and T. Tolker-Nielsen.** 2005. Growing and analyzing biofilms in flow cells, p. 1B2.1-1B2.15. *In* R. Coico, T. Kowalik, J. Quarles, B. Stevenson, and R. Taylor (ed.), Current protocols in microbiology. John Wiley & Sons, New York, NY.
24. **Stewart, P. S., P. K. Mukherjee, and M. A. Ghannoum.** 2004. Biofilm antimicrobial resistance, p. 250–268. *In* M. Ghannoum and G. A. O'Toole (ed.), Microbial biofilms. ASM Press, Washington, DC.
25. **ten Kortenaar, M. V., J. J. M. de Goeij, Z. I. Kolar, G. Frens, P. J. Lusse, M. R. Zuiddam, and E. van der Drift.** 2001. Electroless silver deposition in 100 nm silicon structures. J. Electrochem. Soc. **148:**C28–C33.
26. **Videla, H. A., and W. G. Characklis.** 1992. Biofouling and microbially influenced corrosion. Int. Biodeterior. Biodegradation **29:**195–212.
27. **Wellman, N., S. M. Fortun, and B. R. McLeod.** 1996. Bacterial biofilms and the bioelectric effect. Antimicrob. Agents Chemother. **40:**2012–2014.
28. **Zottola, E. A., and K. C. Sasahara.** 1994. Microbial biofilms in the food processing industry—should they be a concern. Int. J. Food Microbiol. **23:**125–148.

Appendix VI

# Influence of silver additions to type 316 stainless steels on bacterial inhibition, mechanical properties, and corrosion resistance
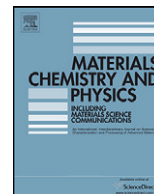
# Influence of silver additions to type 316 stainless steels on bacterial inhibition, mechanical properties, and corrosion resistance

Wen-Chi Chiang [a], I-Sheng Tseng [b], Per Møller [a], Lisbeth Rischel Hilbert [c], Tim Tolker-Nielsen [d], Jiann-Kuo Wu [b],*

[a] Department of Mechanical Engineering, Technical University of Denmark, Kgs. Lyngby, Denmark
[b] Institute of Materials Engineering, National Taiwan Ocean University, Keelung, Taiwan
[c] Force Technology, Brøndby, Denmark
[d] Department of International Health, Immunology and Microbiology, University of Copenhagen, Copenhagen, Denmark

ARTICLE INFO

ABSTRACT

Bacterial contamination is a major concern in many areas. In this study, silver was added to type 316 stainless steels in order to obtain an expected bacteria inhibiting property to reduce the occurrence of bacterial contamination. Silver-bearing 316 stainless steels were prepared by vacuum melting techniques. The microstructure of these 316 stainless steels was examined, and the influences of silver additions to 316 stainless steels on bacterial inhibition, mechanical properties, and corrosion resistance were investigated. This study suggested that silver-bearing 316 stainless steels could be used in areas where hygiene is a major requirement. The possible mechanisms of silver dissolution from the surfaces of silver-bearing 316 stainless steels were also discussed in this report.

## 1. Introduction

Bacterial contamination is a major concern in many areas, such as food industries, water distributing systems, and hospitals, because they may harbor pathogens, causing hygienic risks or diseases in humans, and may also cause other adverse effects, such as microbially influenced corrosion of materials [1–7]. An essential pre-requisite is therefore to ensure that undesired bacterial adhesion and proliferation do not occur, or that surface-adhering bacteria can be efficiently removed. However, the efficient removal of adhering bacteria can sometimes be difficult. Some sites in food processing factories, such as dead ends, joints, and bends in pipes, are vulnerable points where adhering bacteria may well live because of difficult cleaning or disinfecting access [8–10]. In hospitals, all reusable devices, such as surgical instruments, theater tables, and kidney dishes, must be decontaminated between clinical uses and between patients. However, hospital-acquired infections can be transmitted via some inadequately decontaminated or re-contaminated devices. Patients in hospitals and people in general could also be infected via transient contacts with surfaces and objects that have been touched or used by someone carrying pathogenic bacteria, such as taps and door handles [4,5]. Recent studies have helped to give people a better understanding of the relationship between home hygiene and health. Bacteria can be transmitted in the home environment, especially at some "critical points", such as kitchen surface areas, where efficient rinsing is not feasible [3,6].

It is well-known that stainless steels, such as type 304 and 316, have been widely used in above-mentioned areas because of their good corrosion resistance and cleanability [9–12]. Hygienic quality is linked to cleanability of selected steels to ensure that bacterial contamination may not occur [10]. However, stainless steels themselves do not have indigenous bacteria inhibiting properties. It is of high relevance to develop methods for directly inhibiting bacteria on stainless steel surfaces. Different kinds of treatments, such as surface coatings [13–15] and alloying modifications [16–21], have been studied as potential means of inhibiting bacteria on stainless steel surfaces. However, the inhibiting effects provided by surface coatings may deteriorate because of friction, processing, cleaning, or daily use. Alloying modified copper (Cu)-bearing stainless steels have been investigated widely for their bacterial inhibition, corrosion resistance, and mechanical properties [16,17,19–21]. However, there are few studies about silver (Ag)-bearing stainless steels [15,18]. Ag has been used for bacterial inhibition for 2500 years [22]. Ag is a metallic element well-known for inhibiting bacterial activities. Therefore, Ag and its compounds have been introduced into many commercial products to obtain bacteria inhibiting effects, and are considered to have a potential to reduce the risk of infection in many investigations in recent years

* Corresponding author. Tel.: +886 2 24622192x6402; fax: +886 2 24625324.
E-mail addresses: wcc@mek.dtu.dk (W.-C. Chiang), a0055@ntou.edu.tw (J.-K. Wu).

[22–26]. It also has been suggested that Ag can be used as a potential surface for certain hospital and healthcare applications, especially in the areas where problems of hospital-acquired infections are seen [24,26]. Furthermore, from the hygienic point of view, Ag has lower toxicity to human cells and tissues as compared with Cu [23].

Although there is no known official classification of food grade stainless steels, type 316 stainless steel is often referred to as the food grade. Type 316 stainless steel is also one of the most commonly used medical grade materials [12]. In view of these considerations, we decided to investigate the effect of Ag addition to type 316 stainless steels in bacterial inhibition. If effective, these Ag-bearing 316 stainless steels could substitute commonly commercial stainless steels in areas where hygiene is a major requirement. In this study, austenitic Ag-bearing 316 stainless steels were prepared, and influence of Ag addition on their bacterial inhibition, corrosion resistance, and mechanical properties were investigated.

## 2. Experimental

### 2.1. Materials

Ingots with nominal compositions 316 stainless steel, containing 0, 0.03, and 0.09 wt.% Ag respectively, were prepared by repeated melting in a vacuum induction melting (VIM) furnace, and then drop casting to form ingots. The cast ingots, with 6.5 cm diameter and 15 cm height, were forged at 1150 °C to reduce their thickness from 15 to 5 cm, and these were followed by solution treatment at 1050 °C for 5 min. The treated steel samples were prepared for the investigations of microstructure, mechanical properties, corrosion resistance, and bacterial inhibition. As-received pure Ag (99.9% Ag) plates and 304 stainless steels were also prepared to use as comparisons for the investigations of properties of bacterial inhibition and corrosion resistance respectively. The chemical analysis compositions for the investigated steels were determined by the use of an SPECTRO X-LAB 2000 X-ray fluorescence spectroscopy (XRF) and a PerkinElmer AAnalyst 300 flame atomic absorption spectroscopy (FAAS) (for Ag analysis). A Jeol 5900 scanning electron microscope (SEM) equipped with an INCA 400 energy dispersive X-ray (EDX) system were applied to microstructural investigations. Aqua regia solution (1 HNO$_3$:3 HCl) was used to etch the samples for 10 s before microstructural investigations.

### 2.2. Mechanical properties

The effect of Ag addition of 316 stainless steel on mechanical properties was studied by tensile and hardness tests. The tensile samples with gauge dimensions of 3.2 cm × 0.4 cm × 0.5 cm (thickness) were prepared by electrical discharge machining (EDM), and then polished with SiC paper to a final grit size of 1000. Tensile tests were performed at room temperature in a MTS 810 tensile machine at a strain rate of $1 \times 10^{-2}$ s$^{-1}$. A total of three independent tensile tests were conducted with 316, 316-0.03Ag, and 316-0.09Ag. After tensile tests, the fracture surfaces were examined by SEM. The hardness tests were performed by using a Vickers hardness testing machine using 1 kg load. A total of ten independent hardness tests were conducted.

### 2.3. Corrosion properties

The effect of Ag addition of 316 stainless steel on corrosion properties was studied by electrochemical polarization tests. As-received 304 stainless steels were also prepared to use as comparisons for corrosion resistance because 304 steels are also widely used in many areas where hygiene is a major requirement. A total of three independent polarization tests were conducted. For materials with active–passive properties, such as stainless steels, pitting potential measurements are used for ranking the aggressiveness of different media or the corrosion resistance of different alloys in specific solution. A Gill ACM Instrument potentiostat was used for potentiodynamic polarization tests. All samples were polished with SiC paper to a final grit size of 1000 before tests. The roughness of steel surface prepared with this treatment (grit 1000) is approximately $R_a = 0.1$ μm, which is slightly lower than commercially available 2B finish sheet ($R_a$ approximately 0.2 μm). The tests were performed in a typical three-electrode cell setup with platinum (Pt) as a counter electrode and a saturated calomel electrode (SCE) as a reference electrode. The exposed area of the working electrode was 1.25 cm$^2$. 1 M sodium acetate buffer pH 7 containing 3.5 wt.% NaCl solution was used. The experiments were performed under nitrogen gas purging during the tests at room temperature. The polarization curves were recorded at a scan rate of 0.5 mV s$^{-1}$ from the initial potential of −0.4 V versus open-circuit potential, which was recorded after 1.5 h immersion before tests, to the final current density of 1 mA cm$^{-2}$. In this paper, all potentials were reported with respect to saturated hydrogen electrode (SHE). Pitting potential was defined as the potential at which current density exceeded $10^{-2}$ mA cm$^{-2}$ [10].



**Fig. 1.** Experimental set-up of bacteria inhibiting test.

### 2.4. Determination of bacteria inhibiting effect

The purpose of this test was to determine the bacteria inhibiting effect of Ag-bearing 316 stainless steel in comparison with 316 stainless steel and pure Ag in a bacteria-contaminated environment. Fig. 1 shows the schematics of the film stick method used in this study, and this method was basically following Japanese Industrial Standard (JIS) Z 2801: 2000 [27]. The test was performed by using bacteria-containing solutions (suspensions) held in close contact with test surfaces. Samples of 316, 316-0.03Ag, 316-0.09Ag, and pure Ag with dimensions 5 cm × 5 cm × 0.05 cm (thickness) were used, and were polished with SiC paper to a final grit size of 1000 before tests. Escherichia coli (E. coli) ATCC6538P were used as test organisms in this study. E. coli is commonly used as indicator microorganism of an environmental monitoring parameter in many areas where hygiene is a requirement [28]. The test procedures were as follows. Cultivation of a cell suspension of E. coli was carried out at 37 °C in nutrient broth solution, and the initial bacterial concentration was approximately $10^5$ CFU ml$^{-1}$ (colony forming units). 0.4 ml of this nutrient broth solution inoculated with E. coli was then dripped and spread on each sample in order to obtain a contaminated surface, then covered by a sterilized polyethylene film (4 cm × 4 cm) to hold in close contact and incubated at 37 °C for 24 h. A total of three independent tests were conducted. After 24-h incubation, each test surface was rinsed by 10 ml of SCDLP (soybean-casein digest broth with lecithin and polysorbate) solution to collect live bacteria on the surface. Then, for the determination of bacteria inhibiting effect, collected bacteria-containing solutions were used for plating serial dilutions on agar plates to count the colony forming units of E. coli, and the values were counted after 30 h incubation at 37 °C. The bacteria inhibiting rate can be calculated from:

$$\text{Inhibiting rate} (\%) = \frac{\text{CFU}_{\text{Ag–free sample}} - \text{CFU}_{\text{Ag–bearing sample}}}{\text{CFU}_{\text{Ag–free sample}}} \qquad (1)$$

### 2.5. Silver release

The determinations of Ag release from Ag-bearing surfaces in bacteria-containing and bacteria-free solutions were performed by immersion tests. Ag-bearing 316 stainless steels and pure Ag were used as test samples with dimensions 2 m × 2 m × 0.05 cm (thickness), and were polished with SiC paper to a final grit size of 1000 before tests. E. coli were used as test organisms in this study. Cultivation of E. coli was carried out at 37 °C in nutrient broth solution, and the initial bacterial concentration was approximately $10^6$ CFU ml$^{-1}$. Test samples were placed into 15 ml bacteria-containing and bacteria-free nutrient broth solutions respectively. After 24-h immersion tests, the solutions were collected for Ag analyses. Total Ag determinations were analyzed by a PerkinElmer SCIEX ELAN 5000 inductively coupled plasma-mass spectrometer (ICP-MS). Before ICP-MS analysis, a microwave-assisted digestion in acidic solution (1 HNO$_3$:1 test solution) was performed. For each solution, a total of three independent analyses were conducted.

### 2.6. Bacterial activities associated with surfaces in solutions

The purpose of this study was to use microscopic techniques to directly observe bacterial activities associated with the sample surfaces in solutions under conditions of high bacterial load, and furthermore study the inhibiting mechanism. Cultivation of E. coli was carried out at 37 °C in ABTG solution [15], and the initial bacterial concentration was approximately $10^6$ CFU ml$^{-1}$. 316 stainless steel, Ag-bearing 316 stainless steels, and pure Ag were used as test samples with dimensions 0.7 cm × 0.4 cm × 0.05 cm (thickness), and were polished with SiC paper to a final grit size of 1000 before tests. Samples of 316 steel and pure Ag were included as controls along with Ag-bearing 316 steel. Each sample was placed in a dish, 5 ml ABTG solution inoculated with E. coli were transferred to each dish, and the dishes were incubated at 37 °C with shaking at 60 rpm for 24 h. For each test sample, a total of three independent tests were conducted.

After 24-h incubation, the bacterial activities on surfaces in solution were observed by the use of a Zeiss LSM 510 META confocal laser scanning microscope (CLSM), and staining with Molecular Probes LIVE/DEAD BacLight Bacterial Viability Assay, which utilizes the green fluorescent SYTO 9 for staining of cells, and the red fluorescent propidium iodide for staining of membrane-compromised (dead) cells. A 488-nm argon laser was used to excite the SYTO 9-stained cells, and a 543-nm helium/neon laser was used to excite the propidium iodide-stained cells. Simulated 3D images were generated by the use of Bitplane IMARIS software. For the determination of colony forming units of 24-h-old cultures in solutions, serial dilutions of bacteria suspensions were plated on agar plates to count the values of CFU ml$^{-1}$.

**Table 1**
Chemical analysis compositions of investigated stainless steels.

| Steel designation | Composition (wt.%) | | | | | | | | |
|---|---|---|---|---|---|---|---|---|---|
| | C | Si | Mn | P | S | Ni | Cr | Mo | Ag |
| 316 | 0.018 | 0.37 | 1.41 | 0.023 | 0.006 | 12.33 | 17.54 | 2.08 | – |
| 316-0.03Ag | 0.017 | 0.33 | 1.43 | 0.021 | 0.007 | 12.21 | 17.31 | 2.09 | 0.031 |
| 316-0.09Ag | 0.016 | 0.35 | 1.40 | 0.026 | 0.002 | 12.70 | 17.10 | 2.12 | 0.092 |

## 3. Results and discussion

### 3.1. Characterization of Ag-bearing stainless steels

The cast microstructures of investigated steels mainly consisted of austenite and retain delta ($\delta$) ferrite phases. The cast ingots were forged at 1150 °C to eliminate dendrites, voids, segregation, and retain $\delta$-ferrite phases. After forging, Ag-bearing 316 steels had an austenitic microstructure at room temperature. Table 1 shows the analyzed chemical composition of investigated steels. Some studies have shown that Ag has extremely low solubility in steel and precipitates as small particles [29,30]. Ag precipitates in the austenitic matrix were too small to be observed by the use of an optical microscope, and therefore SEM back-scattering electron images (BEI) were performed. Because the atomic weight of Ag is larger than that of iron (Fe), bright particles in BEI images indicate Ag phases, whereas dark areas indicate austenitic matrix (Fig. 2). Based on EDX analyses, Ag phases were confirmed in the austenitic matrix. Similar results have been reported previously [18,30]. In Fig. 2, dispersive fine Ag precipitates were obviously observed in steels containing 0.09 wt.% Ag, however in those containing 0.03 wt.% Ag, the precipitates, although present, were less easily detected.

### 3.2. Mechanical properties

The influence of Ag additions on strength and ductility properties of 316 steels at room temperature is shown in Fig. 3. When the
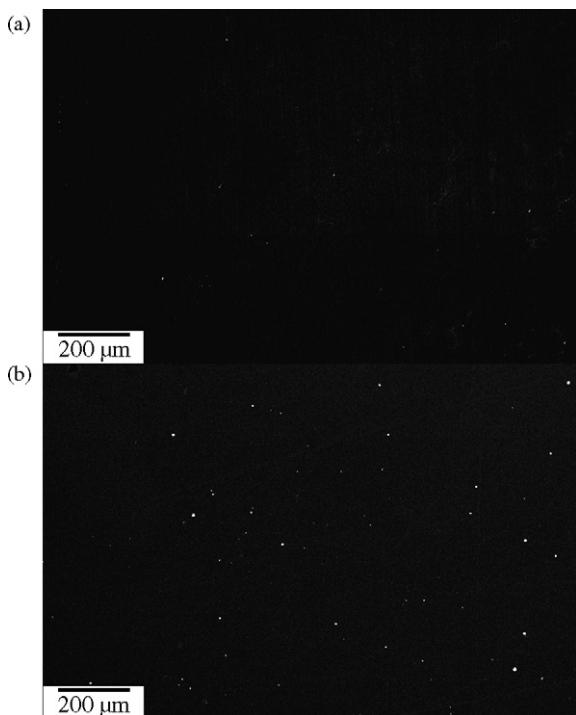


**Fig. 2.** SEM-BEI micrographs of (a) 316-0.03Ag, and (b) 316-0.09Ag. White particles indicate Ag phases.
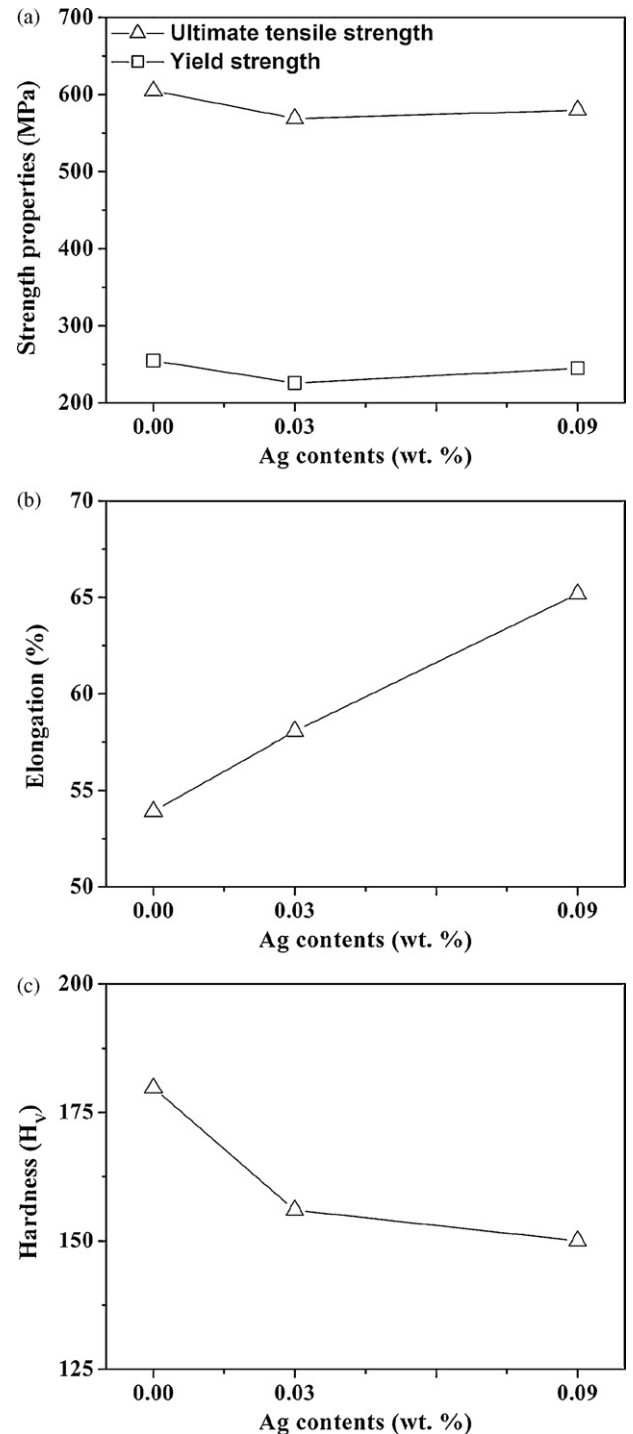


**Fig. 3.** Effect of Ag additions of 316 stainless steels on the mechanical properties. (a) Strength properties, (b) elongation, and (c) Vickers hardness.

**Table 2**
Bacteria inhibiting effects of 316, 316-003Ag, 316-0.09Ag, and pure Ag.

|  | Average CFU cm$^{-2}$ | Inhibiting rate (%)[a] |
|---|---|---|
| 316 | 149 | – |
| 316-0.03Ag | 15 | 89.9 |
| 316-0.09Ag | 3 | 98.0 |
| Pure Ag | <1 | >99.0 |

[a] Inhibiting rate was calculated by Eq. (1).

Ag content of the steels increased from 0 to 0.03 wt.%, the strength properties, both ultimate tensile strength (UTS) and yield strength (YS), were observed to slightly decrease (Table 2) because of the softening effect of Ag. If regarding the Ag-bearing 316 steel as a two-phase alloy (Ag and austenitic phases), the well-known mixture law [31] can be applied by the following equation:

$$\sigma_\Sigma = \sigma_1 V_1 + \sigma_2 V_2 \qquad (2)$$

where $\sigma_1$ and $V_1$ are the strength and volume fraction of austenite, and $\sigma_2$ and $V_2$ are the strength and volume fraction of Ag. However, as shown in Fig. 3 (a), the UTS and YS increased slightly when the Ag content increased from 0.03 to 0.09 wt.%. Some studies have shown that when the Ag content is higher than a certain amount, fine Ag particles can improve strength though precipitation strengthening or grain refinement [30]. The effects of precipitation strengthening or grain refinement caused by more Ag additions mitigate the softening effect of Ag. As shown in Fig. 3(b), the ductility property (elongation) of the steels was observed to greatly increase with increasing Ag content from 0 to 0.09 wt.%, and similar results have been reported previously [30,32]. It is well-known that Ag is a very ductile metal. Therefore, the mixture law can be applied to explain the effect of increasing elongation of 316 steels. Some studies have also shown that Ag can improve the ductility property through grain refinement [30], or acting as a scavenging element for alloys, where it can stabilize or remove interstitial impurities, such as nitrogen [32]. Fig. 3(c) shows that the Vickers hardness of the steels was observed to decrease with increasing Ag content from 0 to 0.09 wt.%, indicating the softening effect of Ag on 316 matrix. Fig. 4 shows the ductile fracture morphologies of the investigated steels after tensile testing at room temperature. The dimple structures were observed on all of the investigated steels, also indicating that the Ag additions of the steels did not change the deformation behavior leading to the final failure. It could be attributed to the 316 matrix being always in a stable austenitic state at room temperature [19]. In Fig. 4(b) and (c), Ag particles (confirmed by SEM-EDX) can be visible at the bottom of some voids, indicating that some large voids were nucleated at Ag particles, which can be regarded as an inclusion.

### 3.3. Corrosion properties

The polarization curves of 316, 316-0.03Ag, 316-0.09Ag, and 304 steels in pH 7 3.5 wt.% NaCl solutions are shown in Fig. 5, and the curves are representative of three independent tests. It can be seen that the range of passive region of Ag-bearing 316 steels was decreased with increasing Ag content from 0 to 0.09 wt.%. Pitting potential (Fig. 6) was defined as the potential at which current density exceeded $10^{-2}$ mA cm$^{-2}$. Below these pitting potentials, a number of short-period current spikes (Fig. 6) in the tests of 304, 316-0.03Ag, and 316-0.09Ag steels were observed, which were attributed to metastable passivity breakdown followed by immediate re-passivation (metastable pitting). Because Ag remained as a second phase on the passive film of Ag-bearing 316 steels and therefore affected the stability of passive film, resulting in a discontinuous passive film on 316 surfaces. Although Ag-bearing 316 steels had a lower corrosion resistance than Ag-free 316 steel in
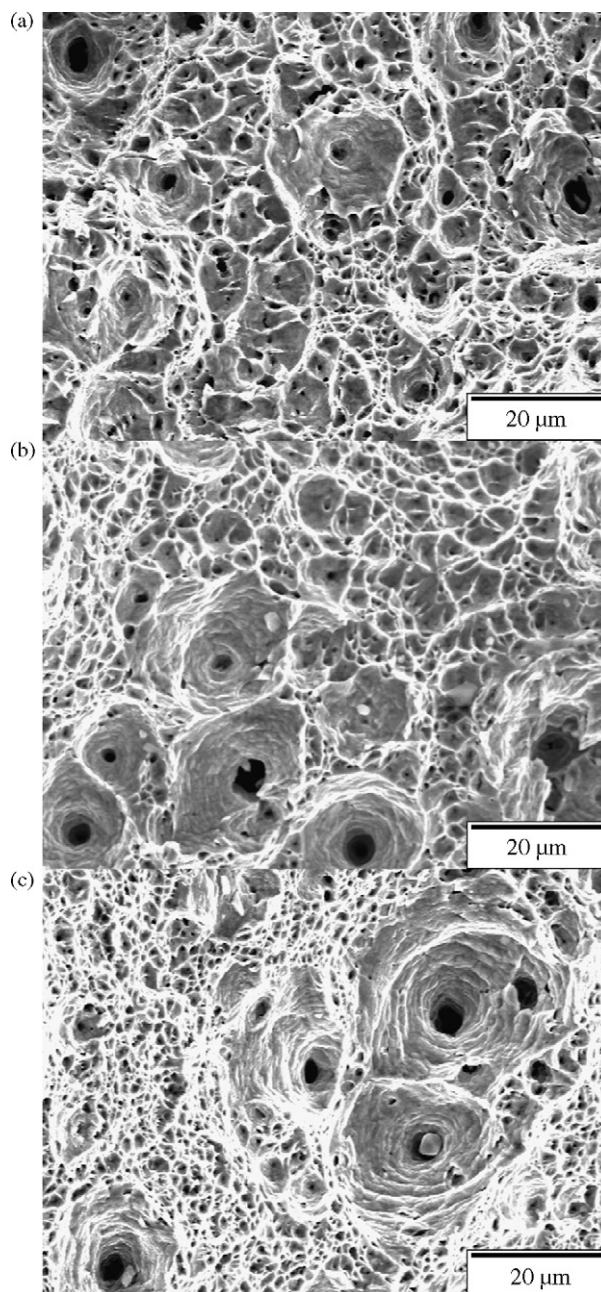


**Fig. 4.** SEM micrographs of fracture morphologies of (a) 316, (b) 316-0.03Ag, and (c) 316-0.09Ag after tensile tests at room temperature.

chloride-containing environments, its corrosion resistance was still better than that of 304 steel (Figs. 5 and 6), which also has been widely used in many areas where hygiene is a major requirement.

According to the Pourbaix diagram of Ag–Cl–H$_2$O in Fig. 7, there is an immune area of Ag where the potential is below 0.25 V (at pH 7). As compared with Fig. 5, it indicates that Ag precipitates on 316 surfaces can remain as Ag phases in normal and low oxidizing environments, and therefore can provide 316 surfaces with the expected bacteria inhibiting effect which is caused by Ag toxicity to bacteria. However, in higher oxidizing environments, such as commonly using oxidizing disinfectant in cleaning procedures of food industries, the inhibiting effect could be diminished due to Ag state conversion or increased Ag dissolution. This study indicated that the operation environment is an important parameter on Ag-bearing steels to obtain an effective bacteria inhibiting property. If the Ag-bearing 316 steel is to be used in the food industries as a bac-
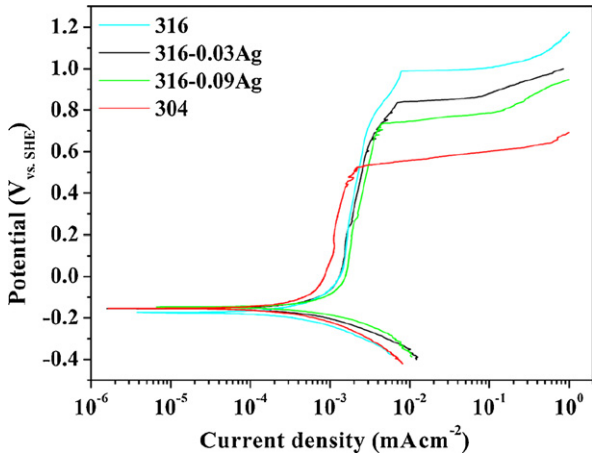
**Fig. 5.** Polarization curves in pH 7 3.5 wt.% NaCl solution. The curves are representative of three independent tests.
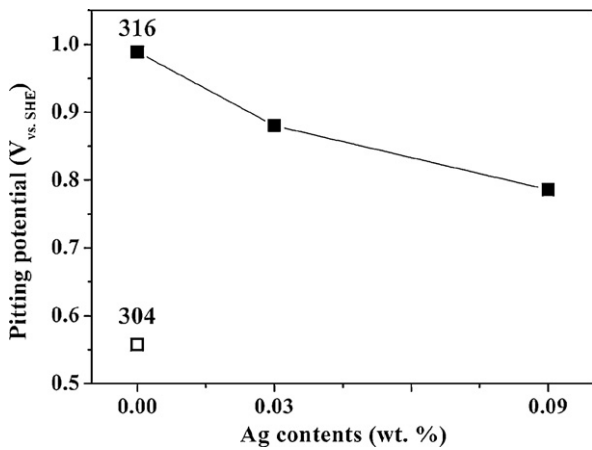


**Fig. 6.** Pitting potentials in pH 7 3.5 wt.% NaCl solution.

teria inhibiting surface, then its corrosion behaviors in the cleaning and disinfecting agents need to be further studied to evaluate the effectiveness of the surfaces after cleaning procedures.

### 3.4. Bacteria inhibiting effect and Ag release

Table 2 shows the results of the bacteria inhibiting effects of the test samples. Tests with 316 steel and pure Ag were included
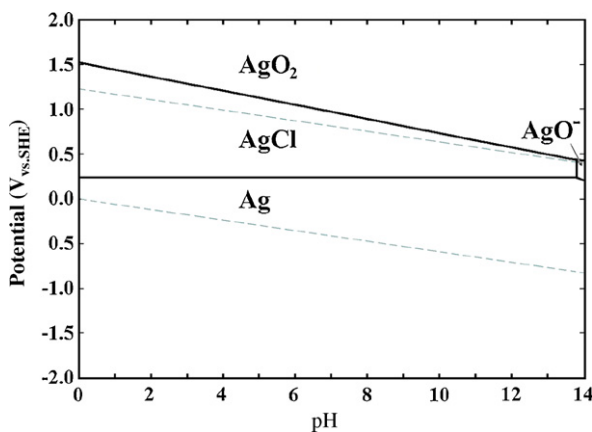


**Fig. 7.** Pourbaix diagram of Ag–Cl–H$_2$O system at 25 °C. It was calculated from Cl$^-$ concentration of 0.6 M (3.5 wt.% NaCl solution) and Ag ions concentration of $10^{-6}$ M.
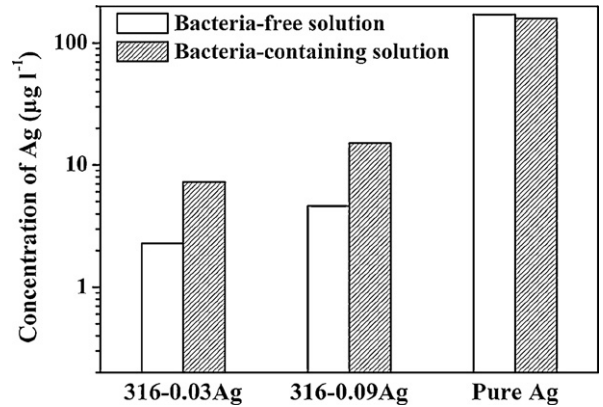


**Fig. 8.** Average concentration of Ag after 24-h immersion in bacteria-free and bacteria-containing solutions.

as controls along with the tests with Ag-bearing 316 steels. It has been reported that the number of live bacteria present on open surfaces in hospitals can be 0–100 CFU cm$^{-2}$ [33]. In this study, the film stick method was used to hold bacteria-containing solutions in close contact with surfaces. Therefore, in the following it is assumed that all CFU mainly originated from adhering bacteria
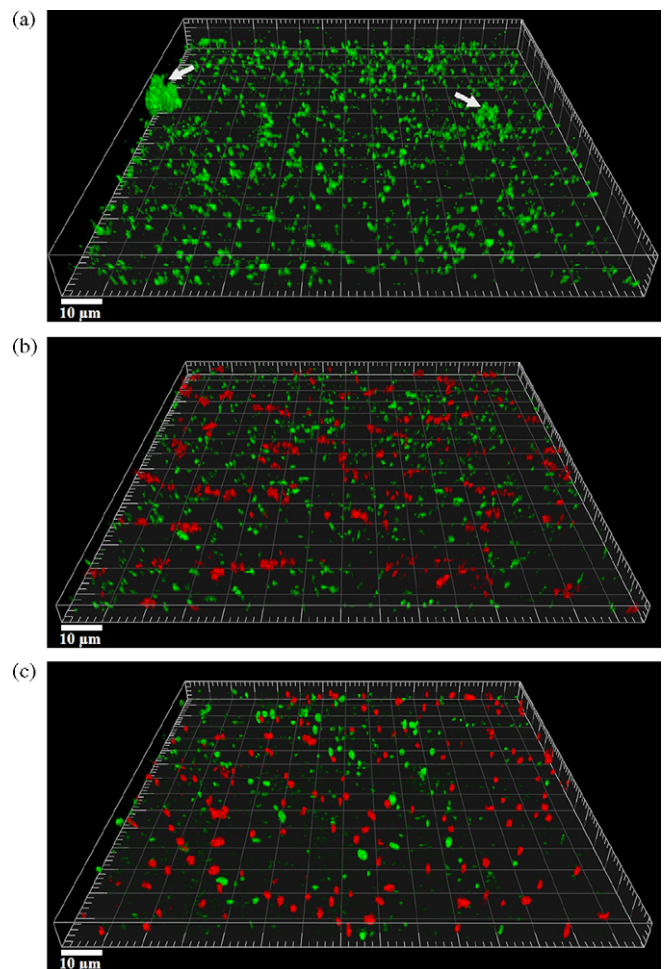


**Fig. 9.** CLSM micrographs of *E. coli* on the surfaces of (a) 316 stainless steel, (b) Ag-bearing 316 stainless steel, and (c) pure Ag. Green fluorescence indicates live bacteria, and red fluorescence indicates dead bacteria. Arrows indicate the formations of microcolonies. The images are representative of three independent experiments. (For interpretation of the references to colour in this figure legend, the reader is referred to the web version of the article.)

that were detached during the rinsing procedure, although some CFU could originate from bacteria in the nutrient broth solution. The average number of live bacteria present on the 316 surface after 24-h incubation was 149 CFU cm$^{-2}$. As shown in Table 2, 316-0.03Ag exhibited a bacteria inhibiting effect (89.9%). When the Ag content was increased to 0.09 wt.%, the steel exhibited an excellent bacteria inhibiting effect (98.0%), and obtained almost a similar rate as pure Ag. Therefore, it seems probable that the dispersive Ag precipitates on the 316 surfaces played an important role in bacterial inhibition. This experiment suggested that Ag-bearing 316 steels may be used in place of traditional stainless steels to help reduce the occurrence of bacterial contamination.

In order to evaluate the Ag ion release rate from Ag-bearing steels and pure Ag surfaces in bacteria-containing and bacteria-free growth media respectively, immersion tests were performed. In the following it is assumed that all Ag were present as Ag ions in solutions, although the analyses measured Ag compounds in total and not only dissolved ions. In Fig. 8, it is shown that the tests of pure Ag gave higher Ag ion release than those of 316-0.03Ag and 316-0.09Ag in bacteria-containing and bacteria-free solutions respectively. Surprisingly, higher Ag ion concentrations in the tests of Ag-bearing steels were measured after 24-h immersion in bacteria-containing solutions compared to those from the immersion in bacteria-free solutions.

### 3.5. Bacterial activities on surfaces in solutions

After 24-hour incubation, bacteria associated with the samples surfaces were LIVE/DEAD stained and visualized by the use of CLSM. As shown in Fig. 9(a), live bacteria formed microcolonies, and no dead bacteria were present on the 316 surface. On the contrary, as shown in Fig. 9(b) and (c), Ag-bearing 316 steels and pure Ag both can cause a reduction in numbers of surface-adhering bacteria, and dead bacteria can be observed on these surfaces, which was in agreement with the tests of determining the inhibiting effect

(Table 2). On the other hand, CFU determinations showed that the solutions with 316, Ag-bearing 316 steels, and pure Ag all contained approximately $10^8$ CFU ml$^{-1}$ of E. coli in the suspension (planktonic phase). It indicated that the numbers of bacteria in the suspension surrounding Ag-bearing 316 steels and pure Ag did not significantly change as compared with the cell numbers in the suspension surrounding 316 steel. Therefore, the lower numbers of live adhering bacteria measured on these Ag-bearing surfaces were not due to a lower numbers of bacteria in the surrounding cell suspension. In Fig. 9, CLSM observations indicated that bacterial adhesion was followed by an inhibiting effect on the Ag-bearing surfaces. Previous studies have shown that the minimum inhibitory concentration of electrically generated Ag ions for some bacterial strains is 30–125 $\mu$g l$^{-1}$, and the necessary concentration for full killing effect is 480–1005 $\mu$g l$^{-1}$ [34]. As combined with the measurements of Ag ion release (Fig. 8), it can be concluded that these Ag-bearing surfaces had an even higher local released Ag concentration near or at the surfaces, which killed the surface-adhering bacteria.

Although the present study indicated that less bacteria adhered to the Ag-bearing 316 steels and pure Ag than to 316 steel in the test involving 24-h incubation, some previous studies [9,24,35] have demonstrated that bacterial microcolonies may form after longer incubation on Ag surfaces. Therefore, if Ag-bearing 316 steel is to be used in hygienic-related areas as a bacteria inhibiting surface, then appropriate cleaning practices need to be applied to maintain the effectiveness of the surfaces.

### 3.6. Mechanism of Ag dissolution from Ag-bearing steel surface

When pure Ag is in normal drinking water, it can be thermodynamically calculated that there is equilibrium with 2 $\mu$g l$^{-1}$ Ag$^+$ at 10 °C to 33 $\mu$g l$^{-1}$ Ag$^+$ at 40 °C (calculated from average Cl$^-$ concentration of 70 mg l$^{-1}$ in Lyngby, Denmark). However, when chemical compounds aggressive to Ag are present in an environment, such as ammonium (NH$_4^+$) and cyanide (CN$^-$) ions, as
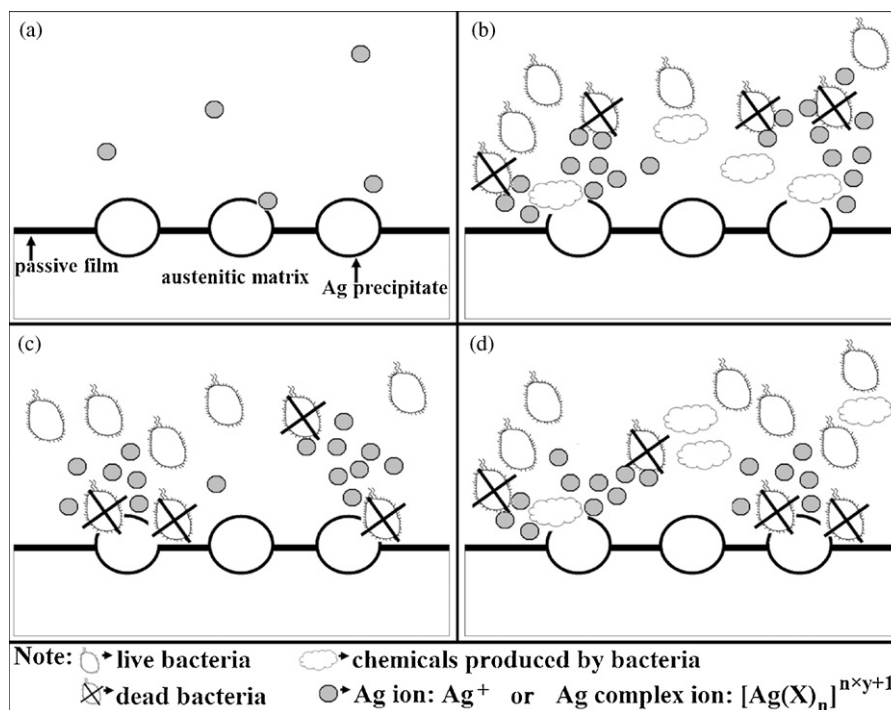


**Fig. 10.** Schematic illustrations of possible mechanisms of Ag dissolution from Ag-bearing 316 surfaces. (a) Mechanism 1: bacteria are not present, and the surface releases small amount of Ag ions. (b) Mechanism 2: bacteria are present, and chemicals produced by bacteria increase Ag dissolution. (c) Mechanism 3: bacteria are present, attach to the surface, and increase Ag dissolution because of the interactions with chemical groups inside bacteria cells. (d) Mechanism 2 + 3. (Ag complex ions [Ag(X)$n$]$^{n \times y+1}$, where X is NH3, CN$^-$, etc., and $y$ is the charge of X)

well as the galvanic effect of Ag and 316 austenitic matrix, the process of increased Ag dissolution can occur by Ag complex formations. These Ag complexes can be effective and have a wide spectrum of bacterial inhibition [36]. The proposed mechanisms are visualized in Fig. 10. As shown in Fig. 10(a), the Ag-bearing 316 surface releases small amounts of Ag ions in bacteria-free solution, but in general this content should not cause any or only a slight inhibiting effect because of low Ag concentration. In Fig. 10(b), when bacteria are present and produce some chemical compounds through their metabolism, the effect of increased Ag dissolution can occur and furthermore improve the bacterial inhibition of the Ag-bearing 316 surfaces. For examples, under anaerobic conditions, a number of bacterial species, e.g. *E. coli*, can perform respiratory reduction of nitrate ($NO_3^-$) to nitrite ($NO_2^-$) and of nitrite to ammonia ($NH_3$) [37,38]. Ammonia or ammonium ion can cause metallic Ag to form Ag complexes (diamminesilver ion). The calculated reaction of Ag dissolution is as follows [39,40]:

$$4Ag + 8NH_4^+ + 4OH^- + O_2 \rightarrow 4[Ag(NH_3)_2]^+ + 6H_2O,$$

$$\Delta G = -227.120 \text{ kJ} (25\,^\circ C) \tag{3}$$
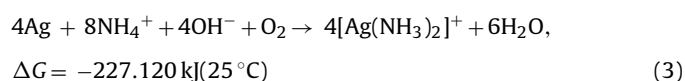
Since the Gibbs free energy ($\Delta G$) for the reaction is negative, this reaction (Eq. (3)) is thermodynamically favorable.

It also has been reported that microbial cyanide biosynthesis, so called microbial cyanogenesis, can occur in some species of bacteria, e.g. *Pseudomonas aeruginosa* (*P. aeruginosa*) [41,42]. Cyanide produced by bacteria can cause metallic Ag to form Ag complexes (dicyanoargentate ion). The calculated reaction of Ag dissolution is as follows [43,44]:

$$4Ag + 8CN^- + O_2 + 4H^+ \rightarrow 4[Ag(CN)_2]^- + 2H_2O,$$

$$\Delta G = -629.430 \text{ kJ} (25\,^\circ C) \tag{4}$$
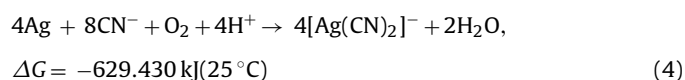
On the other hand, it is well-known that Ag can react with amino acids ($H_2NCHRCOOH$, where R is an organic substituent) or amino groups ($-NH_2$) of membranes or enzymes inside bacterial cells, which eventually kills bacteria [24,36,45]. These reactions can lead to increased Ag dissolution from Ag-bearing surfaces by Ag complex formations. As shown in the mechanism in Fig. 10(c), when bacteria attach to Ag particles on a Ag-bearing 316 surface, they are killed because of interactions with chemical groups inside cells, and furthermore increase Ag dissolution, which can enhance the bacterial inhibition.

## 4. Conclusions

1. The microstructural observation of Ag-bearing 316 stainless steels showed that Ag precipitates as small particles on the steel matrix surfaces because Ag has extremely low solubility in steel.
2. The Ag additions to 316 stainless steels influenced both their strength and ductility properties. The observation of fracture morphologies indicated that Ag additions to steels did not change the deformation behavior.
3. Ag remained as a second phase in the passive film of 316 stainless steels and therefore affected the stability of passive film, resulting in a discontinuous passive film. Therefore, Ag-bearing 316 stainless steels had a lower corrosion resistance than that of 316 stainless steels in chloride-containing solutions.
4. The experiments provided evidences that the Ag addition to type 316 stainless steels can improve their bacteria inhibiting properties, and bacteria can be inhibited on the surfaces of Ag-bearing 316 stainless steels due to the release of toxic levels of Ag ions from their surfaces. Dispersive Ag precipitates on the surfaces of 316 stainless steels played an important role on bacterial inhibition. Good inhibiting properties were obtained already at

0.03 wt.% of Ag additions to 316 stainless steels, but 0.09 wt.% of Ag additions improved the effect.
5. When bacteria were present in solutions, an increased Ag ion release rate was found in this study due to the chemical interactions between Ag phases on 316 surfaces and bacteria.
6. This study suggested that Ag-bearing 316 stainless steels could be used in place of traditional stainless steels to help reduce the occurrence of bacterial contamination giving primarily an inhibiting effect close to the surface, however, the mechanical and corrosion properties are slightly poorer than those of 316 stainless steels.

## References

[1] H.A. Videla, W.G. Characklis, Int. Biodeter. Biodegr. 29 (1992) 195.
[2] E.A. Zottola, K.C. Sasahara, Int. J. Food Microbiol. 23 (1994) 125.
[3] M.V. Jones, Int. Biodeter. Biodegr. 41 (1998) 191.
[4] S.J. Dancer, J. Hosp. Infect. 43 (1999) 85.
[5] A. Rampling, S. Wiseman, L. Davis, A.P. Hyett, A.N. Walbridge, G.C. Payne, A.J. Cornaby, J. Hosp. Infect. 49 (2001) 109.
[6] L.J. Kagan, A.E. Aiello, E. Larson, J. Commun. Health 27 (2002) 247.
[7] J.R. Flanders, F.H. Yildiz, in: M. Ghannoum, G.A. O'Toole (Eds.), Microbial Biofilms, ASM Press, Washington, 2004, p. 314.
[8] T. Mattila-Sandholm, G. Wirtanen, Food Rev. Int. 8 (1992) 573.
[9] M. Hjelm, L.R. Hilbert, P. Møller, L. Gram, J. Appl. Microbiol. 92 (2002) 903.
[10] L.R. Hilbert, D. Bagge-Ravn, J. Kold, L. Gram, Int. Biodeter. Biodegr. 52 (2003) 175.
[11] P. Marshall, Austenitic Stainless Steels: Microstructure and Mechanical Properties, Elsevier Applied Science Publishers, London, 1984, p. 410.
[12] J.A. Disegi, L. Eschbach, Injury 31 (2000) D2.
[13] Y. Ohko, S. Saitoh, T. Tatsuma, A. Fujishima, J. Electrochem. Soc. 148 (2001) B24.
[14] P. Møller, L.R. Hilbert, C.B. Corfitzen, H.J. Albrechtsen, J. Appl. Surf. Finish. 2 (2007) 149.
[15] W.C. Chiang, L.R. Hilbert, C. Schroll, T. Tolker-Nielsen, P. Møller, Electrochim. Acta 54 (2008) 108.
[16] S. Nakamura, S. Suzuki, N. Okubo, M. Hasegawa, K. Miyakusu, CAMP-ISIJ 11 (1998) 1147.
[17] S. Suzuki, S. Nakamura, N. Ookubo, M. Hasegawa, K. Miyakuso, CAMP-ISIJ 12 (1999) 518.
[18] K.R. Sreekumari, K. Nandakumar, K. Takao, Y. Kikuchi, ISIJ Int. 43 (2003) 1799.
[19] I.T. Hong, C.H. Koo, Mater. Sci. Eng. A 393 (2005) 213.
[20] J. Yang, D. Zou, X. Li, J. Zhu, Mater. Sci. Forum 510/511 (2006) 970.
[21] K. Yang, M. Lu, J. Mater. Sci. Technol. 23 (2007) 333.
[22] R.L. Davies, S.F. Etris, Catal. Today 36 (1997) 107.
[23] J.L. Clement, P.S. Jarrett, Met. Based Drugs 1 (1994) 467.
[24] J.M. Schierholz, L.J. Lucas, A. Rump, G. Pulverer, J. Hosp. Infect. 40 (1998) 257.
[25] N. Silvestry-Rodriguez, E.E. Sicairos-Ruelas, C.P. Gerba, K.R. Bright, Rev. Environ. Contam. Toxicol. 191 (2007) 23.
[26] P.D. Bragg, D.J. Rainnie, Can. J. Microbiol. 20 (1974) 883.
[27] Japanese Industrial Standard JIS Z 2801:2000, 2000.
[28] World Health Organization, Guidelines for Drinking-water Quality, vol. 1, WHO, Geneva, 2006.
[29] L.J. Swartzendruber, J. Phase Equil. 5 (1984) 560.
[30] W.B. Morrison, Mater. Sci. Technol. 1 (1985) 954.
[31] K. Cho, J. Gurland, Metall. Trans. 19A (1988) 2027.
[32] Y.F. Gu, Y. Ro, H. Harada, Metall. Mater. Trans. 35A (2004) 3329.
[33] C.J. Griffith, R.A. Cooper, J. Gilmore, C. Davies, M. Lewis, J. Hosp. Infect. 45 (2000) 19.
[34] T.J. Berger, J.A. Spadaro, S.E. Chapin, R.O. Becker, Antimicrob. Agents Chemother. 9 (1976) 357.
[35] W.C. Chiang, C. Schroll, L.R. Hilbert, P. Møller, T. Tolker-Nielsen, Appl. Environ. Microb. 75 (2009) 1674.
[36] N.C. Kasuga, M. Sato, A. Amano, A. Hara, S. Tsuruta, A. Sugie, K. Nomiya, Inorg. Chim. Acta 361 (2008) 1267.
[37] H. Neubauer, F. Goetz, Arch. Microbiol. 154 (1990) 349.
[38] H. Neubauer, F. Götz, J. Bacteriol. 178 (1996) 2005.

[39] E.L. Shock, H.C. Helgeson, Geochim. Cosmochim. Acta 52 (1988) 2009.
[40] Landolt-Börnstein: Thermodynamic Properties of Inorganic Material, Scientific Group Thermodata Europe (SGTE), Springer-Verlag, Berlin-Heidelberg, 1999, Part 1.
[41] C.J. Knowles, Bacteriol. Rev. 40 (1976) 652.
[42] P.A. Castric, J. Bacteriol. 130 (1977) 826.
[43] D.D. Wagman, W.H. Evans, V.B. Parker, R.H. Schumm, I. Halow, S.M. Bailey, K.L. Churney, R.L. Nuttall, J. Phys. Chem. Ref. Data 11 (1982).
[44] E.L. Shock, D.C. Sassani, M. Willis, D.A. Sverjensky, Geochim. Cosmochim. Acta 61 (1997) 907.
[45] S.L. Percival, P.G. Bowler, D. Russell, J. Hosp. Infect. 60 (2005) 1.

Appendix V

# Influence of bacteria on silver dissolution from silver-palladium surfaces

European Corrosion Congress, 2009

# Influence of bacteria on silver dissolution from silver-palladium surfaces

**Wen-Chi CHIANG[1], Lisbeth Rischel HILBERT[2], Casper SCHROLL[3], Per MØLLER[3], Tim TOLKER-NIELSEN[1]**

[1] *Department of International Health, Immunology and Microbiology, University of Copenhagen, Denmark, wenchi@sund.ku.dk*
[2] *FORCE Technology, Denmark, LTH@force.dk*
[3] *Technical University of Denmark, Denmark, pm@mek.dtu.dk*

Abstract
Silver-palladium surfaces are potentially used for bacterial and biofilm inhibition by generating micro-electric fields and electrochemical redox processes, and it is desired that the release of any metal ion will be at low concentration. However, in some specific environments, undesired silver dissolution can occur which can be recognized as a result of corrosion or deterioration of the silver-palladium surface, and will reduce the lifetime of the surface and contaminate the surroundings. The effect of bacteria, biofilm and solution contents on silver stability is therefore of interest, if silver-palladium surfaces are used in biologically active systems. In this study, a series of 24- and 72-hour immersion tests using several solutions was performed for the evaluation of silver dissolution and study of the mechanism. The quantitative data on silver dissolution and the correlation between silver dissolution, solution contents, and surface-associated bacteria were obtained. It was not surprising that chemicals aggressive to silver and silver compounds accelerated silver dissolution due to the formations of silver ions and silver complex ions, but a phenomenon of increased silver dissolution was found associated directly with the presence of bacteria. Experiments showed that surface-associated bacteria greatly increased silver dissolution from the silver-palladium surfaces due to the interactions between cell components and the surfaces, and the amount of surface-associated bacteria enhanced this effect.

Keywords: "silver dissolution", "immersion test", "silver-palladium surface", "bacteria"

## Introduction

Bacterial contamination can cause many adverse effects, such as deterioration of food products and human diseases. Bacteria in natural, industrial and clinical settings most often live in surface associated communities known as biofilm. Bacteria in biofilm are more tolerant to cleaning, disinfecting operations, and antibiotic therapies than their planktonic phases, making these treatments less effective or ineffective [1-8]. It is of high priority to develop effective and non-toxic methods for combating biofilm formations. Therefore, a biofilm preventing silver-palladium (Ag-Pd) surface has been developed, and the results of microstructure observations, electrochemical tests, and anti-biofilm activity have been published [9-12]. The Ag-Pd surface in focus in this paper can inhibit surface-associated bacteria and prevent biofilm formations by generating micro-electric fields itself and redox processes (electrochemical interactions) with bacteria [9-12]. In this way, it is desired that the release of any metal ion will be at low concentration. However, in our previous experiments, the phenomenon of undesired Ag dissolution from Ag-Pd surfaces has been found [10, 11]. Metal dissolution is a result of corrosion or deterioration of materials [13], and will reduce the lifetime of the material and contaminate the surroundings. It has recently been reported that metallic gold (Au) on medical implants can be dissolved by cells, which is called ''dissolucytosis'' [14, 15]. These studies demonstrated that whenever metallic Au surfaces are attacked by membrane-bound dissolucytosis, Au ions are dissolved by surrounding cells or

the effects of cell growth on metallic Au surfaces. These observations indicated that even indigestible noble metals can be attacked by the phenomenon of microbiologically influenced corrosion.

In this report we investigated the correlation between solution contents, surface-associated bacteria, and metal dissolution of Ag-Pd surfaces under a condition of high bacterial load. The objective was to decrease the risk of contamination to a surrounding environment due to metal dissolution. We performed immersion tests to obtain quantitative data, and the amounts of Ag dissolved from Ag-Pd surfaces at different test environment were compared. The mechanism of Ag dissolution behind the effect is also discussed based on thermodynamic considerations and experiments carried out in this study.

## Experimental

Materials and bacteria
To obtain a test sample with a desired Ag-Pd surface, a Ag (99.9% Ag) plate was treated by immersion plating in palladium chloride solution for 3 minutes at ambient temperature. The palladium chloride solution was prepared from 5 vol. % of the stock solution which is prepared from 0.5 $gl^{-1}$ $PdCl_2$ and 4 $gl^{-1}$ NaCl dissolved in water. As-received stainless steel AISI 316 (approximately 68.7% Fe, 16.9% Cr, 10.16% Ni, and 2.02% Mo) was used as a control in this study. The size of the test sample used in this study was 4 mm × 7 mm × 0.5 mm.

In our previous studies [10-12], we employed Ag-resistant bacteria to study the biofilm inhibiting property of Ag-Pd surface. Therefore, Ag-resistant *E. coli* J53[pMG101] [16] and Ag-sensitive *Escherichia coli* (*E. coli*) J53 [17] were used as model organisms in his study. With this setup we can also investigate the correlation between bacterial metal resistance and metal dissolution. Cultivation of a cell suspension of *E. coli* was carried out at 37°C in ABTG solution (bacterial growth medium). The composition of ABTG is shown in Table 1.


*Table 1. Composition of ABTG solution.*

| |
|---|
| 2 $gl^{-1}$ $(NH_4)_2SO_4$ |
| 6 $gl^{-1}$ $Na_2HP\ O_4$ |
| 3 $gl^{-1}$ $KH_2PO4$ |
| 3 $gl^{-1}$ NaCl |
| $1 \times 10^{-3}$ M $MgCl_2$ |
| $1 \times 10^{-4}$ M $CaCl_2$ |
| $1 \times 10^{-5}$ M $FeCl_3$ |
| 6.25 $gl^{-1}$ glucose |
| 25 $mgl^{-1}$ methionine |
| 25 $mgl^{-1}$ proline |
| 2.5 $mgl^{-1}$ thiamine |
| 1000 ml $H_2O$ |

Immersion test and determination of dissolved Ag in solution

The purpose of immersion tests was to investigate the influence of different bacteria-containing ABTG solutions on the metal dissolution from Ag-Pd surface under a condition of high bacterial load. In cold tap water, the amount of naturally occurring bacteria is approximately $10^1$ CFUml$^{-1}$ (colony forming units) [9, 11]. For immersion tests in bacteria-containing solutions, the initial bacterial concentration was approximately $10^6$ CFUml$^{-1}$. Each test was three replicates. As shown in Table 1, the ABTG solution used in this study contains ammonium sulfate (($NH_4)_2SO_4$). It is well-known that the ammonium ion ($NH_4^+$) is aggressive to Ag and its compounds, e.g. AgCl [9].Therefore, tests in bacteria-free ABTG solutions with different ammonium contents were performed to investigate the influence of $NH_4^+$ content on Ag metal dissolution, and also to be used as a control. Table 2 shows test conditions used in this study. Each sample was placed into a dish with 5 ml solution at 37 °C with shaking at 60 rpm for 24 and 72 hours respectively. For each test condition, a total of three independent tests were conducted.

*Table 2. Bacteria-containing and bacteria-free solutions used in the immersion tests.*

| Solution | Model organism | Test duration |
|---|---|---|
| ABTG$^*$ | - | 24 and 72 hours |
| ABTG$^*$ | Ag-sensitive *E. coli* J53 | 24 and 72 hours |
| ABTG$^*$ | Ag-resistant *E. coli* J53[pMG101] | 24 and 72 hours |
| ABTG (25% $NH_4^+$)$^{**}$ | - | 24 hours |
| ABTG (1% $NH_4^+$)$^{***}$ | - | 24 hours |

* The composition of the ABTG solutions used is shown in Table 1.
** The content of $(NH_4)_2SO_4$ in ABTG is reduced from 2 to 0.5 gl$^{-1}$.
*** The content of $(NH_4)_2SO_4$ in ABTG is reduced from 2 to 0.02 gl$^{-1}$.

After 24- and 72-hour immersion tests, the spent solutions were collected for the measurements of Ag concentrations to evaluate the levels of Ag dissolution from Ag-Pd surfaces under different test environments. The measurements of Pd concentrations were also conducted. The collected solutions were diluted, and then acidified (nitric acid) to make a clear solution for analyses. The concentration of total Ag in medium was analyzed by the use of a PerkinElmer SIMA 6000 graphite furnace atomic absorption spectrometry (GFAAS), and the concentration of total Pd in medium was analyzed by the use of a JOBIN YVON JY38S inductively coupled plasma optical emission spectrometry (ICP-OES). A total of three independent analyses were conducted for each solution, and the average concentration was calculated.

Bacterial activity associated with Ag-Pd surface

The purpose of this study was to use microscopic techniques to directly observe bacterial activity associated with Ag-Pd surface under a condition of high bacterial load, and furthermore study the mechanism of metal dissolution. After 24- and 72-hour immersion tests, the bacterial activity on the Ag-Pd surface were observed by the use of a Zeiss LSM 510 META confocal laser scanning microscope (CLSM), and staining with Molecular Probes LIVE/DEAD BacLight Bacterial Viability Assay, which utilizes the green fluorescent SYTO 9 for staining of cells, and the red fluorescent propidium iodide for staining of membrane-compromised cells. A 488-nm argon laser was used to excite the SYTO 9-stained cells, and a 543-nm helium/neon laser was used to excite the propidium iodide-stained cells. Simulated 3-D images were generated by the use of Bitplane IMARIS software.

## Results and discussion

Silver stability

The microstructure of the Ag-Pd surface has been described previously [9-11]. Pd was incompletely deposited as a microhole-structured layer upon Ag. Ag was partially exposed through these microholes. In these microholes, some Ag can react to form silver chloride (AgCl) during Pd deposition. The calculated reaction of AgCl formation at room temperature during Pd deposition is as follows [19-21]:

$$PdCl_4^{2-} + 2Ag \rightarrow 2AgCl + Pd + 2Cl^- \quad \Delta G = -66.907 \text{ kJ (25 °C)} \quad (1)$$
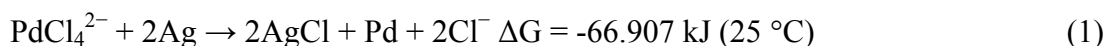
The resulting surface can therefore release Ag ions or compounds like AgCl and theoretically also Pd, if the surface is degraded.
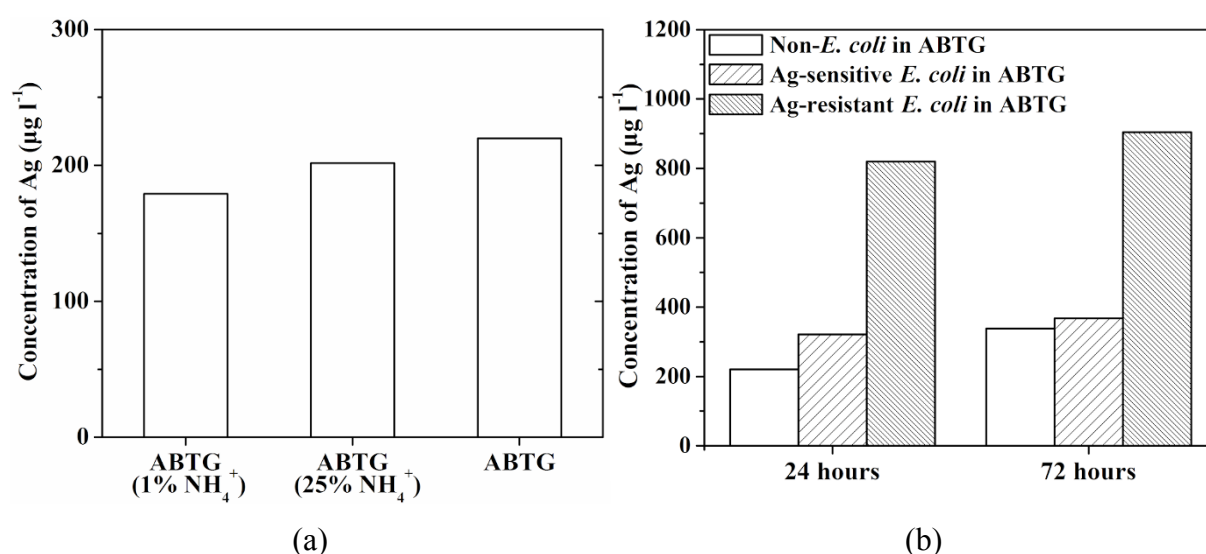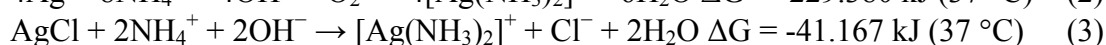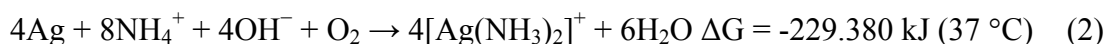


*Fig. 1. Concentration of Ag in different immersion environments. (a) Effects of $NH_4^+$ content in bacteria-free ABTG medium on Ag dissolution after 24-hour immersion, and (b) effects of bacteria in ABTG medium on Ag dissolution after 24- and 72-hour immersion.*

Fig. 1 shows the concentration of Ag dissolved from Ag-Pd surfaces into solutions. The concentration of Pd dissolved from Ag-Pd surfaces was $\leq 2 \text{ µgl}^{-1}$ for all tests, thus indicating no dissolution of this metal. In the following it is assumed that all measured Ag were present as dissolved ions in solutions, although the analyses measured Ag compounds in total and not only dissolved ions. In Fig. 1 (a), it is observed that the dissolved Ag concentration slightly increased with increasing $NH_4^+$ content in medium. The data also show that ABTG solution with only a small amount of $NH_4^+$ content has a strong tendency for Ag dissolution. When $NH_4^+$ is present, the process of increased Ag dissolution can occur by Ag complex (diammine silver ion) formations. The calculated reactions are as follows [22, 23]:

$$4Ag + 8NH_4^+ + 4OH^- + O_2 \rightarrow 4[Ag(NH_3)_2]^+ + 6H_2O \quad \Delta G = -229.380 \text{ kJ (37 °C)} \quad (2)$$
$$AgCl + 2NH_4^+ + 2OH^- \rightarrow [Ag(NH_3)_2]^+ + Cl^- + 2H_2O \quad \Delta G = -41.167 \text{ kJ (37 °C)} \quad (3)$$

Since the Gibbs free energy ($\Delta G$) for these reactions is negative, these calculated reactions are thermodynamically favorable. The test media in itself therefore facilitates Ag dissolution.

In Fig. 1 (b), surprisingly high Ag concentrations were found in the tests of Ag-resistant *E. coli* compared to those from the tests of Ag-sensitive *E. coli* and *E. coli*-free solutions. It was also found that bacteria-containing solutions had a higher rate of Ag dissolution than that of bacteria-free ABTG solutions.

Biofilm prevention
Fig. 2 and Fig. 3 show bacterial activities associated with the test surfaces, which were LIVE/DEAD stained and visualized by the use of CLSM. Samples with 316 steel were included as controls along with the Ag-Pd surface. As shown in Fig. 2, Ag-sensitive and Ag-resistant bacteria both can form biofilm on the 316 surfaces. It can also be observed that the thickness and density of biofilm increased with increasing incubation time from 24 to 72 hours.
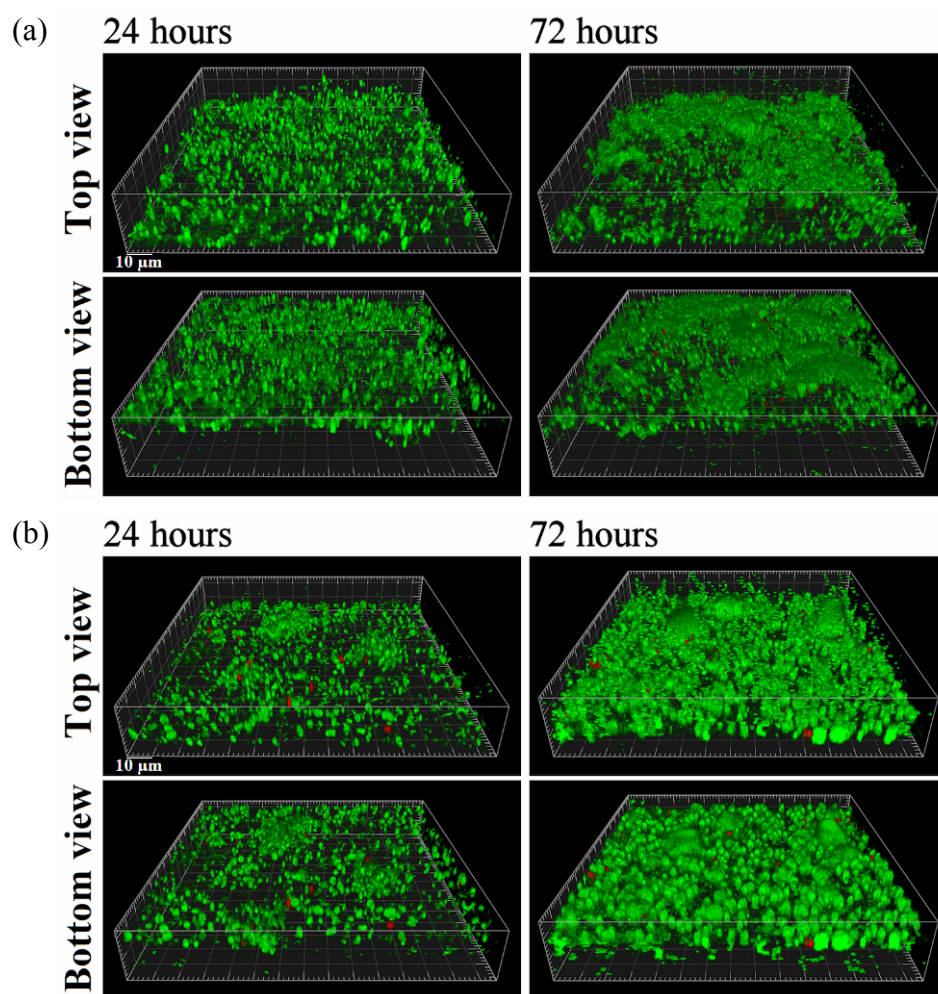


*Fig. 2. CLSM micrographs of 24- and 72-hour-old, LIVE/DEAD-stained (a) Ag-sensitive E. coli J53, and (b) Ag-resistant E. coli J53[pMG101] biofilm on 316 surfaces. The upper panel (top view) shows the biofilm from the growth medium side, whereas the lower panel (bottom view) shows the biofilm from the surface side. The images are representative of three independent experiments. Green fluorescence indicates live cells and red fluorescence indicates dead cells.*
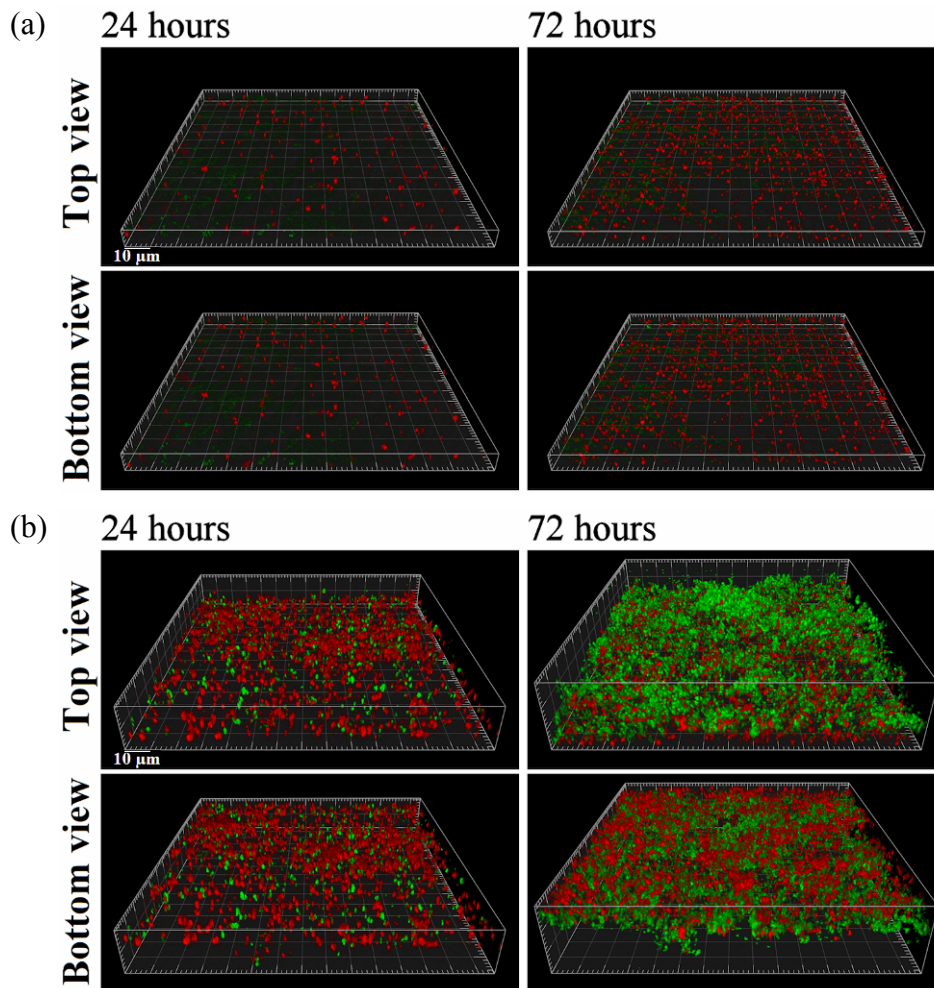
*Fig. 3. CLSM micrographs of 24- and 72-hour-old, LIVE/DEAD-stained (a) Ag-sensitive E. coli J53, and (b) Ag-resistant E. coli J53[pMG101] biofilm on Ag-Pd surfaces. The upper panel (top view) shows the biofilm from the growth medium side, whereas the lower panel (bottom view) shows the biofilm from the surface side. The images are representative of three independent experiments. Green fluorescence indicates live cells and red fluorescence indicates dead cells.*

As shown in Fig. 3 (a), unlike biofilm on the 316 surfaces (Fig. 2), in case of the Ag-sensitive bacteria, the Ag-Pd surface killed surface-associated bacteria and prevented biofilm formation, and more dead bacteria were found after 72-hour immersion. In case of the Ag-resistant bacteria (Fig. 3 (b)), the Ag-Pd was covered with a layer of surface-associated dead bacteria close to the surface after 24-hour immersion. When the surface was consistently exposed to solution with a high bacterial load, the Ag-resistant bacteria from their planktonic phase subsequently formed biofilm upon a conditioning layer of dead bacteria that had developed on the surface (Fig. 4). In agreement with our previous studies [10-12], it demonstrated that the Ag-resistant bacteria close to the Ag-Pd surface were killed due to the micro-electric fields/redox processes.
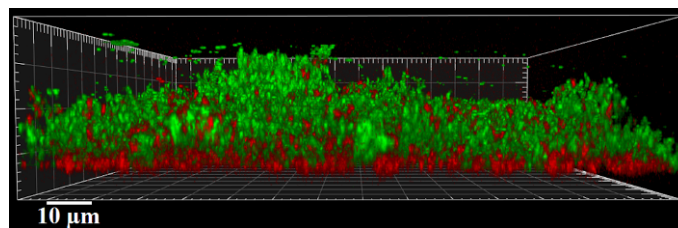
*Fig. 4. CLSM micrograph of a side view of 72-hour-old, LIVE/DEAD-stained Ag-resistant E. coli J53[pMG101] biofilm on Ag-Pd surfaces. Biofilm formed upon a layer of surface-associated dead bacteria. The images are representative of three independent experiments. Green fluorescence indicates live cells and red fluorescence indicates dead cells.*

Comparing Fig. 3 (a) and 3 (b), the apparent difference is that less dead Ag-sensitive bacteria were present close to the surface in the tests of 24-hour immersion, and no obvious biofilm formed in the tests of 72-hour immersion. Taken together with the analyses of Ag concentration as shown in Fig. 1, this can be explained by the ability of Ag-resistant bacteria to tolerate higher Ag concentration than Ag-sensitive bacteria [16, 17]. When chemicals aggressive to Ag-Pd surfaces were present in solution, an increased Ag dissolution occurred and dissolved toxic levels of Ag into the surrounding solution. This killed planktonic Ag-sensitive bacteria in solution in addition to the killing effects of the surface, where low numbers of Ag-sensitive bacteria could not initiate biofilm formation. Therefore less dead Ag-sensitive bacteria were present on the Ag-Pd surface.

Ag dissolution mechanism
As shown in Fig. 1 (b) and Fig. 3, these observations suggested that surface-associated bacteria increased Ag dissolution from the surfaces, and the amount of surface-associated bacteria improved this effect. The tests with Ag-resistant bacteria showed more surface-associated dead bacteria and had an even higher Ag concentration than those of Ag-sensitive bacteria.

The influence of surface-associated bacteria on the increased rate of Ag dissolution can be explained by the interactions between cell components and Ag-Pd surface. It is well-known that Ag can react with amino acids ($H_2NCHRCOOH$, where R is an organic substituent) or amino groups ($-NH_2$) of membranes or enzymes inside bacteria, [24-26]. When surface-associated bacteria were present, these reactions can lead to increased rate of Ag dissolution from the surface by Ag complex formations. Furthermore the silver resistant strain utilises effects like silver binding proteins and efflux pumps, which may possibly affect the silver dissolution rate [16, 17].
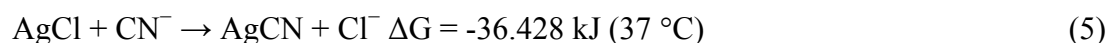
In Fig. 1 (b), the rate of Ag dissolution was observed not to increase proportionally with increasing incubation time from 24 to 72 hours. This can be explained by a steady state of the reaction because of mass-transfer control.

In natural media different from this ABTG designed for optimal biofilm formation in tests, we might find other effects. In some specific environments (not above-mentioned test conditions), a number of bacterial species, e.g. *E. coli*, can perform respiratory reduction of nitrate ($NO_3^-$) to nitrite ($NO_2^-$) and of nitrite to ammonia ($NH_3$) under anaerobic condition [27, 28]. If Ag-Pd surfaces are applied in these environments, these $NH_3$ or $NH_4^+$ ions can cause Ag and AgCl to form Ag complexes (Eq. 2 and Eq. 3). It also has been reported that microbial cyanide biosynthesis, so called microbial cyanogenesis, can occur in some species of bacteria, e.g.

*Pseudomonas aeruginosa* (*P. aeruginosa*) [29, 30]. Cyanide produced by bacteria or already presented in an environment can cause Ag and AgCl to form Ag complexes (dicyanoargentate ion). For Ag dissolution, the calculated reaction is as follows [31, 32]:

$$4Ag + 8CN^- + O_2 + 4H^+ \rightarrow 4[Ag(CN)_2]^- + 2H_2O \quad \Delta G = \text{-626.809 kJ (37 °C)} \qquad (4)$$
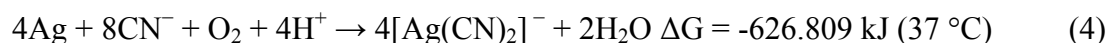
For AgCl dissolution, a series of reactions can happen, and these calculated reactions are as follows [23, 32]:

$$AgCl + CN^- \rightarrow AgCN + Cl^- \quad \Delta G = \text{-36.428 kJ (37 °C)} \qquad (5)$$
$$AgCN + CN^- \rightarrow AgCN^{2-} \quad \Delta G = \text{-23.375 kJ (37 °C)} \qquad (6)$$

Since the Gibbs free energy ($\Delta G$) for these reactions is negative, these calculated reactions are thermodynamically favorable.

## Conclusion

This study indicated that it is important to select applicative environments to avoid the degradation of Ag-Pd surfaces. In some specific environments, an undesired increased Ag dissolution can occur and add to the bacteria inhibiting effect when chemicals aggressive to Ag and AgCl, such as $NH_4^+$ ions, are present. Surface-associated bacteria can increase Ag dissolution from Ag-Pd surfaces due to the interactions between cell components and the surfaces, and the amount of surface-associated bacteria can improve this effect. This could indicate that in a natural environment Ag-dissolution may be low unless bacteria or activating ions are present. Furthermore silver resistant strains seem to enhance this microbiologically influenced corrosion as compared to silver sensitive strains.

Biofilm formation evidently can occur if the Ag-Pd surface becomes covered with a conditioning layer of dead bacteria. Highest bacteria inhibiting efficiency of an Ag-Pd surface may therefore be achieved under conditions where appropriate cleaning processes can be applied.

## References

1.  H.A. Videla, W. G. Characklis, Int. Biodeter. Biodegr. 29 (1992) 195.
2.  E.A. Zottola, K.C. Sasahara, Int. J. Food Microbiol. 23 (1994) 125.
3.  M.V. Jones, Int. Biodeter. Biodegr. 41 (1998) 191.
4.  J.W. Costerton, Int. J. Antimicrob. Ag. 11 (1999) 217.
5.  S.J. Dancer, J. Hosp. Infect. 43 (1999) 85.
6.  A. Rampling, S. Wiseman, L. Davis, A.P. Hyett, A.N. Walbridge, G.C. Payne, A.J. Cornaby, J. Hosp. Infect. 49 (2001) 109.
7.  L.J. Kagan, A.E. Aiello, E. Larson, J. Comm. Health 27 (2002) 247.
8.  J.W. Costerton, B. Ellis, K. Lam, F. Johnson, A.E. Khoury, Antimicrob. Agents Chemother. 38 (1994) 2803.
9.  P. Møller, L.R. Hilbert, C.B. Corfitzen, H.J. Albrechtsen, J. Appl. Surf. Finish. 2 (2007)

149.

10. W.C. Chiang, L.R. Hilbert, C. Schroll, T. Tolker-Nielsen, P. Møller, Corros. Eng. Sci. Technol. 43 (2008) 142.

11. W.C. Chiang, L.R. Hilbert, C. Schroll, T. Tolker-Nielsen, P. Møller, Electrochim. Acta 54 (2008) 108.

12. W.C. Chiang, C. Schroll, L.R. Hilbert, P. Møller, T. Tolker-Nielsen, Appl. Environ. Microb. 75 (2009) 1674.

13. D.A. Jones, Principles and Prevention of Corrosion, 2nd ed., Prentice Hall, Upper Saddle River, NJ, 1996.

14. G. Danscher, Histochem. Cell Biol. 117 (2002) 447.

15. A. Larsen, M. Stoltenberg, G. Danscher, Histochem. Cell Biol. 128 (2007) 1.

16. A. Gupta, K. Matsui, J.F. Lo, S. Silver, Nat. Med. 5 (1999) 183.

17. A. Gupta, M. Maynes, S. Silver, Appl. Environ. Microb. 64 (1998) 5042.

18. G. Bertani, J. Bacteriol. 62 (1951) 293.

19. Thermodynamic Tables for Nuclear Waste Isolation. Prepared by S. L. Philips, F. V. Hale, L. F. Silvester, Lawrence Berkely Laboratory M. D. Siegel, Sandia National Laboratories, 182, 1988.

20. Landolt-Börnstein: Thermodynamic Properties of Inorganic Material, Scientific Group Thermodata Europe (SGTE), Springer-Verlag, Berlin-Heidelberg, Part 1, 1999.

21. Barin I: Thermochemical Data of Pure Substances, VCH Verlags Gesellschaft, Weinheim, 1989.

22. E.L. Shock, H.C. Helgeson, Geochim. Cosmochim. Acta 52 (1988) 2009.

23. Landolt-Börnstein: Thermodynamic Properties of Inorganic Material, Scientific Group Thermodata Europe (SGTE), Springer-Verlag, Berlin-Heidelberg, Part 1, 1999.

24. J.M. Schierholz, L.J. Lucas, A. Rump, G. Pulverer, J. Hosp. Infect. 40 (1998) 257.

25. S.L. Percival, P.G. Bowler, D. Russell, J. Hosp. Infect. 60 (2005) 1.

26. N.C. Kasuga, M. Sato, A. Amano, A. Hara, S. Tsuruta, A. Sugie, K. Nomiya, Inorg. Chim. Acta 361 (2008) 1267.

27. H. Neubauer, F. Goetz, Arch. Microbiol. 154 (1990) 349.

28. H. Neubauer, F. Götz, J. Bacteriol. 178 (1996) 2005.

29. C.J. Knowles, Bacteriol. Rev. 40 (1976) 652.

30. P.A. Castric, J. Bacteriol. 130 (1977) 826.

31. D.D. Wagman, W.H. Evans, V.B.Parker, R.H. Schumm, I. Halow, S.M. Bailey, K.L. Churney, R.L. Nuttall, J. Phys. Chem. Ref. Data 11 (1982).

32. E.L. Shock, D.C. Sassani, M. Willis, D.A. Sverjensky, Geochim. Cosmochim. Acta 61 (1997) 907.